TÉCNICO LISBOA

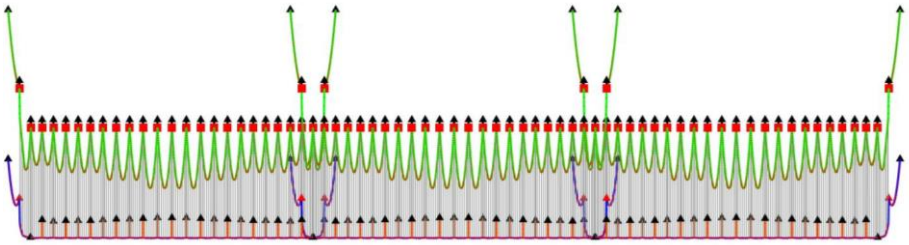

Analysis of the Pantograph-Catenary Interface Quality for the National Overhead Contact Lines and Train Pantographs

Ana Matilde Esteves Macedo

Thesis to obtain the Master of Science Degree in

Mechanical Engineering

Supervisores: Prof. Jorge Alberto Cadete Ambrósio

Dr. Pedro Cabaço Antunes

Examination Committee

Chairperson: Prof. Paulo Rui Alves Fernandes

Supervisor: Dr. Pedro Cabaço Antunes

Member of the Committee: Eng. Sérgio Pissarra de Abreu dos Santos

December 2021

Acknowledgments

I want to thank my supervisor, Prof. Jorge Ambrósio for the patience that he had. I also want to thank for his guidance during this work and for always being accessible and willing to help.

A special thanks to my advisor, Dr. Pedro Antunes, for all the dedication, time, help and motivation that he willingly provided through the entirety of this project. That where essential for the conclusion of this thesis.

I want to thank my parents and siblings for the tough love and the unconditional support that in the toughest moments only a family can provide.

Finally, I want to thank my friends for the support and help provided.

Resumo

Os transportes ferroviários desempenham um papel fulcral no transporte de passageiros e mercadorias, não só devido ao seu custo, segurança e conforto. Mas também devido à sua menor pegada de carbono. O aumento da competitividade dos transportes ferroviários requer que não só as suas velocidades de operação aumentem, como também que sejam mais eficientes energeticamente. A interface entre o pantógrafo e a catenária condicionam a qualidade da transmissão de energia elétrica da infraestrutura para os motores elétricos do veículo, sendo o maior obstáculo tecnológico ao aumento da velocidade de exploração dos comboios nas linhas ferroviárias atuais. Este trabalho tem como objetivo o estudo de duas catenárias distintas de maneira a avaliar os limites à velocidade de operação de veículos ferroviários e os critérios que impedem maiores velocidades. Este estudo vai também focar-se em como pantógrafos distintos podem afetar a interação pantógrafo-catenária. Para tal, uma série de testes vão ser desenvolvidos no âmbito de entender qual é a dinâmica de cada par pantógrafo catenária, para quando as catenárias estas estão sujeitas a operações com pantógrafos simples ou múltiplos. Consequentemente, saber-se-á qual o melhor pantógrafo a usar com cada catenária, tal como as possíveis perdas de velocidades de operação das catenárias, caso o pantógrafo que apresentar menor capacidade de contacto for escolhido.

Palavras-Chave

Dinâmica ferroviário;
Interação pantógrafo-catenária;
Operação pantógrafos múltiplos;
Forças de contacto.

Abstract

The railway systems play a pivotal role in the transport of passengers and goods, not only because of its cost, safety and comfort. But also because of its smaller carbon footprint. Increasing the competitiveness of rail transport requires that not only its exploration velocity increase, but also that it is more energy efficient. The interface between the pantograph and the catenary affects the quality of the transmission of electrical energy from the infrastructure to the vehicle's electric motors, being currently the greatest technological obstacle to increasing the speed of operation of trains on the railway lines. This work aims to study two distinct catenaries in order to assess the limits to the exploration velocity of railway vehicles and the criteria that prevent higher speeds. This study will also focus on how distinct pantographs can affect the pantograph-catenary interaction. For this, a series of tests will be developed in order to understand the dynamics of each catenary pantograph pair, for when the catenaries are subject to operations with single or multiple pantographs. Consequently, it will be known which is the best pantograph to use with each catenary, as well as the possible loss of exploration velocity of the catenaries, if the pantograph with the lowest contact capacity is chosen.

Key words

Railway dynamics;
Pantograph-Catenary interaction;
Multiple pantograph operation;
Contact force.

Table of Contents

List of figures

List of Tables

List of Symbols

Convention	
a, A, α	Scalar
A	Vector
A	Matrix
Subscript	
a_{cw}	Quantity referred to the contact wire
a_i, a_j	Quantity referred to body i and j
a_L	Quantity referred to the linear Euler-Bernoulli beam element
a_G	Quantity referred to the element geometric matrix
a_{pant}	Quantity referred to the pantograph
a_{cat}	Quantity referred to the catenary
a_{max}	Quantity referred to the maximum value
a_{min}	Quantity referred to the minimum value
a_m	Quantity referred to the mean value
$a_{dropper}$	Quantity referred to the dropper
a_0	Quantity referred to the initial value
Superscript	
a^e	Quantity referred to the element
a^m	Quantity referred to body m
Overscript	
$\dot{a}$	First time derivative
$\ddot{a}$	Secund time derivative
Latim Symbols	
T	Tension
m_{cw}	Linear mass of the contact wire
d	Position at the dropper
d^S	Nominal position
l	Length of the dropper
M, m	Mass
K, k	Stiffness
C, c	Damping
F, f	Force
a	Acceleration
v	Velocity
d	Displacement
g	Gravity

δ	Penetration
z	Position on the z coordinate
r	Specific radius
S	Statistical
s	Variation in spring length
L	Spring length
y	Lump mass height
α	Stiffness proportional factor
β	Damping proportional factor
F_c, f^c	Contact force
f^g	Gravitational force
f^d	Dropper slacking force
F_a	Aerodynamic force
F_s	Static force
F_{up}	Uplift force
σ	Standard deviation

List of Acronyms

CW	Contact wire
S_{min}, SMin	Statistical minimum
S_{max}	Statistical maximum
FEM	Finite element model
CL	Contact loss
σ	Standard deviation
Max	Maximum
Min	Minimum

1 Introduction

The railway system is an important network which allows the safe transportation of goods and passengers across different points in the world. The rising interiorization of the ecological footprint that is left on earth is leading countries to implement higher oil taxes. These measures result in an increase in oil prices, in an attempt to reduce greenhouse gases emissions. Higher oil prices lead, companies and individuals to invest more in electric vehicles as a means of transportation. In order to improve the competitiveness and attractiveness of trains, they need to be faster, more reliable, and more cost-efficient than the alternatives. While maintaining the passengers' level of comfort and safety. One way of improving the attractiveness of railway vehicles is by decreasing the passenger travel cost. However, this change in the cost cannot be felt by the railway operators. Consequently, there is a need to reduce the overall operation costs. The railway operators give special importance to the increase of compatibility between systems from various countries creating an increase in the distances of transportation and the decrease of maintenance costs, while increasing the operation speed. When the operation speed of a railway vehicle is above a maximum validated speed there is a risk of damaging some of the system components, either on the infrastructure or the vehicle side. If the catenaries ends up damaged then the maintenance costs would naturally increase, since the cost of the catenary maintenance is not only the cost of the required maintenance, but also the cost of not being able to use the track during the period of the maintenance actions. If the operator is not able to utilize the tracks, the passengers or the goods have to travel using other means of transportation, directly lowering the railway operator results and preventing the track to be in use, which leads to a lower reliability of the system.

By comparing the railway system with other means of transportation it is possible to determine the ideal one for each scenario. From short to medium distances the railway system is a viable alternative to air transportation since it has better energy efficiency and causes less pollution. For longer distances, the railway system is still the most economic for transportation of goods. Despite the advantages such as the cost-effectiveness of the system, one cannot forget a big factor that comes into play, the initial investment. In order to get such a land network, a large investment is required in order to build the infrastructure, vehicles, and tracks, as well as plan, design, and development of an efficient system.

In this day and age, electric railway vehicles are the safest, more ecological, and cost-effective means of transportation. In these systems, the transference of energy occurs from the catenaries to the pantographs, therefore the contact pantograph-catenary is an important factor to take into consideration. The catenary is an overhead structure, whose purpose is to carry electric energy. This structure is composed of different types of cables and their supports elements. The pantograph is a device mounted on top of the railway vehicle. Whose objective is to carry the energy from the catenary contact wire to the railway vehicle motor. The limiting factor of the maximum velocity achieved by the railway vehicle is the ability to maintain this contact as uninterrupted and as constant as possible [1]. This occurs because the railway vehicle motors need to receive the necessary electrical energy for their proper operation. During a contact loss, the energy supplied to the motors is interrupted. Which might also lead to arcing

between the contact strip of the pantograph and the contact wire. When arcing is detected, this leads to higher localized electro-mechanic wear of both components.

An increase of the mean contact force would imply a better contact between the catenary and pantograph, with fewer contact losses situations. This would improve the electric energy transference to the train and allow higher velocities of operation. However, this strategy also comes with its downsides associated, such as the higher component wear, due to the involved friction in the contact [2,3]. Consequently, leading to an increase in maintenance operation and costs. Lowering the mean contact force leads to a higher chance of contact losses, which in turn would lower the energy that the motors would receive. Therefore, it would not be possible to maintain high velocities and the occurrence of arcing would also be detected. In the end, a balance between the characteristics of the contact and the system wear generated is of utmost importance. This balance would ensure a better contact quality at higher speeds while lowering the necessary maintenance cycles of the system. The parameters required to evaluate the contact according with the norm EN50367 are the mean contact force, the standard deviation, the maximum contact force, the maximum steady arm uplift, and the contact loss percentage.

In order to obtain higher exploration velocities for catenaries, initially designed for lower velocities requires some changes in the catenary structures are needed. One way to obtain higher speeds is by increasing the tension on the wires by lowering the contact wire linear mass. Both of these changes lead to a higher elastic wave propagation speed, which in turn results in better contact quality. However, changing the wires tension is not always possible since the catenary supports may not be dimensioned to support these forces and changing the existent supports is extremely expensive to be a viable option. Another way to improve the catenary-pantograph contact quality is by increasing the uniformity of the catenary stiffness using stich wire, however the use of stitch wires is less used with the passage of time, since it is a costly design and there are better and cheaper designs that improve the uniformity of the stiffness [4,5,6]. The stiffness is controlled via the dropper distance around the steady-arms. For both stitch and simple catenary types there is a pre-sag of 1/1000 to further improve the uniformity of the stiffness [7–9].

Different pantograph-catenary pairs may show significant differences in their dynamic analysis. It is necessary to study the required pantograph-catenary interaction for all of the pantographs that are expected to operate in that catenary. Virtual studies are best suited to analyse the suitability of different pairs, since they are cheaper, faster, broader in range, and easier to execute than a physical test. The implementation of computational tools capable of simulating the dynamics of the pantograph-catenary was required to enable such analysis. Today, these computational tools are used not only to validate pantographs, infrastructures, and vehicles, but also to optimize the operating conditions and designs. In the case of validating an infrastructure design, the computational tools are essential, since the only way of testing the changes obtained by the infrastructures designs alterations in a physical setting involves large resources such as man labour and the stopping the vehicle operation in the track.

Computational code *PantoCat* [10] which allows for the dynamic analysis of catenary finite element models and pantograph multibody models is extensively used in this work. This computational tool considers the catenary structure and pantograph optimization design [11–13], critical catenary section [14–16], catenary damping effects [9,17], single and multiple pantograph operations [18–20],

and aerodynamic direct and indirect effects on the catenary and catenary irregularities [21–24]. It also allows for the modelling of fully nonlinear pantograph multibody models. Most of the numerical tools developed deal with simulations of the between the pantograph and catenary for straight tracks [25,26], the software used in this study is one that can implement curves and track elevations to simulate the catenary models in a more realistic manner.

This study as an objective to analyse the dynamic behaviour of two different catenaries, in order to identify their trains speeds at which they can be operated. In order to further study their operation range, cases with single and multiple pantographs are considered. The contact quality is studied for five different scenarios for each catenary. The scenarios differences consist in the number of pantographs operated simultaneously and their respective separation i.e., the distance between them when mounted on the train rooftop. These studies consider the overlapping zone of the catenary, i.e., the transition between two catenary sections, that represents a singularity in the catenary. Using the *PantoCat* software the dynamic results for the catenary pantograph interaction are obtained to be analysed. Their interaction is studied for a speed range of 120 km/h until the operation velocity of a single pantograph operation becomes invalid by the European norms [27]. The railway vehicles are simulated with velocities with 5 km/h increments.

This thesis starts by giving a brief introduction to the catenary pantograph dynamics, chapter 2 describes the catenary and the pantograph systems, as well as the methods used for their modelling. This chapter also describes the methods used to represent the contact interaction and how to validate and analyse the dynamic results obtained from the pantograph-catenary contact interaction simulation. Chapter 3 presents the data necessary for the pantographs and catenaries models. In chapter 4 the contact dynamic presented and discussed. Important dynamic results for a single pantograph interaction, followed by all of the results relevant for the multiple pantographs interaction are presented and discussed. Chapter 5 includes the general conclusions of this work, as well as the suggestions for future works.

2 Pantograph-Catenary Dynamics and Numerical Modelling

This chapter includes a definition of the typical catenary components, their use and typical problems. The catenary topology and its modelling method is explained. Afterwards, being the numerical model of the pantograph defined in the process. After the numerical models of the structural components of the catenary are defined, the numerical method requires to analyse the pantograph-catenary contact interaction is described. Finally, the parameters used for the acceptance of the pantograph-catenary compatibility are presented, as well as their acceptance thresholds, according to the existing norms.

2.1 Catenary Modelling and Analysis

Railway catenaries are periodic structures mounted along the railway track. That supply the electricity to the trains running on the tracks below. Although the actual type, of construction, of the catenary differs for each track, they all share the same basic main components. Figure 2.1 represents part of a typical catenary system in which the base is composed of support, console, and stay, is what supports the messenger wire and the contact wire [27]. The messenger wire is responsible to support the contact wire in a position that allows the correct pantograph interaction. The contact wire is responsible for suppling the railway vehicle with the required electricity. The steady arm ensures not only the necessary stagger of the messenger and contact wire, but also the correct compliance with the supports. Finally, there are the droppers which help the connect the contact wire to the messenger wire, supporting and the contact wire and controlling the contact wire elasticity and sag i.e., the contact wire geometry. Occasionally one can also find a stitch wire in the connectivity of the messenger wire with the stay to improve the uniform stiffness around the steady arm. The general catenary structure is represented in Figure 2.1. The catenary has a maximum length for each span, the distance between supports. The span length can be altered if needed, for the case of curves or due to obstacles in the catenary construction. Each catenary has a limited length, generally below 1.5 km, so that the contact wire can be feed with electricity in independent sections and, in case of need, be replaced in specific locations [29].

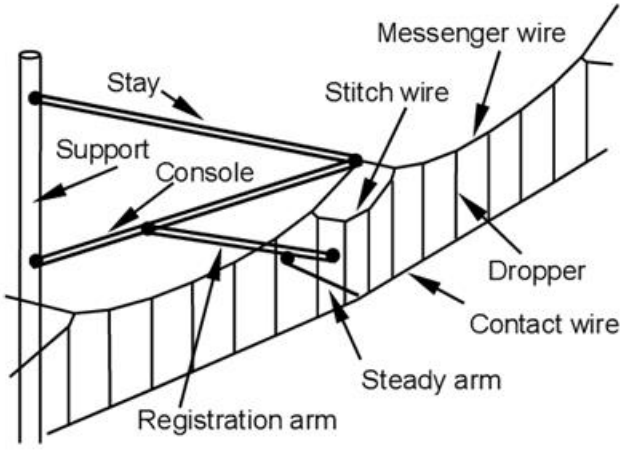

Figure 2.1: Structural elements of a typical catenary

The contact wire and the messenger wire are tensioned, with high axial forces, generally realized by using large masses that hang at the first and last support of each section. Each catenary section has a maximum length of 1.5 km, and a catenary is composed by various catenary sections. This distance allows the tension in the wire to be kept constant along the catenary while maintaining a good balance between the cost and physical constraints. However, a distance of only 1.5 Km is not enough to cover all the track. Therefore, each track requires several catenary sections in succession. The continuity of the contact between the pantograph and the catenary is essential, this problem is fixed by the overlapping section at the start and end of each section, represented in Figure 2.2, i.e., sections composed by a span that overlaps the existing and incoming contact wires of two sequential sections and spans that connect the catenary section to the “hanging masses” [27].

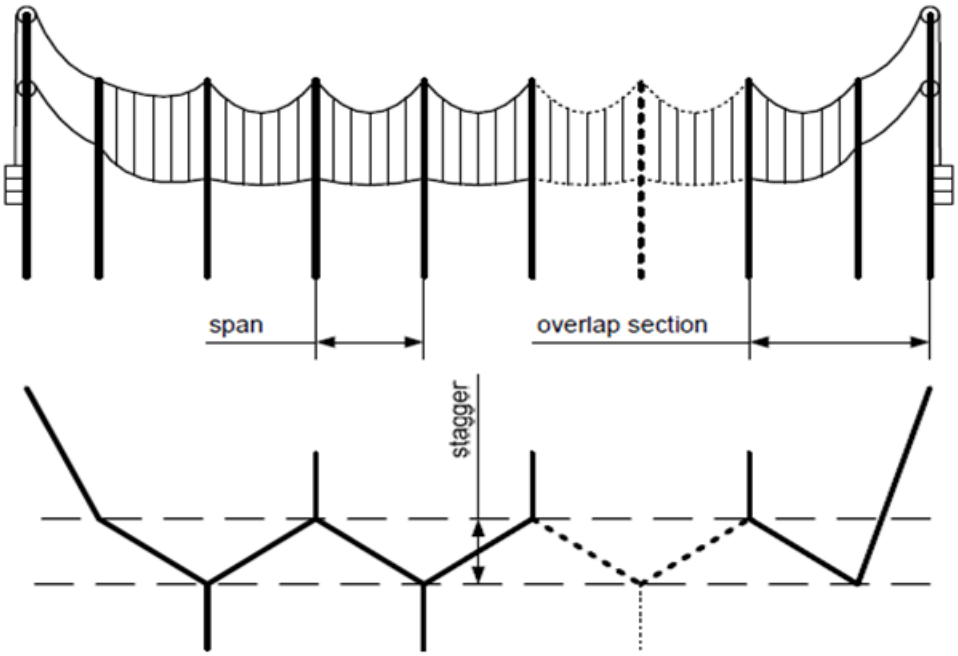

Figure 2.2: Side and top views of a catenary section

The stagger is the lateral displacement, shown in Figure 2.2, of the contact and messenger wire. Its purposes are: to avoid excessive friction, heat, and grooves on the pantograph contact strip, distributing it along a larger area, which helps to maintain the contact force, between the catenary and the pantograph; to allow that the catenary follows the track when curving. The stagger is imposed at the supports by the steady arm, this design considers the track geometry, the contact strip length, the operational requirements, and the weather tolerances that can be imposed either by the standards or by infrastructures managers.

There are two main issues in the modelling of the catenary, these are the line tension and the dropper slacking. The line tension is normally achieved by a weight pulley system mounted at each end of the catenary section, as seen in Figure 2.3. This mechanism ensures the line tension of the catenary wires is kept as constant as possible, even when the variation of the temperature leads to changes in the messenger and contact wire lengths.

Figure 2.3: Representation of a weights line tensioning system

The linear tension of the wires must ensure that the oscillation of the wire derived by the contact between the pantograph and the catenary has a wave propagation speed faster than the train. This avoids the increase of the catenary oscillation amplitude and the bending effects of the wires which, in turn, would prevent a good pantograph contact. The increase of the bending effects leads to an increase both the wear and the potential for wire breakage. This tension helps attenuate the sag, favouring a more constant contact force with fewer perturbations. In principle, the more sag a catenary has in the contact wire the less constant the contact force will be, creating a system with more contact perturbations. However, in some catenary construction the existence of pre-sag is important to ensure a more constant contact wire stiffness [7–9]. The wave propagation speed of the contact wire is called critical velocity. This velocity corresponds to the critical point where if increased, the amplitude of the catenary oscillations is so high that the contact quality between the catenary and the pantograph deteriorate significantly. In order to maintain a safe margin, the actual maximum operation velocity for a railway vehicle is 70% of the critical velocity [28], as seen in EN 50119. The catenary wave propagation velocity is given by

$$v_c = \sqrt{\frac{T_{cw}}{m_{cw}}} \tag{2.1}$$

The dropper slacking, i.e. the dropper bending due to its compression instability represented in Figure 2.4, has a nonlinear behaviour. The dropper's purpose is to support the contact wire, maintaining it in the correct position. Therefore, droppers have a constant stress tension until the pantograph passes under them. At this point in time the dropper loses the tension force and is suddenly subjected to compression forces. However, droppers are cables, so they offer no resistance against compression forces, which constitutes a nonlinearity that requires that the numerical methods used in the analysis can handle them. Since these nonlinearities are localized and have a known behaviour. They can be solved using corrective measure [9].

Figure 2.4: Arcing and dropper slacking in a standard railway vehicle operation

When modelling the catenary only its deformed geometry is known, i.e., the geometry that results from the application of the gravitational force and the tension forces on an unknown initial geometry. However, the geometry that can be modelled is the unknown undeformed geometry, which creates a serious initialization modelling problem. Which consists in finding the undeformed catenary geometry, that, after loading, leads to the deformed geometry already known. This requires an inverse initial problem to be solved, known as catenary model initialization. Figure 2.5 represents the finite element model of an unloaded generic catenary, where the sag is inexistent, while Figure 2.6 represents the top, side views, and sag view of the same catenary finite element model after the natural loads are applied.

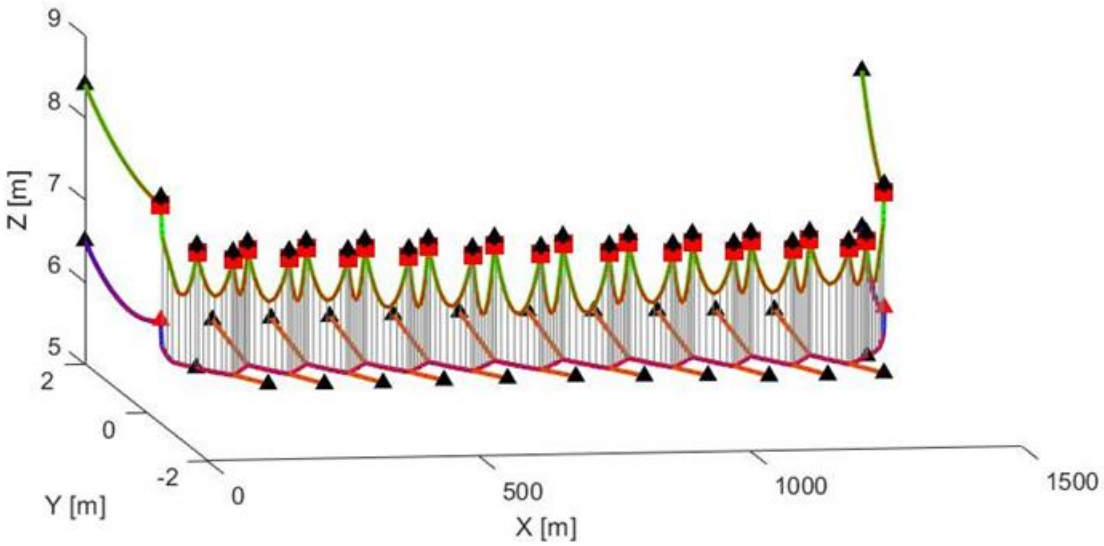

Figure 2.5: Generic catenary model in its undeformed state

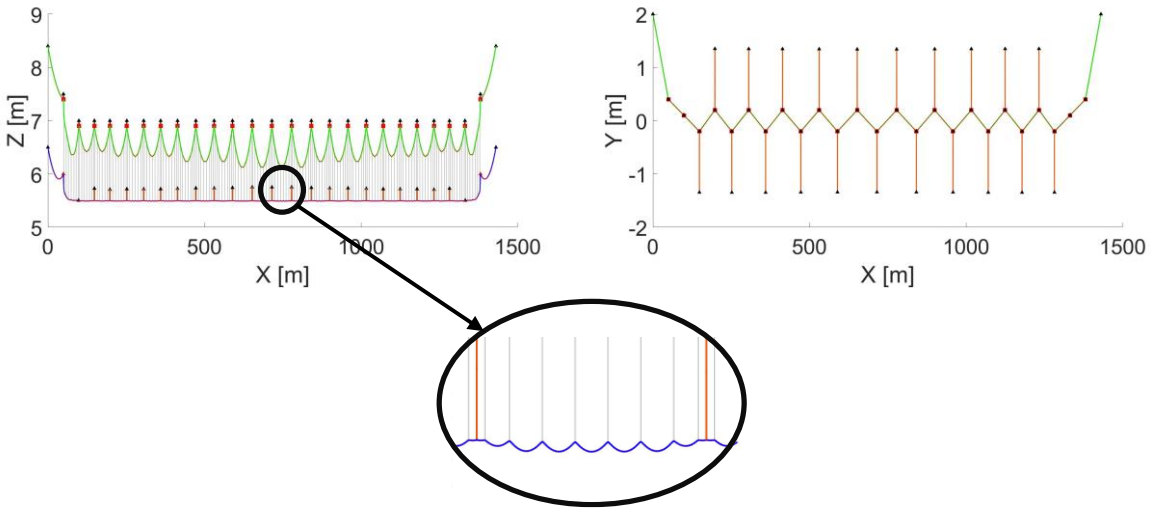

Figure 2.6: Side, top, and sag view of a generic loaded catenary model

The catenary initialization is a minimalization problem where the objective function finds the length of each dropper so that the difference between the statistical deformed catenary geometry and the undeformed geometry is minimized. This problem is described as:

$$min\left(\sum_{1}^{m}\|\boldsymbol{d}_{CW}^{m}(x) - \boldsymbol{d}_{CW}^{S}\|\right) \qquad (2.2)$$

$$subject\ to\ x\colon [\boldsymbol{l}_0^1, \boldsymbol{l}_0^2, \ldots, \boldsymbol{l}_0^m]$$

Where the initial length of each dropper i, a design variable known for each catenary model, is represented as $\boldsymbol{l}_0^i$. The nominal contact wire position at each dropper is set as $\boldsymbol{d}_{CW}$, while the already deformed contact wire position is represented as $\boldsymbol{d}_{CW}^S$. The minimization problem is solved, firstly for each span. Afterwards, the iteration process on the entire optimization problem is repeated, until convergence is obtained. It is common that three turns are enough when starting with initial dropper lengths close to those of the deployed catenaries. The farther away the initial length of the dropper is to the deployed the worst the catenary model is and the less accurate the results obtained from further studies of this catenary are if extra iterations are not used in this tunning.

When a railway vehicle passes in a track, it disturbs the catenary creating a motion that is defined by small deformations and rotations of the complete system which is nonlinear. The single source for the nonlinear response is the dropper slacking. This makes the linear finite element method ideal for the catenary system modelling and analysis, provided that the nonlinear dropper slacking can be handled efficiently.

The dynamic equilibrium equations of the catenary system are obtained using [29,30].

$$\boldsymbol{M}\boldsymbol{a} + \boldsymbol{C}\boldsymbol{v} + \boldsymbol{K}\boldsymbol{d} = \boldsymbol{f} \qquad (2.3)$$

Which includes the finite element global mass matrix $\boldsymbol{M}$, the stiffness matrix $\boldsymbol{K}$ and the damping matrix $\boldsymbol{C}$ of the catenary model. The accelerations, velocities and displacements vector are represented as $\boldsymbol{a}$, $\boldsymbol{v}$ and $\boldsymbol{d}$ respectively, while the sum of the applied nodal forces is $\boldsymbol{f}$ which include the gravity and

pantograph contact forces. The contact wire and the messenger wire have a high-tension force applied which changes the way how the catenary stiffness is structured. These wires are modelled as finite element beams and their element stiffness given by

$$\boldsymbol{K_i^e} = \boldsymbol{K_L^e} + F\boldsymbol{K_G^e} \tag{2.4}$$

In which $\boldsymbol{K_i^e}$ represents the stiffness matrix of each element. This matrix is dependent on the $\boldsymbol{K_L^e}$ the stiffness matrix of an Euler-Bernoulli beam element as well as $\boldsymbol{K_G^e}$,the element geometric matrix and F is the axial tension force that the wires are subjected to. The global stiffness matrix and global mass matrix are implemented by assembling all the element matrices according to the catenary model mesh [29].

The damping behaviour of the catenary is represented by proportional damping, also known as Rayleigh damping [30].The element damping matrix is obtained by using

$$\boldsymbol{C^e} = \alpha^e\boldsymbol{K^e} + \beta^e\boldsymbol{M^e} \tag{2.5}$$

Where α^e and β^e are the stiffness and mass proportional factors, which are defined, by the norms, to represent an adequate damping response of the system. The total force vector, used in equation (2.3) in a particular instant is given by the sum of all individual forces applied in the catenary as

$$\boldsymbol{f} = \boldsymbol{f^g} + \boldsymbol{f^c} + \boldsymbol{f^d} \tag{2.6}$$

Which includes the gravitational force $\boldsymbol{f^g}$, the contact force $\boldsymbol{f^c}$, and the dropper slacking compensation forces $\boldsymbol{f^d}$. This vector must be evaluated at each time step since the applied forces in the system are variable.

The force vector $\boldsymbol{f^d}$ contains the dropper compensation forces derivated due to the dropper slacking. When there is no dropper slacking the droppers will perform as a finite element bar element, which are included in the initial element stiffness matrix $\boldsymbol{K}$. However, in the presence of slacking a force equal to $\boldsymbol{K_{droppers}^e}\boldsymbol{d}_{dropper}$ is added to the dynamic equations (2.3) right-hand-side as $\boldsymbol{f^d}$ to balance the dropper compression forces implicit in the left-hand-side equation (2.3) [9].

The computational code PantoCat, used in this work, includes a Newmark time integration algorithm [29,31] with a trapezoidal rule to solve the governing dynamic equilibrium equations. This particular method is applied due to its unconditional stability nature when used implicitly and its proven robustness in FEM applications of the type of the ones used in this work [9].

2.2 Pantograph Modelling and Analysis Methods

The pantograph collects the energy from the catenaries and transfers it to the train motors. A good model of the pantograph is essential to be able to obtain reliable results for the dynamic interaction with the catenary. The pantographs are generally modelled as linear lump-mass models. Even though nonlinear multibody models can be used, the lump-mass model is more commonly applied due to its simplicity. The parameters of the lump-mass models cannot be measured experimentally or modelled by any process, therefore, they have no physical meaning. The characteristics of these models are obtained by knowing the frequency and amplitude of the motion of the pantograph when excited in a

specialized test rig and by matching the lump-mass model response that was acquired experimentally [1,33]. When this model is applied to pantographs, they are made of two or more masses connected by springs and dampers. Figure 2.7 represents a four lump-masses pantograph model, where m_3 and m_4 have independent movement from each. This model only has one dimensional motion, originated from the contact force with the contact wire, represented as F_c in Figure 2.7 .

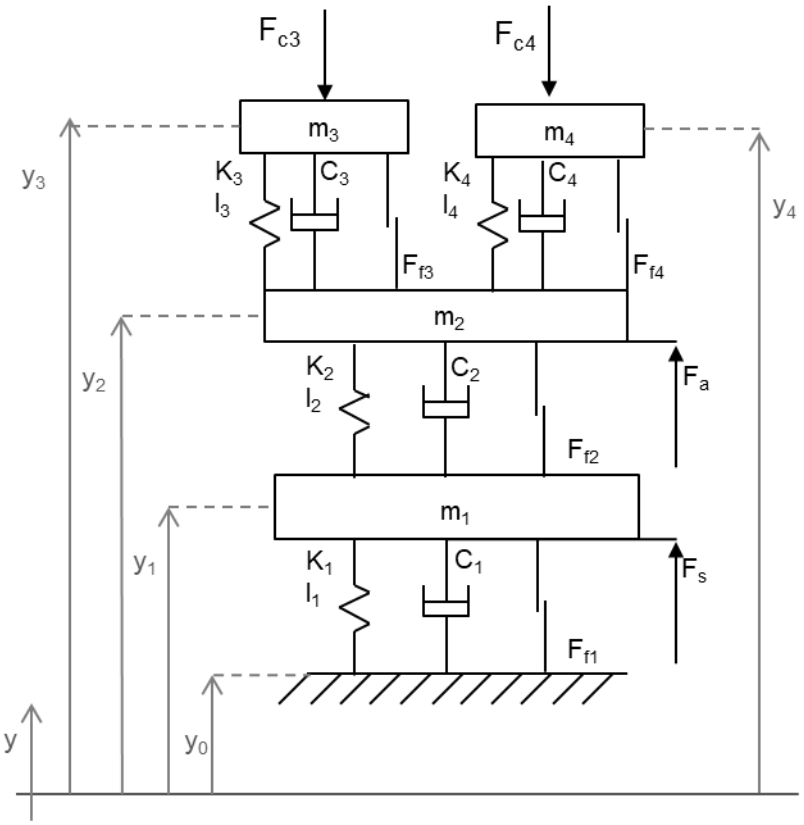

Figure 2.7: Representation of a 4 lump-masses model

The pantograph equations of motion of the model represented in Figure 2.7 has four lump masses , m_1, m_2, m_3 and m_4. These masses are linked to each other via springs, K_1, K_2, K_3 and K_4, and dampers C_1, C_2, C_3 and C_4, and written as:

$$m_1\ddot{y}_1 + C_1(\dot{y}_1 - \dot{y}_0) - C_2(\dot{y}_2 - \dot{y}_1) + K_1(y_1 - y_0 - l_1) - K_2(y_2 - y_1 - l_2) = -m_1.g + F_{f1}(\Delta v_{01}) - F_{f2}(\Delta v_{12}) + F_s \tag{2.7}$$

$$m_2\ddot{y}_2 + C_2(\dot{y}_2 - \dot{y}_1) - C_3(\dot{y}_3 - \dot{y}_2) - C_4(\dot{y}_4 - \dot{y}_2) + K_2(y_2 - y_1 - l_2) - K_3(y_3 - y_2 - l_3) - K_4(y_4 - y_2 - l_4) = -m_2 g + F_{f2}(\Delta v_{12}) - F_{f3}(\Delta v_{23}) - F_{f4}(\Delta v_{24}) + F_a \tag{2.8}$$

$$m_3\ddot{y}_3 + C_3(\dot{y}_3 - \dot{y}_2) + K_3(y_3 - y_2 - l_3) = -m_3 g + F_{f3}(\Delta v_{23}) - F_{c3}(t) \tag{2.9}$$

$$m_4\ddot{y}_4 + C_4(\dot{y}_4 - \dot{y}_2) + K_4(y_4 - y_2 - l_4) = -m_4 g + F_{f4}(\Delta v_{24}) - F_{c4}(t) \tag{2.10}$$

In which the relative velocity between linked masses is given by

$$(\Delta v_{ij}) = v_i - v_j \tag{2.11}$$

The equation of motion requires that a ground constraint is used in the model. The restriction on the pantograph lump-mass model ensures that the ground is fixed, which is expressed by

$$y_0 = constant \implies \dot{y}_0 = \ddot{y}_0 = 0 \tag{2.12}$$

Outside of the specific lump-mass model parameters the equations of motion consider other parameters that can be variable and do not define the pantograph model just like the friction force between the lump masses ($F_{\mathrm{f1}}, F_{\mathrm{f2}}, F_{f3}, F_{\mathrm{f4}}$), and the gravitational constant (g). The friction force must be evaluated at each time, since it is proportional to the difference in velocities Δv_{ij} between the adjacent masses, as seen in equation (2.12). The free length of the springs (l_1, l_2, l_3, l_4) is also considered, these parameters are variable and help determine the lump-masses height relative to the ground height (y_0). F_{a} is the aerodynamical force, this force normally is not present when considering the pantograph lump-mass model, however this model considers it. F_{s} is the uplift force, this force is applied at the base of the pantograph, this means that in the lump-mass model it will be applied in the lower mass. The uplift force is used to regulate the contact force $F_{\mathrm{c}}(t)$ parameters, like the mean contact force, its amplitude, and standard deviation The contact force $F_{\mathrm{c}}(t)$ is applied to the contact strips of the pantograph, in the lump-mass model this force is applied to the top mass or masses and has to be evaluated every time step. In the case where two different top masses are considered, the contact forces applied are independent of one another.

Since the catenary is modelled with a finite element model the catenary equations are written in a matrix form. So to be able to use the pantograph model in the same code, or in a similar finite element code, the equations (2.7) to (2.12) need to be rewritten as a vector matrix represented in equation (2.13).

$$\boldsymbol{M_{pant}a} + \boldsymbol{C_{pant}v} + \boldsymbol{K_{pant}d} = \boldsymbol{f_{pant}} \tag{2.13}$$

Where the parameter $\boldsymbol{M_{pant}}$, $\boldsymbol{C_{pant}}$, $\boldsymbol{K_{pant}}$ and $\boldsymbol{F_{pant}}$ can be expressed by:

$$\boldsymbol{M_{pant}} = \begin{bmatrix} m_4 & 0 & 0 & 0 \\ 0 & m_3 & 0 & 0 \\ 0 & 0 & m_2 & 0 \\ 0 & 0 & 0 & m_1 \end{bmatrix} \tag{2.14}$$

$$\boldsymbol{C_{pant}} = \begin{bmatrix} C_4 & 0 & -C_4 & 0 \\ 0 & C_3 & -C_3 & 0 \\ -C_4 & -C_3 & C_4 + C_3 + C_2 & -C_2 \\ 0 & 0 & -C_2 & C_1 + C_2 \end{bmatrix} \tag{2.15}$$

$$\boldsymbol{K_{pant}} = \begin{bmatrix} K_4 & 0 & -K_4 & 0 \\ 0 & K_3 & -K_3 & 0 \\ -K_4 & -K_3 & K_4 + K_3 + K_2 & -K_2 \\ 0 & 0 & -K_2 & K_1 + K_2 \end{bmatrix} \tag{2.16}$$

$$\boldsymbol{f_{pant}} = \begin{bmatrix} -m_4 g + F_{f4}(\Delta v_{24}) - F_{c4}(t) + K_4 l_4 \\ -m_3 g + F_{f3}(\Delta v_{23}) - F_{c3}(t) + K_3 l_3 \\ -m_2 g + F_{f2}(\Delta v_{12}) - F_{f3}(\Delta v_{23}) - F_{f4}(\Delta v_{24}) + F_a + K_2 l_2 - K_3 l_3 - K_4 l_4 \\ -m_1 g + F_{f1}(\Delta v_{01}) - F_{f2}(\Delta v_{12}) + F_s + K_1(l_1 + y_0) - K_2 l_2 \end{bmatrix} \quad (2.17)$$

When a three lump mass is modelled the equation motion constraint equations are different from the one previously mentioned. The Figure 2.8 represents a three lump mass pantograph model.

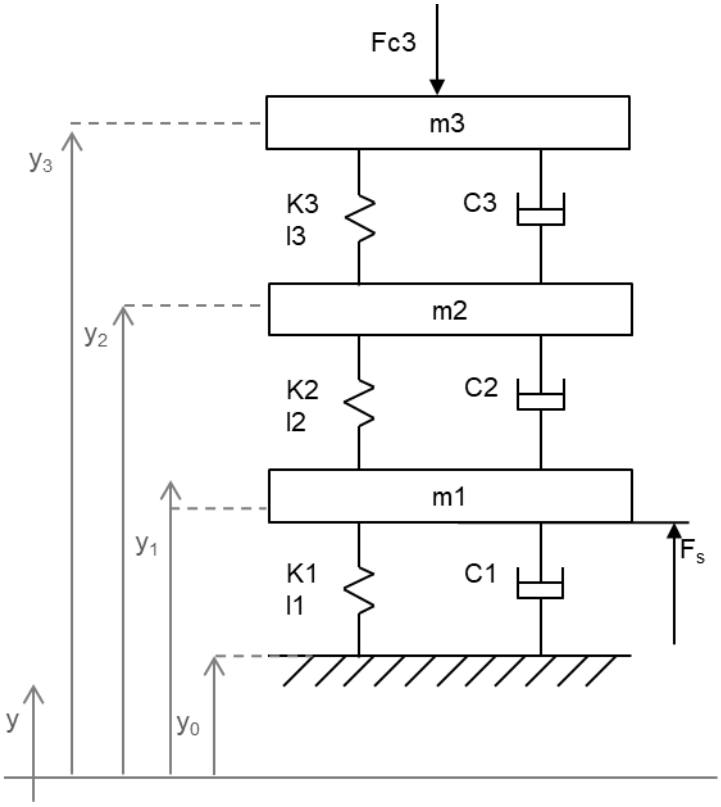

Figure 2.8: Representation of a 3 lump-masses model

For this model, the values of the parameter $\boldsymbol{M_{pant}}$, $\boldsymbol{C_{pant}}$, $\boldsymbol{K_{pant}}$ and $\boldsymbol{F_{pant}}$ that define the equation of motion, equation (2.13), of the lump-mass model represented by Figure 2.8, are defined by:

$$\boldsymbol{M_{pant}} = \begin{bmatrix} m_3 & 0 & 0 \\ 0 & m_2 & 0 \\ 0 & 0 & m_1 \end{bmatrix} \quad (2.18)$$

$$\boldsymbol{C_{pant}} = \begin{bmatrix} C_3 & -C_3 & 0 \\ -C_3 & C_3+C_2 & -C_2 \\ 0 & -C_2 & C_1 + C_2 \end{bmatrix} \quad (2.19)$$

$$\boldsymbol{K_{pant}} = \begin{bmatrix} K_3 & -K_3 & 0 \\ -K_3 & K_3+K_2 & -K_2 \\ 0 & -K_2 & K_1 + K_2 \end{bmatrix} \quad (2.20)$$

$$\boldsymbol{f_{pant}} = \begin{bmatrix} -m_3 g - F_{c3}(t) + K_3 l_3 \\ -m_2 g + K_2 l_2 - K_3 l_3 \\ -m_1 g + F_s + K_1(l_1 + y_0) - K_2 l_2 \end{bmatrix} \tag{2.21}$$

2.3 Catenary Pantograph Interaction

In a railway system, the contact pantograph-catenary is due to the interaction between the pantograph contact strip and the catenary contact wire. This contact allows the flow of energy necessary for the train operation. However, it is also the technological limit for the velocity operations of existing electric railways. A proper contact between the pantograph and the catenary must be kept ensuring the reliability of the train operation as well as its efficiency. A contact loss can create arcing which in its turn leads to higher localized wear on the pantograph contact strip, lowering its overall reliability. In contrast, when the contact force of the system is too high the potential of loss of contact is reduced, but the wear of the contact strip increases. Therefore, the contact force needs to be maintained within specific limits, in order to not only avoid loss of contact but also to prevent high wear.

The pantograph-catenary contact is represented in Figure 2.9 (a). The contact wire, whose cross-section is represented by Figure 2.9 (b), has a cylindrical section made of a copper alloy, while the contact strip has a flat surface of contact, made of carbon, as shown its cross-section in Figure 2.9 (c). A penalty formulation of the contact force , which involves the geometry and materials properties of the contact wire and contact strip, is used in this work [35] This procedure defines the contact force as a function of the interference between the two surfaces.

(a) (b) (c)

Figure 2.9: Pantograph-catenary contact: (a) pantograph bow and contact wire; (b) contact wire cross-section; (c) contact strip cross section

The solution of the contact problem is divided into three different steps that must be solved in each time step for each contact strip. The first step consists of identifying a particular finite element of the contact wire in which contact may be occurring. In this step the position of the points of the contact from a previous iteration is considered as the candidate for the new location of the contact point. Then, the correct location of the potential points of contact of the contact wire and contact strip is found iteratively. Finally, in the third step, the relative penetration, or separation, between the contacting surfaces is obtained being checked if contact between the elements considered exists. The relative penetration between contact wire and strip is

$$\delta = (z_{pant} + r_{pant}) - (z_{cat} - r_{cat}) \quad (2.22)$$

Where (2.22), z_{pant} and z_{cat} represent the z position coordinate of the potential points of the pantograph and the catenary respectively, and r_{pant} and r_{cat} represent the specific radius of the contact wire and contact strip. For a positive relative penetration value, the contact exists, while negative and null values represent a separation between surfaces and, therefore, a non-contact situation.

2.4 Maximum operation velocity in a catenary

To find the exploration velocity that a railway vehicle can travel, it is necessary to know the catenary and the pantograph that are in operation. Different catenary pantograph pairs leads to different operating conditions and, consequently, are subjected to different velocities of exploration. In order to identify the exploration velocity in a particular catenary several quantities associated to the contact force must be measured and verified for compliance.

The contact between the catenary and the pantograph is enforced by an uplift force f_{up}, applied to the mass m_1 of the lump mass pantograph model. This force is constant throughout the operation and needs to be calculated, in such a way that the mean contact force, F_m, between the pantograph and the catenary follows the standards EN50367. The standard EN50367 specifies that the F_m must be inside the interval defined by two predefined values designated by minimum mean contact force $F_{m,min}$ and the maximum mean contact force $F_{m,max}$. Only when the mean contact force has a value between the $F_{m,min}$ and $F_{m,max}$ can the quality of the contact be analysed. The contact quality is evaluated by a series of statistical measures of the contact force, F_c, resulting from the interaction pantograph-catenary. This F_c is first filtered with a cut-of frequency of 20Hz as specified by the norms. The norms also stipulate a series of parameters that the F_c and their statistical measures must verify for an acceptable operation velocity by the norm EN50367. These limit parameters can be observed in Table 2.1. When one of these parameters, exceeds the threshold, the railway vehicle is prevented to operate at that speed. If the F_m fails to be between its limits, the uplift force of the simulation must be adjusted until, F_m is inside the boundaries, only then can the other parameters be analysed. For a more conservative analysis, F_m must be as close to the maximum mean contact force as possible.

Table 2.1: Contact quality validation parameters according to EN50367

	v ≤ 200 km/h	200 km/h < v ≤ 250 km/h	v > 250 km/h
$F_{m,min}$ [N]	$0.00047v^2+60$		
$F_{m,max}$ [N]	$0.00047v^2+90$	$0.00097v^2+70$	
$F_{c,max}$ [N]	300	350	
σ_{max} [N]	≤ 0.3 F_m		
Statistical minimum [N]	> 0		
Steady arm uplift [mm]	≤ 120		
Contact loss [%]	≤ 0.1		≤ 0.2

The parameters stipulated by the norms and presented in Table 2.1 are the mean contact force F_m, maximum contact force F_{max}, as well as the statistical measures of the contact force defined by the

standard deviation, σ, the statistical minimum, S_{min}, and the contact loss percentage $CL_{\%}$. A negative value of S_{min} implies a possibility of contact loss, being calculated by

$$S_{min} = F_m - 3\sigma \quad N \tag{2.23}$$

These statistical values are obtained by the assumption in a realistic situation the contact force behaves like a normal distribution [36].It must be noted that currently it is being questioned if the statistical measures of the contact performance should be updated and even if new measures should be included in the norm, but with no result so far.

3 Subsystem modelling

The objective of this work consists of evaluating the limits of the operation condition of two different catenaries operating with two types of pantographs that equip the railway vehicle in exploration. In this study, both catenaries are modelled with multiple sections and, therefore, with overlapping sections, on a straight track scenario. Since the railway operators emphasize the interoperability of the systems, both catenaries are studied with the two different pantographs models, which represent the type of pantographs in operation. The simulation considers the pairing of each pantograph with each of the catenaries. Each system is simulated with a single and multiple pantograph operations for a broad range of vehicle velocities. For the multiple pantograph operations considered each simulation scenario involves a different pantograph separations. The distance between these two pantographs considered in this work are 35 m, 85 m, 100 m, and 200 m, which corresponds to common pantograph locations in the train operations with multiple units.

3.1 Pantograph Models

Two generic pantographs are modelled in this work and designated Pant1 pantograph and Pant2 pantograph. These pantographs are modelled via lump-mass models. The car height for both pantographs is assumed to be 4 m i.e., it is assumed that they are mounted on the roof of the railway vehicle. Figure 3.1 represents the Pant1 pantograph lump-mass being its modelling parameters shown also.

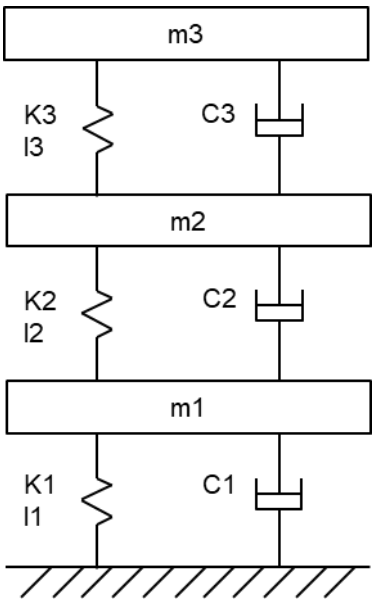

Parameter	Value	Unit
M_1	4.5	KG
M_2	6.27	KG
M_3	4.27	KG
C_1	54.1	Ns/m
C_2	0	Ns/m
C_3	30	Ns/m
K_1	1	N/m
K_2	8000	N/m
K_3	7000	N/m

Figure 3.1: Pant1 pantograph lump-mass model and parameters

The Pant2 pantograph model shown in Figure 3.2 has an unusual topology. Since contrary to the previous, it includes four masse, friction forces, nonlinear springs, and a bump-stop between m_3 and m_4. The friction forces are not represented in the table included in Figure 3.2, since these forces are

dependent on the difference of velocities between the adjacent masses, or between m_1 and the ground, which is the railway vehicle roof.

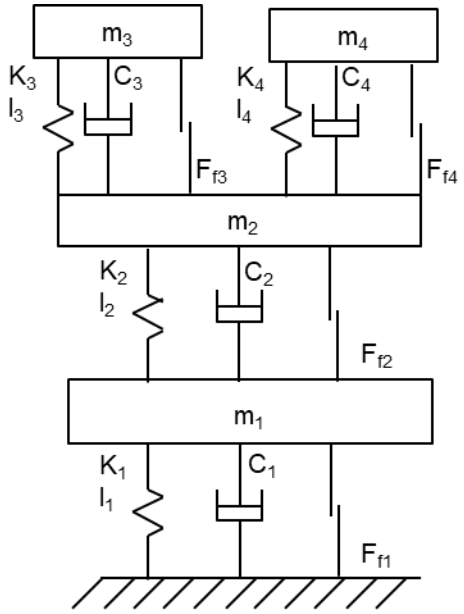

Parameter	Value	Unit
M_1	10.15	KG
M_2	10.45	KG
M_3	2.88	KG
M_4	2.88	KG
C_1	60	Ns/m
C_2	0	Ns/m
C_3	0	Ns/m
C_4	0	Ns/m
K_1	80	N/m
K_2	13500	N/m
K_3	k(s)	N/m
K_4	k(s)	N/m

Figure 3.2: Pant2 pantograph lump mass model and parameters

The Pant2 pantograph lump-mass model has two equal nonlinear springs, each of them is supporting one mass. The variation of the spring length is given as

$$s_i = \left|L_i^0 - L_i\right| \tag{3.1}$$

Where L_i^0 represents the undeformed length of the spring and L_i represents the length of the spring in the current time step. This pantograph model has a bump-stop spring that limits the compression of K_3 and K_4. This means that both of these springs cannot have a length deformation larger than 52mm. In this model, the bump-stop is represented using a spring with a large rigidity that starts acting when the s_i value surpasses 52 mm. The nonlinear upper mass suspension spring stiffness is given as

$$k_i(s) = \begin{cases} 2200, & if \quad 0 \le s_i < 10\,mm \\ 2500, & if\ 10 \le s_i < 20\,mm \\ 3050, & if\ 20 \le s_i < 30\,mm \\ 3650, & if\ 30 \le s_i < 40\,mm \\ 4600, & if\ 40 \le s_i < 52\,mm \\ 10^6, & if\ s_i \ge 52\ mm \end{cases} \tag{3.2}$$

3.2 Catenary Models

The catenaries modelled are designated by LP10 and LP12. These catenaries include various sections, each one with maximum length of 1431 m. The catenary sections include four different types of spans, each of them characterized in Table 3.1 and Table 3.2.

For the modelling of the catenaries include geometric and material parameters. For the LP10 catenary,. the geometry and materials are represented in Table 3.1. Table 3.2 presents the parameters requires for the modelling of the catenary LP12.

Table 3.1: LP10 modelling parameter

Catenary length [m]		1431	Contact wire height [m]	5.5
Number of spans		26	Nº Droppers/Span	Table 3.6
Nº Spans at nominal height [m]		26	Inter-dropper distance [m]	Table 3.6
Span length [m]*		49.5 - 63	Stagger [m]	+/- 0.200
Wave propagation speed [km/h]		369	Maximum velocity [km/h]	258
	Contact wire	Messenger wire	Droppers	Steady arm
Section [m^2]	$1.07x10^{-4}$	$6.50x10^{-5}$	$1.20x10^{-5}$	$2.16x10^{-4}$
Linear Mass [kg/m]	0.951	0.59	0.11	0.572
Young Modulos [Pa]	$1.2x10^{11}$	$8.5x10^{10}$	$8.500x10^{10}$	$7.0x10^{10}$
Tension [N]	10000	10000	-	-
Claw/Clamp mass [kg]	0.175	0.175	-	0.55
Length [m]	-	-	Table 3.6	1.168
Mass [kg]	-	-	-	0.600

One of the most important differences between the catenaries used in this work is the axial tension applied to the contact wire and messenger wire, which has higher values for LP12. Since both catenaries have the same contact wire linear mass, this allows a higher wave propagation velocity in the LP12 catenary, which leads to the possibility of higher exploration velocities.

Table 3.2: LP12 modelling parameters

Catenary length [m]		1431	Contact wire height [m]	5.5
Number of spans		26	Nº Droppers/Span	Table 3.7
Nº Spans at nominal height [m]		26	Inter-dropper distance [m]	Table 3.7
Span length [m]*		49.5 - 63	Stagger [m]	+/- 0.200
Wave propagation speed [km/h]		404	Maximum velocity [km/h]	283
	Contact wire	Messenger wire	Droppers	Steady arm
Section [m^2]	$1.07x10^{-4}$	$6.50x10^{-5}$	$1.20x10^{-5}$	$2.16x10^{-4}$
Linear Mass [kg/m]	0.951	0.59	0.11	0.572
Young Modulos [Pa]	$1.2x10^{11}$	$8.5x10^{10}$	$8.5x10^{10}$	$7.0x10^{10}$
Tension [N]	12000	12000	-	-
Claw/Clamp mass [kg]	0.175	0.175	-	0.55
Length [m]	-	-	Table 3.7	1.168
Mass [kg]	-	-	-	0.600

Both catenaries have the same section length 1431 m, as well as the number of spans 26. The catenary models have symmetric catenary sections i.e., the catenary spans mirror the existing spans in terms of geometry and structure. The catenaries have various types of span, being their lengths and order of appearance in the catenary described in Table 3.3.

Table 3.3: Length of the catenary spans

Span number	1	2	3	4	5	6	7	8	9	10	11	12	13
Span lenght [m]	49.5	49.5	49.5	49.5	54	54	54	54	58.5	58.5	58.5	63	63
Span number	14	15	16	17	18	19	20	21	22	23	24	25	26
Span lenght [m]	63	63	58.5	58.5	58.5	54	54	54	54.0	49.5	49.5	49.5	49.5

The initial value of the dropper length differs for each catenary, due to the difference of initial sag that both catenaries have. Figure 3.3 represents the sag of a catenary, that is given by a value, between 0‰ and 1‰ of the span Length. The initial sag being 1‰, means that the maximum sag of the span under study is 1‰ of the length of the respective span. In order to obtain the initial sag on each dropper it is considered that the initial and final dropper has an initial sag of 0 mm. Then, the parabolic equation containing these three points is determined, which allows the calculation of the initial sag of the other droppers.

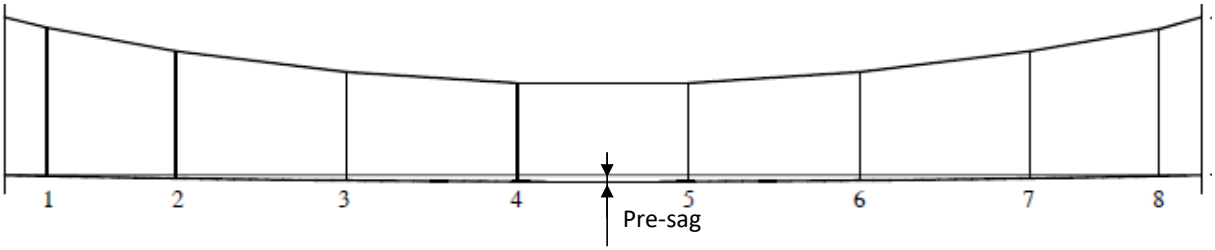

Figure 3.3: Generic representation of the pre-sag in a span

The dropper numeration in Table 3.4 and Table 3.5 is the same used by Figure 3.3. These tables present the droppers position for each span type, as well as each dropper length for the LP10 and LP12 catenary respectively.

The catenaries have a different initial sag value, being LP10 the catenary where the initial sag is 0‰, and LP12 the catenary where the initial sag is 1‰. The size of the pre-sag has an impact on the initial length of the droppers to consider. Table 3.5 indicates the position, length, and initial sag of each dropper according to the span length for the LP12 catenary.

When comparing Table 3.4 to Table 3.5 it can be observed that the difference in the length of the droppers between the catenaries. LP12 leads to higher initial dropper length, for the catenary with initial sag.

Table 3.4: Dropper and pre-sag initial geometric parameters of the LP10 catenary

Span lenght [m]	Dropper	Dropper nº							
		1	2	3	4	5	6	7	8
63	Position [m]	2.25	9.00	18.00	27.00	36.00	45.00	54.00	60.75
	Lenght [m]	1.288	1.011	0.755	0.627	0.627	0.755	1.011	1.288
	Pre-sag [mm]	0	0	0	0	0	0	0	0
58.5	Position [m]	2.25	9.00	15.75	24.75	33.75	42.75	49.50	56.25
	Lenght [m]	1.296	1.042	0.862	0.734	0.734	0.862	1.043	1.296
	Pre-sag [mm]	0	0	0	0	0	0	0	0
54	Position [m]	2.250	9.000	18.000	27.000	36.000	45.000	51.750	
	Lenght [m]	1.304	1.075	0.883	0.819	0.883	1.076	1.304	
	Pre-sag [mm]	0	0	0	0	0	0	0	
49.5	Position [m]	2.25	9.00	15.75	24.75	33.75	40.50	47.25	
	Lenght [m]	1.312	1.107	0.974	0.910	0.974	1.107	1.312	
	Pre-sag [mm]	0	0	0	0	0	0	0	

Table 3.5: Dropper and pre-sag initial geometric parameters of the LP12 catenary

Span lenght [m]	Dropper	Dropper nº							
		1	2	3	4	5	6	7	8
63	Position [m]	2.25	9.00	18.00	27.00	36.00	45.00	54.00	60.75
	Lenght [m]	1.307	1.127	0.961	0.878	0.878	0.961	1.127	1.307
	Pre-sag [mm]	0	2.572	4.958	6.151	6.151	4.958	2.572	0
58.5	Position [m]	2.25	9.00	15.75	24.75	33.75	42.75	49.50	56.25
	Lenght [m]	1.314	1.153	1.039	0.958	0.958	1.039	1.153	1.314
	Pre-sag [mm]	0	2.559	4.388	5.688	5.688	4.388	2.559	0
54	Position [m]	2.25	9.00	18.00	27.00	36.00	45.00	51.75	
	Lenght [m]	1.320	1.180	1.063	1.024	1.063	1.180	1.320	
	Pre-sag [mm]	0	2.544	4.686	5.400	4.686	2.544	0	
49.5	Position [m]	2.25	9.00	15.75	24.75	33.75	40.50	47.25	
	Lenght [m]	1.327	1.206	1.128	1.090	1.128	1.206	1.327	
	Pre-sag [mm]	0	2.525	4.158	4.950	4.158	2.525	0	

The existence of overlapping spans in the catenaries is extremely important, because it permits the railway tracks to be longer. However, they result in contact singularities. The overlapping, when badly modelled leads to bigger displacements of the pantograph head which in turn augments the possibilities for contact loss. Since the overlapping includes a zone where the pantograph enters in contact with two different catenaries sections the contact force in this zone is higher, eventually forcing the reduction of the exploration velocity of the catenary. The model for the overlapping sections include 4 spans where both sections will coexist side by side. The middle spans has the same nominal contact wire height in both catenary sections. However, at adjacent posts, one of the contact wires is elevated by 0.5 m, while at the last support of each section the contact wires is elevated by 1 m. At the overlapping

zone, the stagger is also modified, since there are two sections side by side. Figure 3.4 represents how the top view of the overlapping looks like.

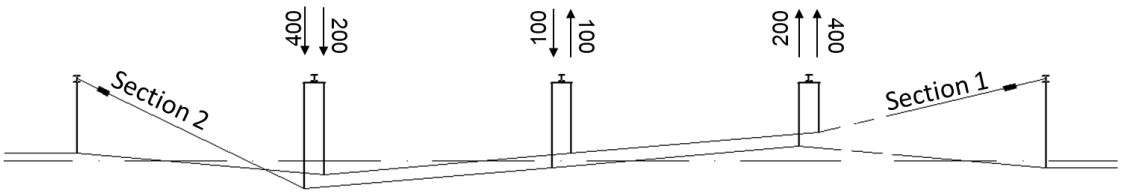

Figure 3.4: Catenary sections overlapping top view representation

Figure 3.5 (c) represents the top view, Figure 3.5 (b) lateral view of the catenary meshes by using the data in Table 3.1, Table 3.3, and Table 3.4 are shown. The static deformation of the LP10 catenary is accounted for being the general view presented, while Figure 3.6 (a), of the static deformed mesh of LP10. In Figure 3.5 (b) is visible the different span lengths, since the overall dropper length decreases with the span length increase.

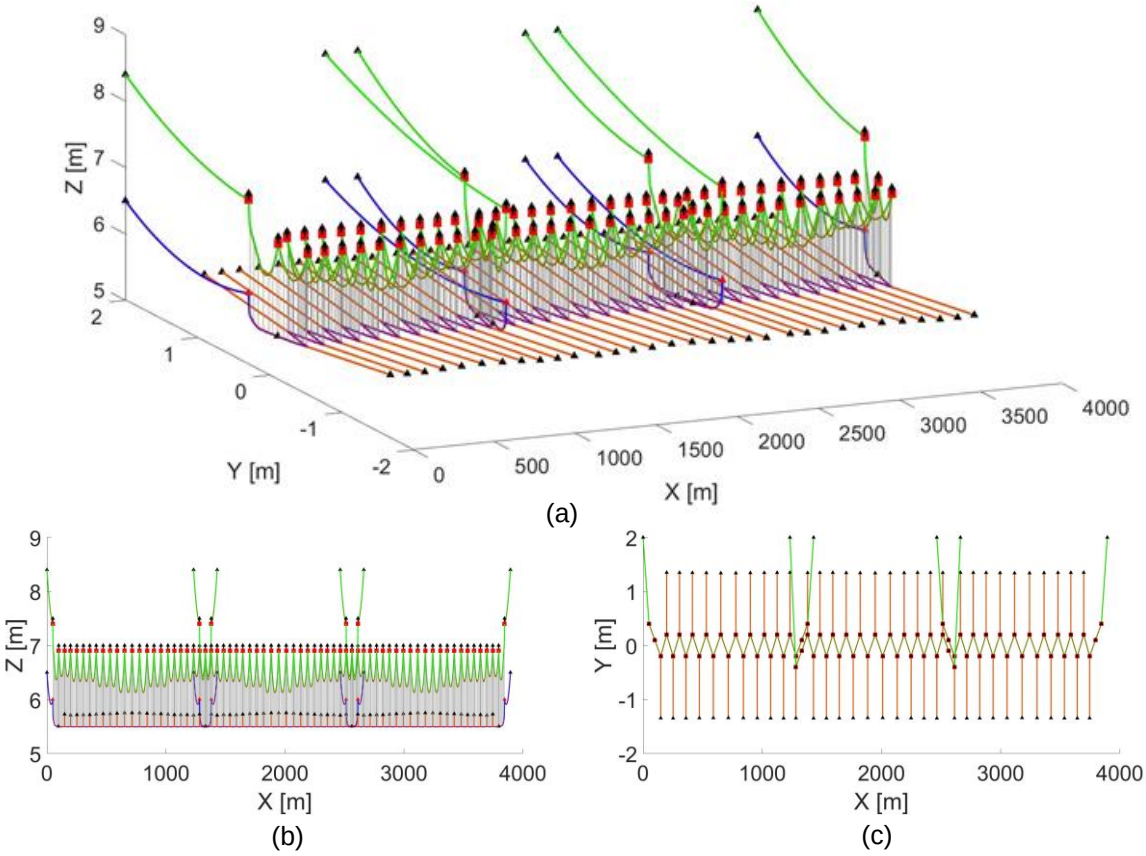

Figure 3.5: Finite element mesh LP10 catenary the static deformation (a) general view (b) lateral view (c) top view

Figure 3.6 (c) represents the top view, Figure 3.6 (b) lateral view of the catenary meshes by using the data in Table 3.2, Table 3.3, and Table 3.5 are shown. The static deformation of the LP12

catenary is accounted for being the general view presented, while Figure 3.6 (a), of the static deformed mesh of LP10. In Figure 3.6 (b) is visible the different span lengths, since the overall dropper length decreases with the span length increase, in this figure the pre-sag is also visible.

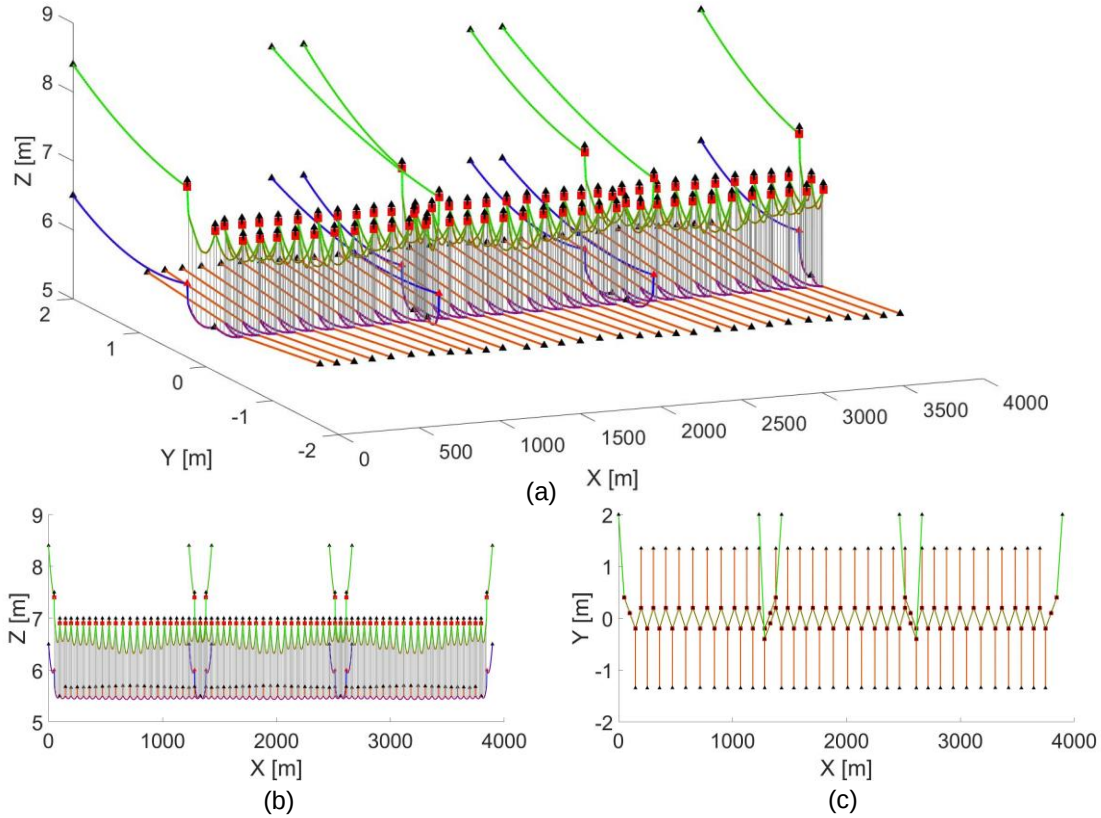

Figure 3.6: Finite element mesh LP12 catenary the static deformation (a) general view (b) lateral view (c) top view

4 Dynamic Analysis of Pantograph Catenary Interaction

The objective of this work is to determine the operational conditions of two different catenary models, LP10 and LP12, in interaction with two different pantographs, Pant1 and Pant2. In this sense, five different case scenarios are here considered, for each different pantograph-catenary pair. One scenario consists in the study of the pantograph-catenary interaction when there is a single operating pantograph, while the other four scenarios consider catenary operations with multiple pantographs. Moreover, at each of these case scenarios, the evaluation of the pantograph-catenary behaviour is analysed at different speeds and pantographs separations.

The zone of interest considered starts at 900m and ends at 1705m, for both catenaries One of the reasons why the zone of interest is here is the existence of the overlapping near the middle of this zone. Another reason for this choice is the ability to study the contact parameter for many span lengths. Figure 4.1 and Figure 4.2 represent the FEM mesh, taking the static deformation into account, of the zone of interest of the LP10 and LP12 catenaries, respectively.

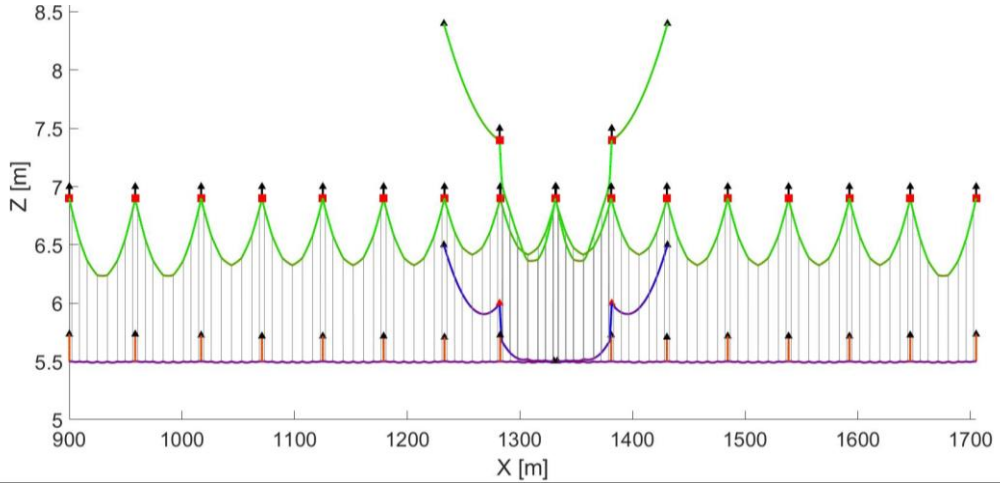

Figure 4.1: Lateral view of the static deformed FEM of the zone of interest of LP10

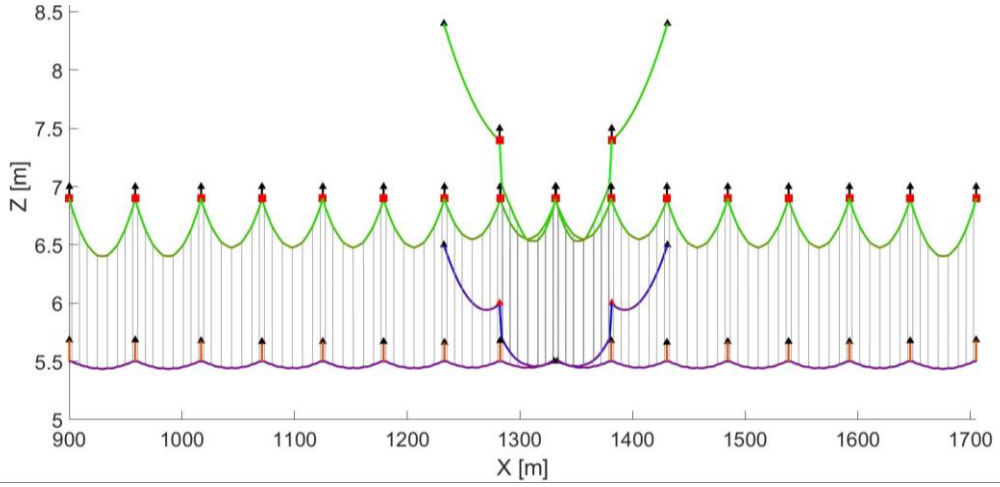

Figure 4.2: Lateral view of the static deformed FEM of the zone of interest of LP12

All dynamic analyses performed are analysed considered the contact quality parameters detailed in chapter 2.4 as well as its corresponding thresholds. These are required to be respected in order to find the catenary-pantograph operating conditions at which these systems are allowed to operate. Table 4.1 summarizes these parameters. In addition to these, three other parameters related to the statistical analysis of contact forces are employed to evaluate each dynamic analysis. These are the minimum contact force, the statistical maximum and minimum. Note that the minimum contact force, F_{min}, result is one of the other important parameters of the contact force F_c. The minimum contact force is a positive or null value, never being negative. Having this force as a null value it means that there is an occurrence of contact loss, CL. The occurrence of negative minimum contact forces are numerical artefacts that result from the filtering process, they do not have any physical meaning and their real value is 0 N. The contact force statistical maximum and statistical minimum do not set directly any operational threshold for operation. However, these statistical parameters help to take into consideration the probability of a contact loss occurring or a high contact force

Table 4.1: Contact quality validation parameters

	v ≤ 200 km/h	200 km/h < v ≤ 250 km/h	v > 250 km/h
$F_{m,min}$ [N]	$0.00047v^2+60$		
$F_{m,max}$ [N]	$0.00047v^2+90$	$0.00097v^2+70$	
$F_{c,max}$ [N]	300	350	
σ_{max} [N]	≤ 0.3 F_m		
Statistical minimum [N]	> 0		
Steady arm uplift [mm]	≤ 120		
Contact loss [%]	≤ 0.1		≤ 0.2

For ease of reference, each of the full set of pantograph-catenary analyses performed in this work is identified following the designation "**Cat_Pant**_S**XXX**_V**YYY**", where **Cat** refers the corresponding evaluated catenary model. **Pant** refers to the type of pantograph used. **XXX** is the value of the pantograph separation, in meters and **YYY** is the train speed, in km/h.

4.1 Single Pantograph

Taking only into consideration the rated wave propagation speed rated for a catenary system, as described in chapter section 2.1, the maximum operating velocity on a given catenary is 70% of the wave propagation speed. However, this fact excludes the dynamic interaction between the pantograph and the catenary. In this sense many other aspects are required to be taken into account when evaluating the exploration velocity for a given pantograph-catenary pair, such as the dynamic response of the pantograph, the catenary system design characteristics and the interaction between both.

4.1.1 LP10 dynamic analysis

The dynamic analysis results obtained of the interaction of the LP10 catenary and the Pant1 pantograph, for various speeds are represented in Table 4.2 and Figure 4.3.

Table 4.2: LP10_Pant1_S0 results for single pantograph, running at various speeds

Speed [km/h]	Pant	Contact Force [N]								Contact loss			Steady Arm Uplift [m]
		F_{max}	F_{min}	ΔF	F_m	σ	σ / F_m	S_{max}	S_{Min}	$CL_{\#}$	CL_t [s]	$CL_{\%}$ [%]	
120	Single	298.5	-10.2	308.7	96.5	14.3	0.15	139.5	53.6	1	0.0	0.03	0.030
125	Single	285.5	-11.2	296.7	97.1	15.2	0.16	142.7	51.6	1	0.0	0.04	0.030
130	Single	280.9	-3.8	284.7	97.7	16.8	0.17	148.2	47.3	1	0.0	0.00	0.030
135	Single	277.0	0.0	277.0	98.3	18.7	0.19	154.5	42.1	0	0.0	0.00	0.030
140	Single	251.0	24.7	226.4	99.0	19.7	0.20	158.3	39.8	0	0.0	0.00	0.033
145	Single	212.1	50.8	161.3	99.6	19.7	0.20	158.6	40.7	0	0.0	0.00	0.035
150	Single	241.4	30.2	211.2	100.5	19.6	0.20	159.4	41.5	0	0.0	0.00	0.039
155	Single	188.4	57.8	130.6	101.0	19.8	0.20	160.5	41.6	0	0.0	0.00	0.043
160	Single	171.1	53.6	117.6	101.9	19.7	0.19	161.0	42.7	0	0.0	0.00	0.048
165	Single	207.1	41.5	165.6	102.5	19.1	0.19	159.8	45.2	0	0.0	0.00	0.059
170	Single	290.3	3.4	286.9	103.3	20.8	0.20	165.8	40.8	0	0.0	0.00	0.052
175	Single	345.8	-17.8	363.7	104.2	23.2	0.22	173.7	34.7	1	0.0	0.07	0.050
180	Single	357.2	-28.3	385.5	105.1	26.1	0.25	183.5	26.8	1	0.0	0.08	0.051

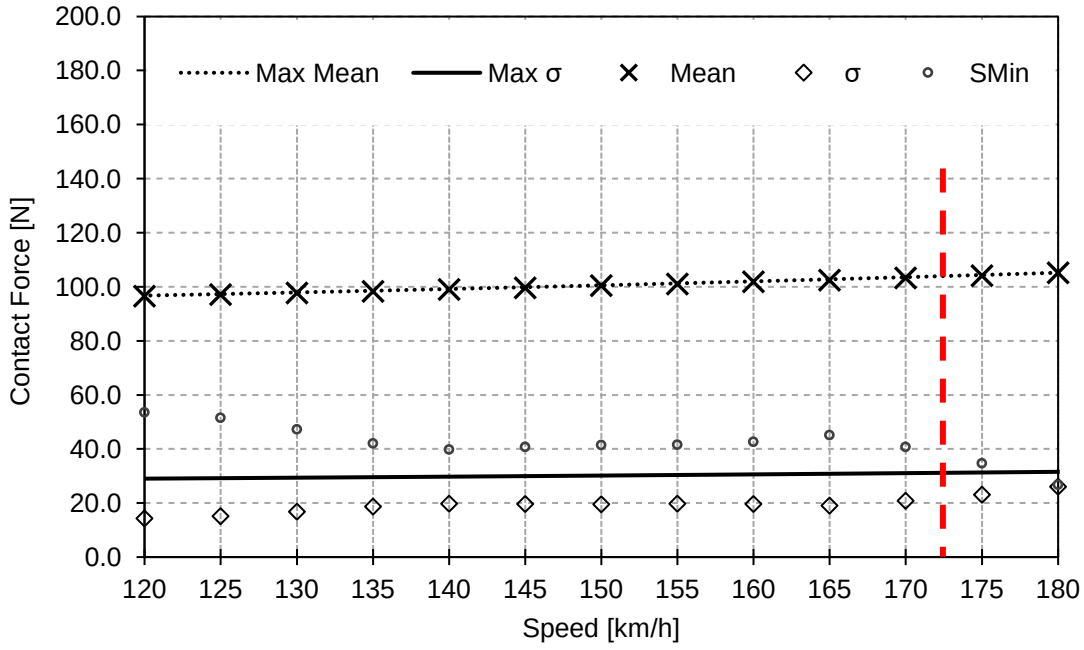

Figure 4.3: LP10_Pant1_S0 results for single pantograph, running at various speeds

Looking at Figure 4.3 all of the contact forces parameters are within their limiting threshold. However, observing Table 4.2 it is possible to observe any contact force parameter that does not respect the limits stipulated in Table 4.1. Table 4.2 has the maximum and minimum forces represented, as well as their amplitude, which allow to conclude that the maximum limit force, of 300 N, is surpassed for 175 km/h. So, the limit operating velocity for this pantograph catenary pairing is 170 km/h. In Table 4.2 the

existence of contact losses is observed for lower velocities. However, these contact losses occur in less than 1% of the simulation, permitting then this train operation speeds. The contact force of the catenary-pantograph interaction at 175 km/h is observed in Figure 4.4.

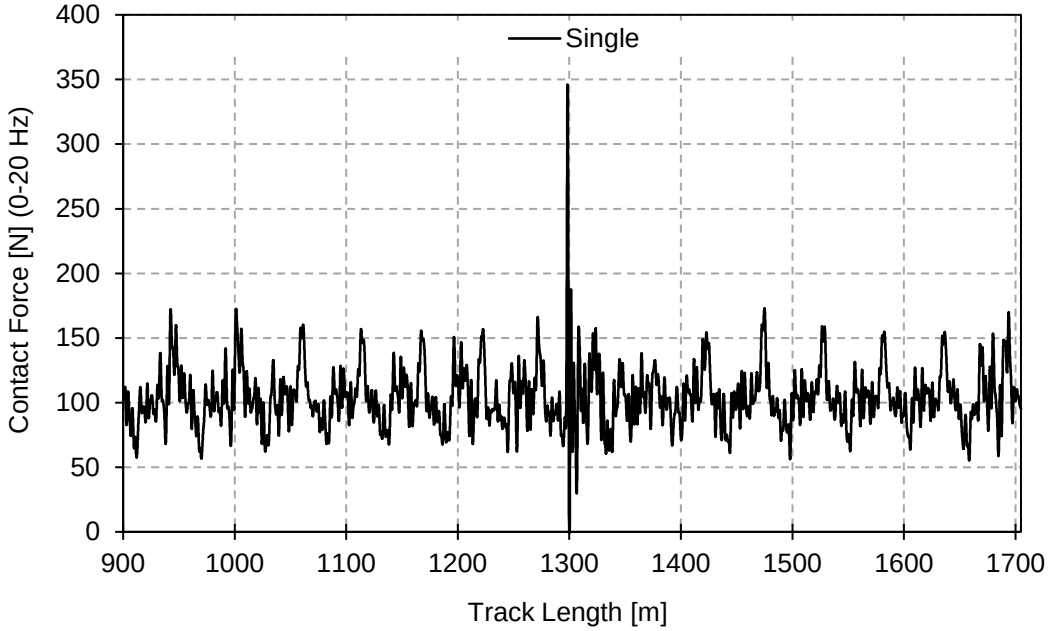

Figure 4.4: Contact forces results for LP10_Pant1_S0_V175

In Figure 4.4 the maximum force observed is located where the two sections overlap. Since this force surpasses the limiting threshold, the limiting factor of this catenary is the overlapping model.

The dynamic analysis results obtained of the interaction of the LP10 catenary and the Pant2 pantograph, for various speeds are represented in Table 4.3 and Figure 4.5.

Table 4.3: LP10_Pant2_S0 results for single pantograph, running at various speeds

Speed [km/h]	Pant	Contact Force [N]								Contact loss			Steady Arm Uplift [m]
		F_{max}	F_{min}	ΔF	F_m	σ	σ / F_m	S_{max}	S_{Min}	$CL_{\#}$	CL_t [s]	$CL_{\%}$ [%]	
120	Single	283.8	-4.7	288.5	96.7	18.7	0.19	152.8	40.6	1	0.0	0.00	0.032
125	Single	247.3	31.5	215.8	97.1	18.7	0.19	153.3	41.0	0	0.0	0.00	0.034
130	Single	290.5	4.2	286.3	97.8	22.8	0.23	166.1	29.4	0	0.0	0.00	0.032
135	Single	246.5	42.4	204.1	98.4	23.5	0.24	168.8	28.1	0	0.0	0.00	0.033
140	Single	212.3	29.8	182.5	99.1	24.9	0.25	173.8	24.5	0	0.0	0.00	0.037
145	Single	181.8	47.4	134.4	99.6	24.0	0.24	171.7	27.6	0	0.0	0.00	0.040
150	Single	217.3	47.2	170.1	100.5	25.7	0.26	177.7	23.3	0	0.0	0.00	0.044
155	Single	178.2	42.3	135.9	101.1	26.2	0.26	179.8	22.4	0	0.0	0.00	0.045
160	Single	181.2	26.8	154.4	102.0	25.2	0.25	177.7	26.3	0	0.0	0.00	0.056
165	Single	248.4	-10.0	258.5	102.4	27.1	0.26	183.7	21.1	1	0.0	0.07	0.061
170	Single	305.6	16.0	289.6	103.1	28.8	0.28	189.7	16.6	0	0.0	0.00	0.055
175	Single	331.3	13.9	317.4	104.2	32.1	0.31	200.5	7.8	0	0.0	0.00	0.055
180	Single	359.1	-10.4	369.5	105.0	37.1	0.35	216.2	-6.3	2	0.0	0.11	0.056

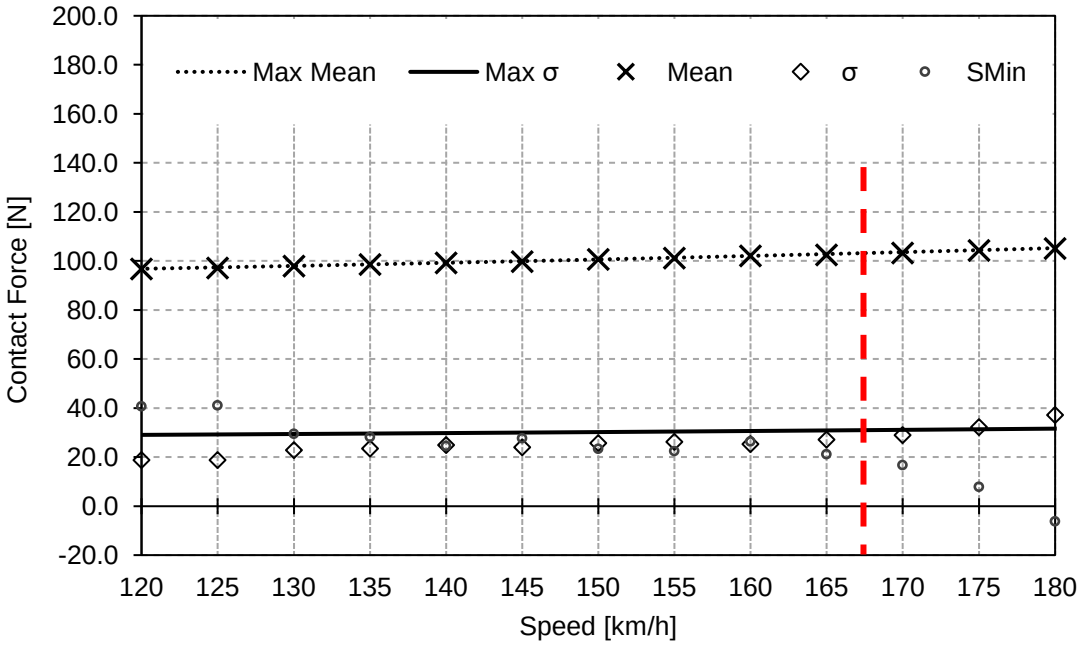

Figure 4.5: LP10_Pant2_S0 results for single pantograph, running at various speeds

Looking at Figure 4.5 all of the contact forces parameters are within their limiting threshold, until the speed reaches 175 km/h, where the standard deviation of the contact force exceeds the maximum threshold. However, observing Table 4.3 it is possible to observe that the maximum force exceeds the 300 N for 170 km/h. Even though there are contact losses for lower speeds than 170 km/h, these contact losses occur for less than the limiting 0.1 %. So, the limit operating velocity for of this catenary pantograph pair is 165 km/h. Figure 4.6 represents the contact force along the track for a speed of 170 km/h.

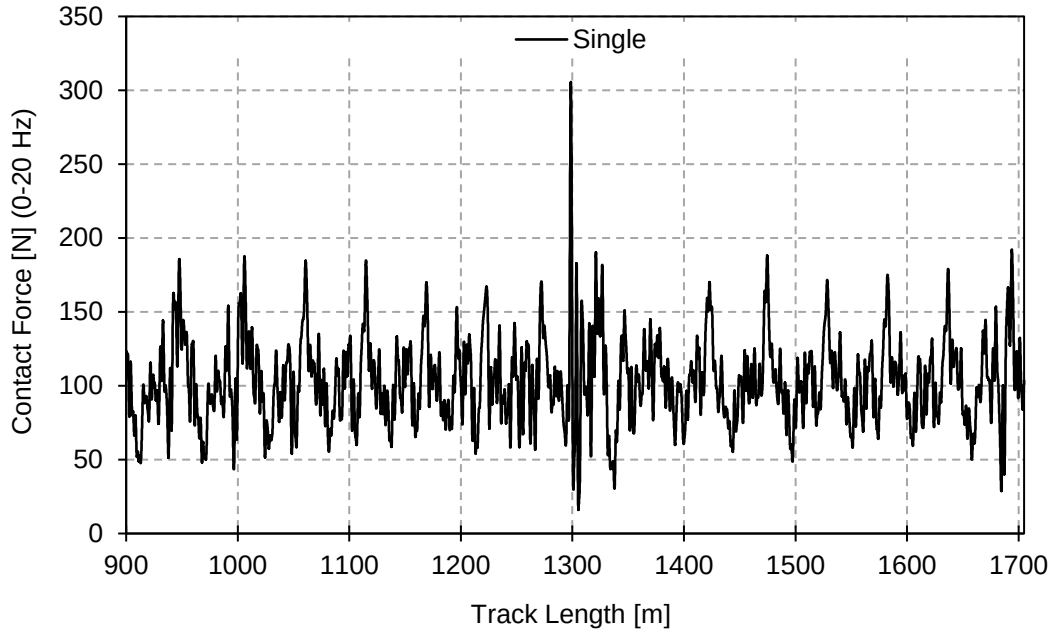

Figure 4.6: Contact forces results for LP10_Pant2_S0_V170

Looking at Figure 4.6, the maximum force is observed to occur where the catenaries sections overlap and nowhere else. So, the limiting factor of this pantograph catenary pairing is the maximum force, derived from the overlapping arrangement.

When comparing the maximum steady arm uplift results at the analysed cases with both used pantographs, Figure 4.7, it is observed that this parameter tends to increase along with the speed and is significantly similar for the different pantographs.

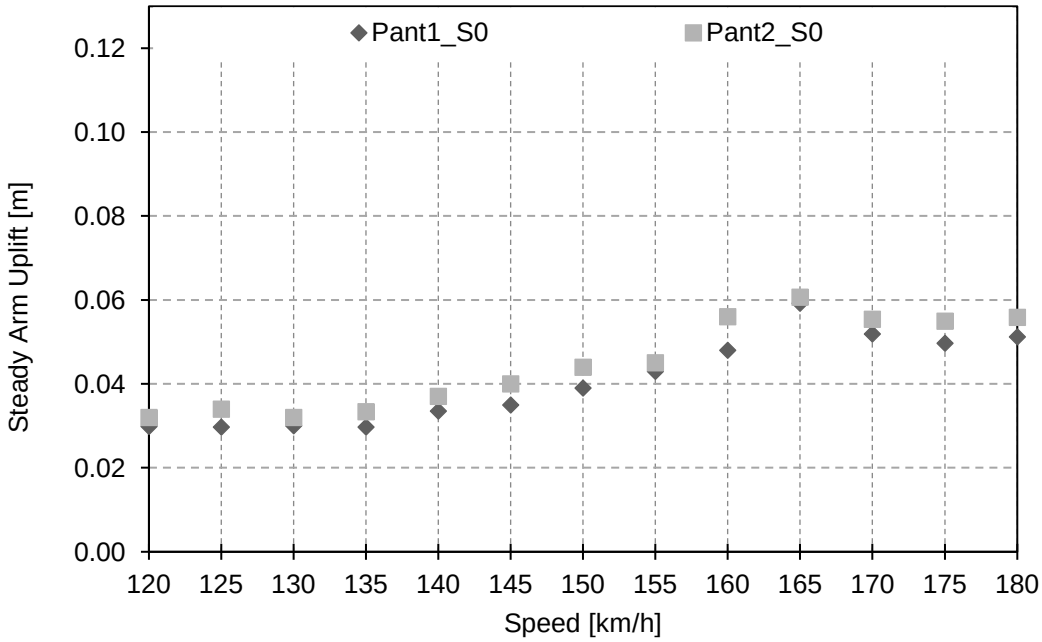

Figure 4.7: Steady arm uplift for LP10 simulated for each pantograph and for various speeds

The maximum steady arm uplift found, of 0.061 m, occurs for the Pant2 pantograph at the velocity of 165 Km/h. Even though this figure represents maximum steady arm uplifts for higher velocities than the exploration velocity, it is possible to conclude that the maximum steady arm does not surpass the limiting threshold for any of the dynamic analysis.

Taking into account 70% of the wave propagating rated for the LP10 catenary system, the maximum permissible train speed on the is 258km/h. Since this velocity does not consider the catenary pantograph interaction having a smaller maximum exploration velocity is to be expected. With the Pant1 pantograph a maximum velocity of 170 km/h was found, and when the pantograph is changed to the Pant2 it will be 165 km/h. This difference of velocities is only 5 km/h when considering a single pantograph. So, the maximum operating velocity for the LP10 catenary is 165 km/h and its limiting factor is the overlapping arrangement, since the only parameter that surpasses its respective limit threshold is the maximum force, that occurs where the two catenary sections overlap.

4.1.2 LP12 dynamic analysis

When the catenary is exchanged, from the LP10 to the LP12 catenary the maximum operating velocity is expected to increase. This is because of the increase of the line tension. The dynamic analysis results obtained of the interaction of the LP12 catenary and the Pant1 pantograph, for various speeds are represented in Table 4.4 and Figure 4.8.

Table 4.4: LP12_Pant1_S0 results for single pantograph, running at various speeds

Speed [km/h]	Pant	Contact Force [N]								Contact loss			Steady Arm Uplift [m]
		F_{max}	F_{min}	ΔF	F_m	σ	σ / F_m	S_{max}	S_{Min}	$CL_{\#}$	CL_t [s]	$CL_{\%}$ [%]	
120	Single	134.0	67.0	67.0	96.6	10.0	0.10	126.7	66.5	0	0.0	0.00	0.019
125	Single	148.6	65.6	83.0	97.2	10.5	0.11	128.8	65.6	0	0.0	0.00	0.018
130	Single	150.5	60.4	90.1	97.8	10.8	0.11	130.3	65.3	0	0.0	0.00	0.018
135	Single	145.8	58.8	87.0	98.4	10.7	0.11	130.5	66.3	0	0.0	0.00	0.018
140	Single	143.7	63.8	80.0	99.1	12.0	0.12	135.2	62.9	0	0.0	0.00	0.017
145	Single	149.4	61.2	88.2	99.7	13.0	0.13	138.5	60.8	0	0.0	0.00	0.015
150	Single	153.7	47.1	106.6	100.5	16.0	0.16	148.6	52.4	0	0.0	0.00	0.017
155	Single	155.5	48.4	107.2	101.1	17.6	0.17	153.8	48.3	0	0.0	0.00	0.019
160	Single	160.9	55.3	105.5	102.0	17.0	0.17	152.9	51.1	0	0.0	0.00	0.019
165	Single	150.8	59.8	91.0	102.7	15.8	0.15	149.9	55.4	0	0.0	0.00	0.020
170	Single	159.4	54.3	105.1	103.5	16.6	0.16	153.3	53.7	0	0.0	0.00	0.022
175	Single	162.0	61.0	101.0	104.3	16.9	0.16	155.2	53.5	0	0.0	0.00	0.027
180	Single	158.5	61.9	96.7	105.1	17.3	0.16	157.0	53.2	0	0.0	0.00	0.027
185	Single	162.3	57.2	105.2	106.0	17.5	0.16	158.4	53.6	0	0.0	0.00	0.027
190	Single	162.4	53.5	108.8	106.8	17.2	0.16	158.3	55.3	0	0.0	0.00	0.029
195	Single	168.2	56.1	112.1	107.7	16.8	0.16	158.2	57.2	0	0.0	0.00	0.033
200	Single	186.8	62.3	124.5	108.7	17.3	0.16	160.7	56.7	0	0.0	0.00	0.031
205	Single	175.6	45.3	130.3	110.7	19.2	0.17	168.4	52.9	0	0.0	0.00	0.028
210	Single	167.2	54.5	112.7	112.7	20.3	0.18	173.6	51.8	0	0.0	0.00	0.031
215	Single	173.2	58.6	114.6	114.8	23.0	0.20	183.9	45.8	0	0.0	0.00	0.035
220	Single	186.9	62.2	124.7	116.9	24.7	0.21	190.9	42.9	0	0.0	0.00	0.041
225	Single	197.5	59.7	137.8	119.0	25.6	0.22	195.9	42.2	0	0.0	0.00	0.047
230	Single	205.7	62.7	143.0	120.9	26.5	0.22	200.6	41.3	0	0.0	0.00	0.050
235	Single	212.7	62.1	150.6	123.4	27.1	0.22	204.8	42.1	0	0.0	0.00	0.060
240	Single	246.5	69.8	176.7	125.7	27.3	0.22	207.6	43.9	0	0.0	0.00	0.060
245	Single	300.2	11.5	288.7	127.9	28.3	0.22	212.7	43.1	0	0.0	0.00	0.063
250	Single	260.2	31.9	228.4	130.3	29.3	0.23	218.3	42.3	0	0.0	0.00	0.063
255	Single	319.9	11.3	308.6	132.9	31.5	0.24	227.3	38.5	0	0.0	0.00	0.068
260	Single	283.9	11.0	272.8	135.3	32.6	0.24	233.1	37.4	0	0.0	0.00	0.072
265	Single	380.1	-38.8	419.0	137.7	36.4	0.26	246.9	28.6	1	0.0	0.15	0.076

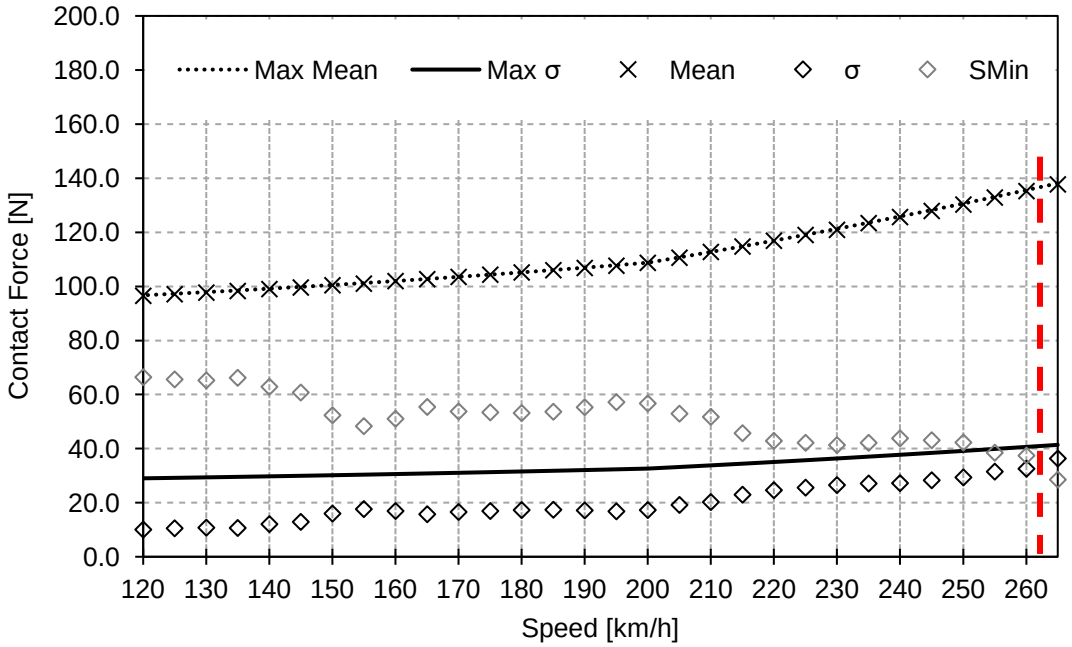

Figure 4.8: LP12_Pant1_S0 results for single pantograph, running at various speeds

Observing Figure 4.8 all of the presented forces parameters can be seen to stay between their respective standard thresholds. With this, there is only two more parameters that can be limiting the exploration velocity, which are the contact loss and the maximum force. Table 4.4 expresses that the maximum force threshold, of 350 N, is surpassed at 265 km/h, and the existence of contact loss that also surpasses its threshold limit for the same velocity. So, the maximum operating velocity for the LP12_Pant1 pairing is 260 km/h, and tits limiting parameters are the contact loss and the maximum force. In Figure 4.9 the contact force, along the track, of the LP12_Pant1_S0_V265 operation is represented.

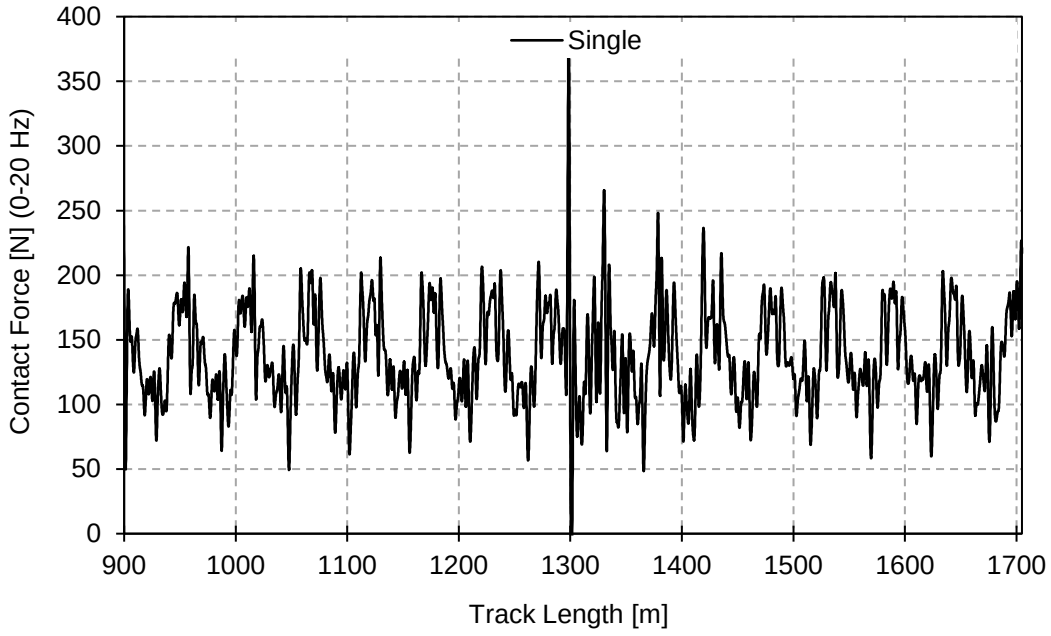

Figure 4.9: Contact forces results for LP12_Pant1_S0_V265

The location of the maximum contact force and the contact loss can be observed in Figure 4.9. Where, the maximum contact force and the contact loss are located in the same place, this place is where the catenary sections overlap. So, the limiting factor of this operation pantograph catenary is the overlapping arrangement.

The pantograph is exchanged, from the Pant1 to the Pant2 pantograph, so the dynamic behaviour also suffers alterations. The dynamic analysis results obtained of the interaction of the LP12 catenary and the Pant2 pantograph, for various speeds are represented in Table 4.5 and Figure 4.10.

Table 4.5: LP12_Pant2_S0 results for single pantograph, running at various speeds

Speed [km/h]	Pant	Contact Force [N]								Contact loss			Steady Arm Uplift [m]
		F_{max}	F_{min}	ΔF	F_m	σ	σ / F_m	S_{max}	S_{Min}	$CL_{\#}$	CL_t [s]	$CL_{\%}$ [%]	
120	Single	156.0	11.3	144.7	96.7	11.5	0.12	131.2	62.2	0	0.0	0.0	0.018
125	Single	175.8	45.1	130.7	97.1	12.3	0.13	133.9	60.4	0	0.0	0.0	0.018
130	Single	168.4	42.6	125.9	97.7	13.2	0.14	137.4	58.0	0	0.0	0.0	0.018
135	Single	160.9	47.3	113.6	98.4	14.0	0.14	140.5	56.4	0	0.0	0.0	0.019
140	Single	167.6	54.5	113.1	99.1	15.5	0.16	145.5	52.8	0	0.0	0.0	0.018
145	Single	159.7	47.8	111.9	99.6	16.4	0.16	149.0	50.3	0	0.0	0.0	0.017
150	Single	184.6	25.5	159.1	100.5	19.6	0.20	159.4	41.6	0	0.0	0.0	0.018
155	Single	167.4	36.5	131.0	101.3	20.9	0.21	163.9	38.6	0	0.0	0.0	0.020
160	Single	166.6	47.3	119.3	102.0	20.0	0.20	162.1	41.9	0	0.0	0.0	0.020
165	Single	163.3	37.7	125.6	102.7	19.3	0.19	160.6	44.7	0	0.0	0.0	0.022
170	Single	164.3	42.8	121.4	103.5	20.4	0.20	164.8	42.2	0	0.0	0.0	0.024
175	Single	168.7	48.3	120.4	104.3	20.7	0.20	166.2	42.3	0	0.0	0.0	0.028
180	Single	176.0	54.7	121.4	105.2	21.2	0.20	168.8	41.5	0	0.0	0.0	0.029
185	Single	169.7	47.2	122.5	105.9	21.1	0.20	169.3	42.5	0	0.0	0.0	0.028
190	Single	163.9	47.4	116.5	106.8	20.5	0.19	168.2	45.5	0	0.0	0.0	0.029
195	Single	183.0	53.3	129.7	107.8	20.2	0.19	168.5	47.1	0	0.0	0.0	0.033
200	Single	193.1	48.5	144.6	108.6	21.9	0.20	174.4	42.8	0	0.0	0.0	0.031
205	Single	181.1	35.3	145.8	110.6	25.2	0.23	186.1	35.0	0	0.0	0.0	0.032
210	Single	187.7	43.8	143.9	112.7	27.9	0.25	196.3	29.1	0	0.0	0.0	0.037
215	Single	204.2	45.8	158.4	114.7	30.6	0.27	206.6	22.9	0	0.0	0.0	0.042
220	Single	208.9	41.2	167.8	116.9	32.7	0.28	214.9	18.9	0	0.0	0.0	0.046
225	Single	210.9	35.6	175.2	118.8	34.3	0.29	221.6	15.9	0	0.0	0.0	0.051
230	Single	238.2	34.3	203.9	121.2	36.2	0.30	229.9	12.4	0	0.0	0.0	0.058
235	Single	247.1	35.4	211.7	123.4	37.4	0.30	235.5	11.2	0	0.0	0.0	0.059
240	Single	287.2	42.9	244.2	125.4	38.6	0.31	241.1	9.7	0	0.0	0.0	0.060
245	Single	294.3	36.1	258.2	127.5	38.9	0.31	244.2	10.8	0	0.0	0.0	0.061
250	Single	492.6	-50.1	542.7	129.1	54.1	0.42	291.3	-33.1	1	0.0	0.2	0.070
255	Single	974.4	-69.7	1044.2	131.6	87.6	0.67	394.4	-131.1	18	0.4	3.1	0.131
260	Single	613.1	-73.2	686.2	134.2	93.7	0.70	415.3	-146.9	34	0.5	4.7	0.102
265	Single	884.8	-83.1	967.9	136.0	98.6	0.73	431.8	-159.8	24	0.4	3.8	0.115

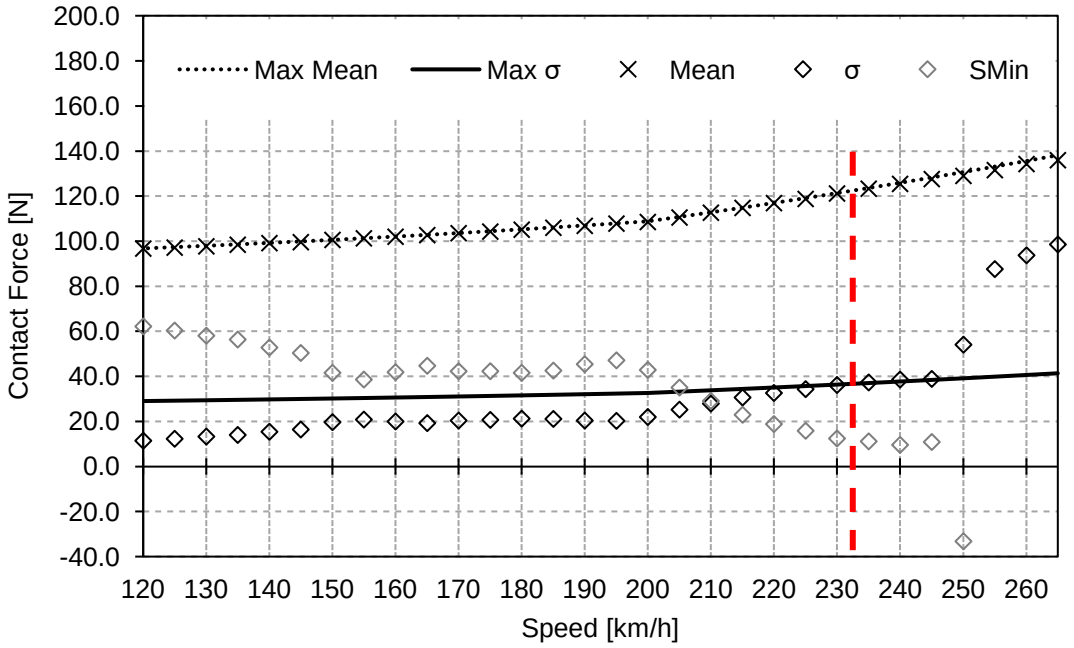

Figure 4.10: LP12_Pant2_S0 results for single pantograph, running at various speeds

Observing Figure 4.10 it is possible to note that the standard deviation surpasses the line of the maximum standard deviation for speeds superior to 230 km/h. Moreover, no other parameter is outside the limits expressed by Table 4.1. From Table 4.5 it is possible to observe that the ratio between the standard deviation and the mean contact force is bigger than 0.3 for 235 km/h, since this parameters at this velocity is in grey. Looking at simulations with inferior speeds then 235 km/h, Table 4.5 shows that no other contact force parameter surpasses the standard threshold. So, the exploration velocity is 230 km/h and the limiting parameter is the standard deviation. In Figure 4.11 the contact force along the track for 235 km/h is observed.

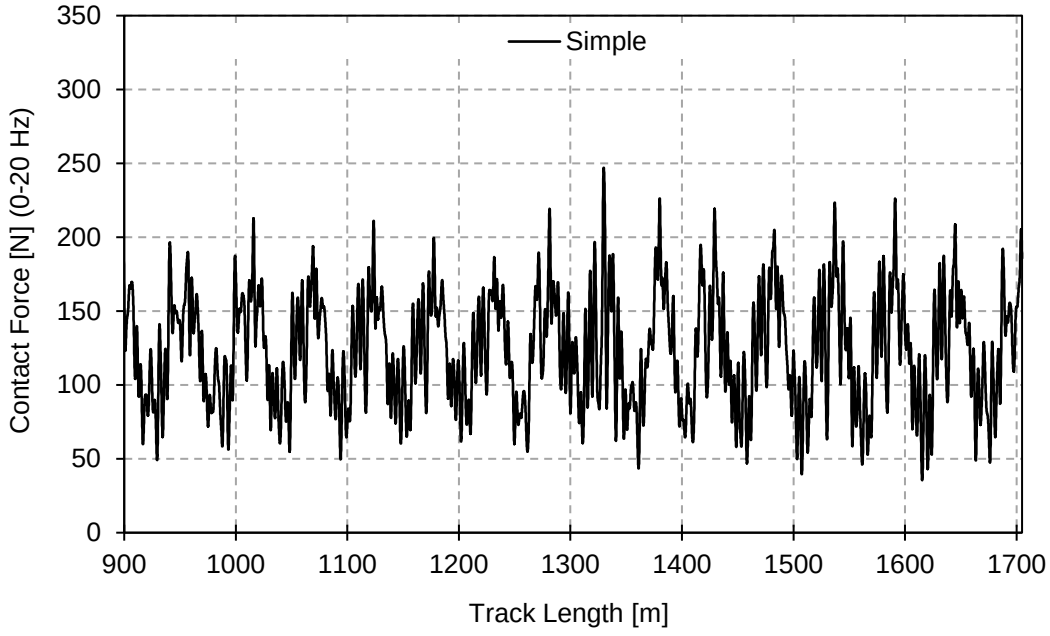

Figure 4.11: Contact forces results for LP12_Pant2_S0_V235

In Figure 4.11 it is possible to observe that when the catenaries sections overlap is where the maximum force occurs, just like it happens for LP12_Pant2_S0_V265. However, in the LP12_Pant2_S0_V235 operation the maximum force does not exceed the threshold limit.

Figure 4.12 represents the maximum steady arm uplift that occurs for LP12 catenary, for each velocity studied and for each pantograph.

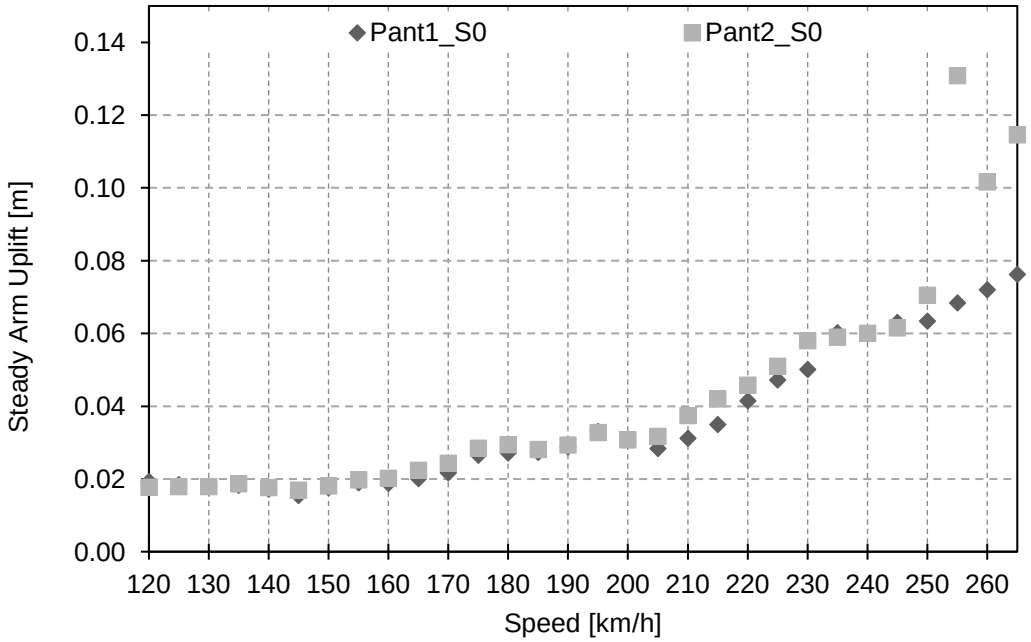

Figure 4.12 Steady arm uplift for LP12 simulated for each pantograph and for various speeds

Comparing the maximum steady arm uplift of both pantographs, as represented in, Figure 4.12, it is observed that this parameter tends to increase along with the speed, and they are significantly similar for the different pantographs until the velocity of 250 km/h is reached. The maximum steady arm uplift occurs for the Pant2 pantograph at the velocity of 255 Km/h, with a value of 0.131 m, as mentioned previously the exploration velocity of LP12_Pant2 pair is 230 km/h. When considering only velocities of exploration permitted by standard the maximum steady arm uplift of LP12 is 0.072 m when the Pant1 pantograph is in operation at 260km/h.

Taking into account 70% of the wave propagating rated for the LP12 catenary system, the maximum permissible train speed on the is 283km/h. Since this velocity does not consider the catenary pantograph interaction having a smaller maximum exploration velocity is to be expected. With the Pant1 pantograph a maximum velocity of 260 km/h was found, and when the pantograph is changed to the Pant2 it will be 230 km/h. This difference of velocities is 30 km/h when considering a single pantograph. So, the maximum operating velocity for the LP12 catenary is 230 km/h and its limiting factor is the standard deviation.

Comparing the two catenaries, it is possible to observe that the LP12 can be used for higher exploration velocities. It is also possible to say that the Pant2 pantograph has a lower exploration velocity than the Pant1 pantograph for both catenaries. It is also possible to observe that difference between the maximum velocity for each catenary with the maximum velocity if the pantograph catenary interaction is not considered is higher for the LP10 catenary. This occurs because the LP10 catenary is limited by the maximum force located in the overlapping section.

4.2 Multiple Pantograph

When studying the operation condition of a railway vehicle on a catenary, the maximum operation speed occurs when only one pantograph is running in the catenary. This is because the elastic propagation wave propagates forward and backward from the pantograph position. When the operation is under multiple pantograph conditions, in this case, two pantographs working simultaneously, both pantographs will generate a propagation wave. Which interferes with the contact characteristics of the catenary with the other pantograph. Normally the trailing pantograph suffers from the wave generated by the leading pantograph. This leads to an effect on the contact parameters of the trailing pantograph. However, for some pantograph separations, the leading pantograph is the one that tends to be affected by the propagation wave of the trailing pantograph. Figure 4.13 represents leading and trailing pantograph according to the travel direction of the train.

Figure 4.13: Multiple pantograph operation

4.2.1 LP10 dynamic analysis

The dynamic analysis results obtained of the interaction of the LP10 catenary and the Pant1 pantograph, considering 2 pantographs, with a separation between them of 35 m, for various speeds are represented in Table 4.6 and Figure 4.14.

Table 4.6: LP10_Pant1_S35 results for multiple pantographs, running at various speeds

Speed [km/h]	Pant	Contact Force [N]								Contact loss			Steady Arm Uplift [m]
		F_{max}	F_{min}	ΔF	F_m	σ	σ/F_m	S_{max}	S_{Min}	$CL_{\#}$	CL_t [s]	$CL_{\%}$ [%]	
120	Leading	262.1	50.1	212.0	96.5	12.0	0.12	132.5	60.5	0	0.0	0.00	0.045
	Trailing	207.1	48.3	158.7	96.5	12.1	0.12	132.7	60.4	0	0.0	0.00	
125	Leading	250.2	58.1	192.2	97.1	12.5	0.13	134.7	59.6	0	0.0	0.00	0.039
	Trailing	179.2	27.5	151.7	97.1	12.3	0.13	133.9	60.3	0	0.0	0.00	
130	Leading	253.8	52.9	200.9	97.7	14.4	0.15	140.9	54.5	0	0.0	0.00	0.040
	Trailing	200.7	34.1	166.6	97.7	13.4	0.14	137.9	57.5	0	0.0	0.00	
135	Leading	268.4	48.8	219.6	98.3	16.3	0.17	147.2	49.5	0	0.0	0.00	0.046
	Trailing	228.3	37.9	190.5	98.3	14.9	0.15	143.1	53.6	0	0.0	0.00	
140	Leading	261.0	13.4	247.6	99.0	19.0	0.19	156.1	42.0	0	0.0	0.00	0.052
	Trailing	188.9	52.3	136.6	99.0	15.4	0.16	145.3	52.8	0	0.0	0.00	
145	Leading	239.0	24.5	214.5	99.6	18.6	0.19	155.4	43.8	0	0.0	0.00	0.059
	Trailing	266.6	9.0	257.6	99.6	18.7	0.19	155.6	43.6	0	0.0	0.00	
150	Leading	224.8	55.0	169.9	100.5	16.4	0.16	149.6	51.3	0	0.0	0.00	0.061
	Trailing	298.7	50.4	248.3	100.4	18.4	0.18	155.5	45.3	0	0.0	0.00	
155	Leading	187.0	64.9	122.2	100.9	15.4	0.15	147.2	54.7	0	0.0	0.00	0.063
	Trailing	198.1	61.1	137.0	100.9	11.9	0.12	136.6	65.3	0	0.0	0.00	
160	Leading	173.7	63.7	110.1	101.8	16.4	0.16	151.1	52.6	0	0.0	0.00	0.066
	Trailing	207.5	53.9	153.6	101.8	12.8	0.13	140.2	63.5	0	0.0	0.00	
…	…	…	…	…	…	…	…	…	…	…	…	…	…

Speed [km/h]	Pant	Contact Force [N]								Contact loss			Steady Arm Uplift [m]
		F_{max}	F_{min}	ΔF	F_m	σ	σ/F_m	S_{max}	S_{Min}	$CL_{\#}$	CL_t [s]	$CL_{\%}$ [%]	
165	Leading	186.2	55.1	131.0	102.5	20.1	0.20	162.9	42.2	0	0.0	0.00	0.063
	Trailing	404.5	-44.2	448.7	102.6	26.8	0.26	183.1	22.1	1	0.0	0.10	
170	Leading	193.2	46.7	146.5	103.3	20.7	0.20	165.5	41.1	0	0.0	0.00	0.068
	Trailing	410.7	-45.8	456.6	103.5	28.3	0.27	188.3	18.6	1	0.0	0.10	
175	Leading	238.3	11.6	226.6	104.2	22.5	0.22	171.8	36.6	0	0.0	0.00	0.071
	Trailing	395.5	-40.2	435.7	104.3	31.0	0.30	197.2	11.3	1	0.0	0.10	
180	Leading	270.9	10.2	260.6	105.1	25.1	0.24	180.4	29.9	0	0.0	0.00	0.068
	Trailing	365.0	-36.5	401.6	105.1	32.7	0.31	203.1	7.2	1	0.0	0.09	

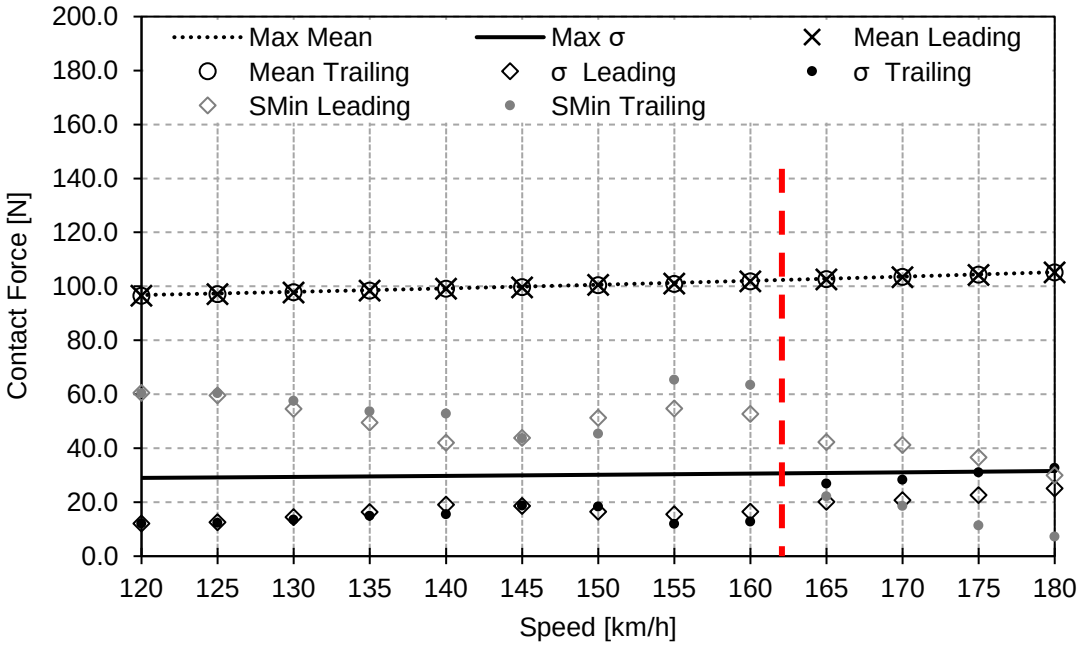

Figure 4.14: LP10_Pant1_S35 results for multiple pantographs operation, running at various speeds and the speed limit for this case

Looking at the dynamic analysis parameters of the LP10_Pant1_S35, presented in Figure 4.14, it is observed that the standard deviation of the trailing pantograph, for 180 km/h is the only value outside their respective thresholds. While Table 4.6 expresses the existence of a maximum forces, of the trailing pantograph, above the 300 N limit. This surpassing of the maximum force limit occurs for operation speeds of 165 km/h and higher. So, the limiting factor for the LP10_Pant1_S35 case is the maximum contact force on the leading pantograph, and the LP10_Pant1_S35 limit exploration velocity is 160 km/h Figure 4.15 represents the contact force along the track, of each pantograph, for the LP10_Pant1_S35_V165 operation.

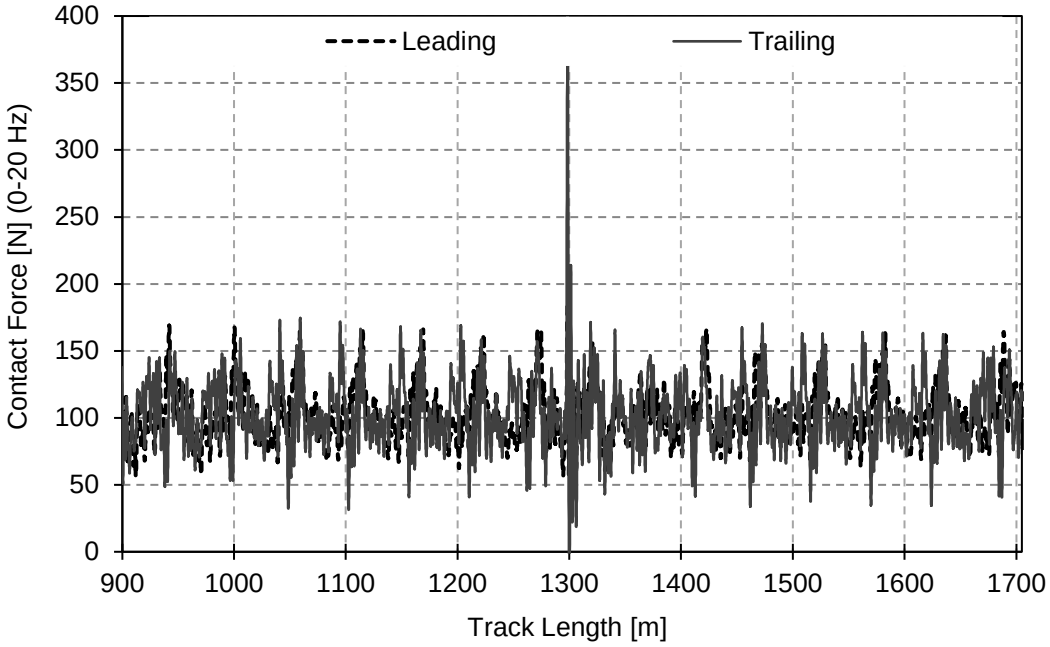

Figure 4.15: Contact forces results for LP10_Pant1_S35_V170

Looking at Figure 4.15 it is possible to determine that the maximum force, which is located where the two catenary sections overlap So, the LP10_Pant1_S35 limit exploration velocity is 160 km/h and the limiting factor is the maximum force that occurs due to the overlapping arrangement.

The dynamic analysis results obtained of the interaction of the LP10 catenary and the Pant1 pantograph, considering 2 pantographs, with a separation between them of 85 m, for various speeds are represented in Table 4.7 and Figure 4.16.

Table 4.7: LP10_Pant1_S85 results for multiple pantographs, running at various speeds

Speed [km/h]	Pant	Contact Force [N]								Contact loss			Steady Arm Uplift [m]
		F_{max}	F_{min}	ΔF	F_m	σ	σ/F_m	S_{max}	S_{Min}	$CL_{\#}$	CL_t [s]	$CL_{\%}$ [%]	
120	Leading	247.3	55.7	191.7	96.5	12.3	0.13	133.4	59.6	0	0.0	0.00	0.031
	Trailing	283.2	46.1	237.1	96.5	15.3	0.16	142.4	50.6	0	0.0	0.00	
125	Leading	241.7	58.0	183.7	97.1	13.3	0.14	136.9	57.3	0	0.0	0.00	0.031
	Trailing	264.0	48.1	215.9	97.1	15.4	0.16	143.4	50.9	0	0.0	0.00	
130	Leading	282.2	-6.4	288.6	97.7	17.0	0.17	148.7	46.8	1	0.0	0.03	0.032
	Trailing	279.7	5.9	273.8	97.7	19.6	0.20	156.5	38.9	0	0.0	0.00	
135	Leading	267.7	4.4	263.3	98.3	18.6	0.19	154.2	42.4	0	0.0	0.00	0.032
	Trailing	260.4	-7.3	267.7	98.3	24.5	0.25	171.9	24.8	1	0.0	0.03	
140	Leading	234.8	31.8	203.0	99.0	19.7	0.20	158.3	39.8	0	0.0	0.00	0.037
	Trailing	193.5	21.6	171.9	99.1	27.2	0.27	180.7	17.5	0	0.0	0.00	
145	Leading	249.9	23.8	226.1	99.6	20.6	0.21	161.3	37.9	0	0.0	0.00	0.047
	Trailing	174.9	32.4	142.5	99.6	25.8	0.26	176.9	22.4	0	0.0	0.00	
150	Leading	227.6	40.8	186.8	100.5	19.5	0.19	158.9	42.0	0	0.0	0.00	0.054
	Trailing	218.2	39.8	178.5	100.4	23.2	0.23	170.1	30.6	0	0.0	0.00	
…	…	…	…	…	…	…	…	…	…	…	…	…	…

Speed [km/h]	Pant	Contact Force [N]								Contact loss			Steady Arm Uplift [m]
		F_{max}	F_{min}	ΔF	F_m	σ	σ/F_m	S_{max}	S_{Min}	$CL_{\#}$	CL_t [s]	$CL_{\%}$ [%]	
155	Leading	218.4	40.6	177.8	101.0	19.9	0.20	160.6	41.4	0	0.0	0.00	0.055
	Trailing	170.0	42.4	127.5	101.0	22.6	0.22	168.8	33.1	0	0.0	0.00	
160	Leading	233.0	40.1	192.9	101.9	20.8	0.20	164.4	39.5	0	0.0	0.00	0.064
	Trailing	166.0	34.9	131.1	101.9	24.1	0.24	174.3	29.6	0	0.0	0.00	
165	Leading	181.9	55.2	126.7	102.6	20.8	0.20	165.1	40.1	0	0.0	0.00	0.064
	Trailing	256.9	6.6	250.4	102.6	26.2	0.26	181.4	23.9	0	0.0	0.00	
170	Leading	181.1	48.7	132.3	103.4	21.1	0.20	166.6	40.2	0	0.0	0.00	0.060
	Trailing	381.0	-22.5	403.5	103.4	30.3	0.29	194.1	12.6	1	0.0	0.07	
175	Leading	208.9	45.9	163.0	104.2	21.2	0.20	167.9	40.5	0	0.0	0.00	0.060
	Trailing	439.9	-44.7	484.5	104.2	34.9	0.33	208.9	-0.5	2	0.0	0.16	
180	Leading	249.4	4.4	245.1	105.1	23.3	0.22	174.9	35.3	0	0.0	0.00	0.065
	Trailing	425.2	-42.5	467.7	105.1	36.0	0.34	213.1	-2.9	1	0.0	0.09	

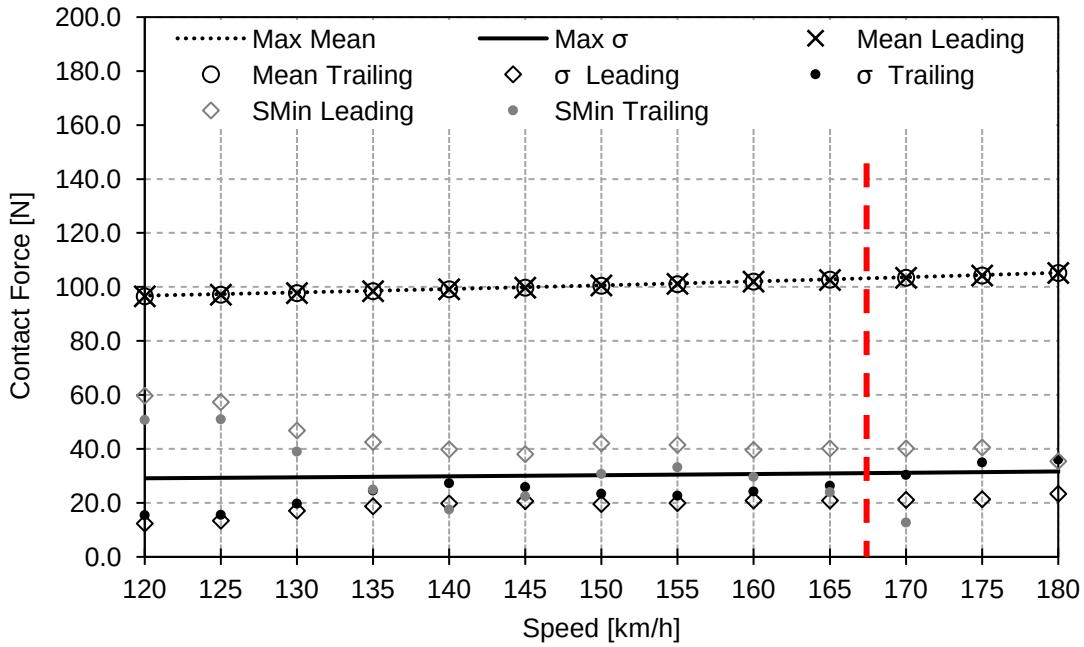

Figure 4.16: LP10_Pant1_S85 results for multiple pantographs operation, running at various speeds and the speed limit for this case

Looking at Figure 4.16 is observed that the statistical minimum, of the trailing pantograph, is negative for the speeds of 175 km/h and 180 km/h, and that the standard deviation, of the trailing pantograph, surpasses the maximum standard deviation line for these same velocities. However, when Table 4.7 is observed, the maximum contact force can be analysed, and it is found that at 170 km/h and for higher velocities the maximum contact force of the trailing pantograph, exceed the 300 N. So, the maximum operating velocity is 165 km/h and the operating limiting factor is the maximum force observed in the trailing pantograph. Figure 4.17 represents the contact force along the track, for each pantograph, for the LP10_Pant1_S85_V170 operation.

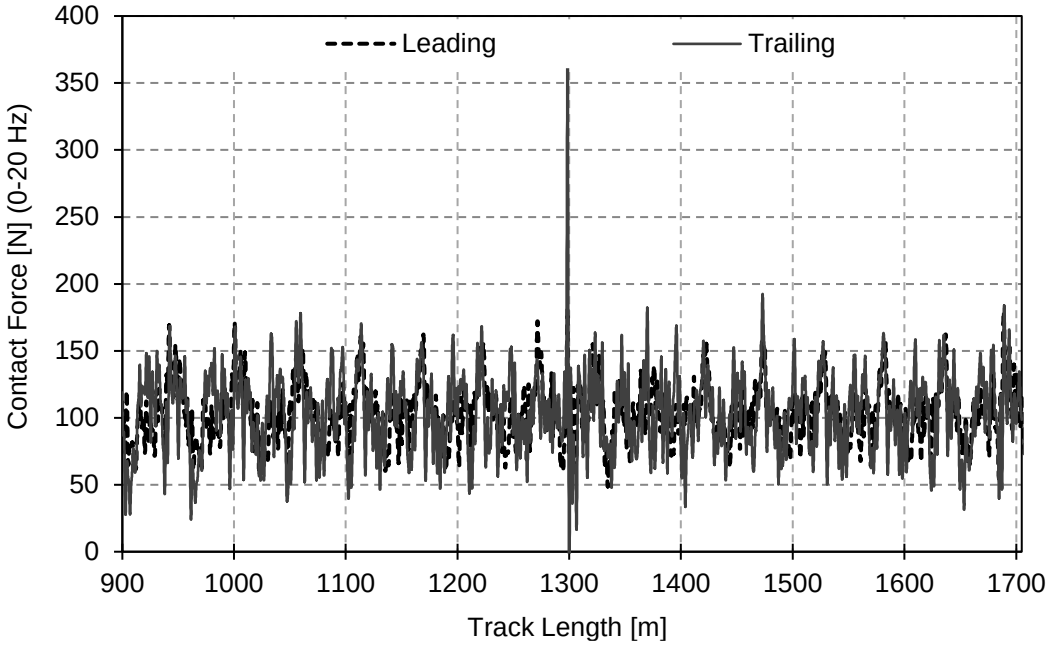

Figure 4.17: Contact forces results for LP10_Pant1_S85_V170

In Figure 4.17 the maximum force is observed to occur for the trailing pantograph and it is located where the two catenary sections overlap. So, this operation limiting factor is the maximum force of the trailing pantograph, that occurs due to the overlapping arrangement. Comparing the LP10_Pant1_S85 dynamic analysis to the LP10_Pant1_S35, it is possible to observe that the maximum velocity is higher for LP10_Pant1_S85, and the limiting factor of the operations is the same.

The dynamic analysis results obtained of the interaction of the LP10 catenary and the Pant1 pantograph, considering 2 pantographs, with a separation between them of 100 m, for various speeds are represented in Figure 4.18 and Table 4.8.

Table 4.8: LP10_Pant1_S100 results for multiple pantograph operation, running at various speeds

Speed [km/h]	Pant	Contact Force [N]								Contact loss			Steady Arm Uplift [m]
		F_{max}	F_{min}	ΔF	F_m	σ	σ/F_m	S_{max}	S_{Min}	$CL_{\#}$	CL_t [s]	$CL_{\%}$ [%]	
120	Leading	250.8	55.8	195.0	96.5	12.3	0.13	133.3	59.7	0	0.0	0.00	0.034
	Trailing	297.6	40.1	257.5	96.5	14.8	0.15	140.9	52.1	0	0.0	0.00	
125	Leading	285.4	-9.1	294.5	97.1	15.3	0.16	143.1	51.2	1	0.0	0.03	0.032
	Trailing	266.7	19.2	247.5	97.1	16.6	0.17	146.9	47.4	0	0.0	0.00	
130	Leading	277.1	-1.7	278.8	97.7	16.9	0.17	148.4	47.0	1	0.0	0.00	0.030
	Trailing	229.9	18.6	211.4	97.7	17.5	0.18	150.4	45.1	0	0.0	0.00	
135	Leading	264.7	5.5	259.2	98.3	18.6	0.19	154.3	42.4	0	0.0	0.00	0.029
	Trailing	270.5	15.8	254.7	98.3	20.0	0.20	158.2	38.4	0	0.0	0.00	
140	Leading	255.5	49.3	206.2	99.0	17.5	0.18	151.6	46.4	0	0.0	0.00	0.033
	Trailing	265.6	34.8	230.8	99.0	20.5	0.21	160.4	37.6	0	0.0	0.00	
145	Leading	210.4	60.9	149.6	99.6	17.3	0.17	151.6	47.7	0	0.0	0.00	0.037
	Trailing	275.8	36.0	239.8	99.7	24.1	0.24	171.9	27.4	0	0.0	0.00	
…	…	…	…	…	…	…	…	…	…	…	…	…	…

Speed [km/h]	Pant	Contact Force [N]								Contact loss			Steady Arm Uplift [m]
		F_{max}	F_{min}	ΔF	F_m	σ	σ/F_m	S_{max}	S_{Min}	$CL_{\#}$	CL_t [s]	$CL_{\%}$ [%]	
150	Leading	192.4	59.4	133.0	100.5	17.4	0.17	152.8	48.1	0	0.0	0.00	0.043
	Trailing	252.2	20.6	231.6	100.5	26.4	0.26	179.7	21.2	0	0.0	0.00	
155	Leading	158.8	59.4	99.4	101.1	19.6	0.19	159.9	42.2	0	0.0	0.00	0.050
	Trailing	181.7	19.2	162.4	101.0	28.4	0.28	186.2	15.7	0	0.0	0.00	
160	Leading	165.8	51.9	113.9	101.8	20.0	0.20	161.8	41.8	0	0.0	0.00	0.068
	Trailing	179.8	10.4	169.3	101.8	26.3	0.26	180.6	23.0	0	0.0	0.00	
165	Leading	194.5	50.6	143.9	102.5	19.4	0.19	160.5	44.4	0	0.0	0.00	0.071
	Trailing	201.1	27.4	173.6	102.6	23.7	0.23	173.8	31.5	0	0.0	0.00	
170	Leading	305.2	-4.9	310.1	103.2	20.8	0.20	165.6	40.9	1	0.0	0.03	0.069
	Trailing	237.1	16.5	220.6	103.4	23.4	0.23	173.7	33.1	0	0.0	0.00	
175	Leading	380.6	-28.1	408.7	104.2	23.0	0.22	173.3	35.0	1	0.0	0.08	0.066
	Trailing	239.0	2.2	236.8	104.3	27.2	0.26	185.9	22.7	0	0.0	0.00	
180	Leading	410.7	-41.4	452.1	105.1	26.3	0.25	184.0	26.3	1	0.0	0.10	0.071
	Trailing	238.5	5.5	232.9	105.2	28.5	0.27	190.8	19.7	0	0.0	0.00	

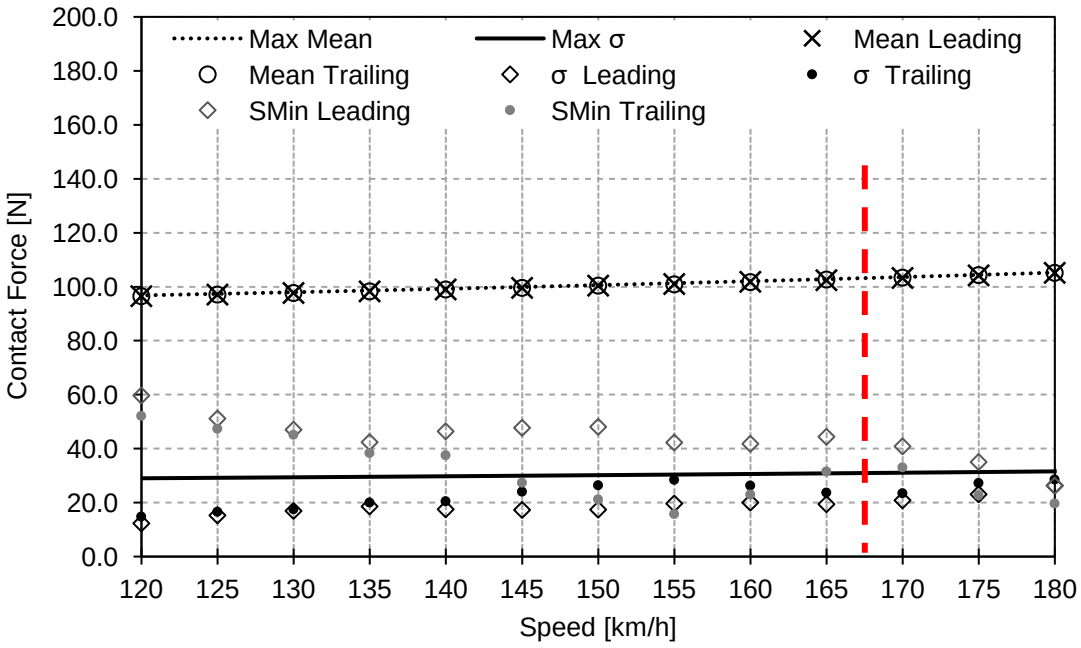

Figure 4.18: LP10_Pant1_S100 results for multiple pantograph operation, running at various speeds and the speed limit for this case

Observing Figure 4.18 all of the contact forces simulation results are found to be between their respective limit thresholds. However, when Table 4.8 is observed it is found that the maximum force surpasses the threshold limit, of 300 N, for an operation of 170km/h. This results, at first glance lock to be the same as the obtained for LP10_Pant1S85. However, the pantograph that is limiting higher velocities is the leading pantograph instead of the trailing one. The standard deviation and the mean force of the trailing pantograph is higher than the leading pantograph. This expresses that even with the trailing pantograph being affecting by the contact parameters of the leading pantograph, the limiting pantograph in this case is the leading pantograph. The maximum exploration velocity for the

LP10_Pant1_S100 is 165 km/h and the limiting factor is the maximum contact force. Figure 4.19 represents the contact force along the track, for each pantograph, for the LP10_Pant1_S100_V170 operation.

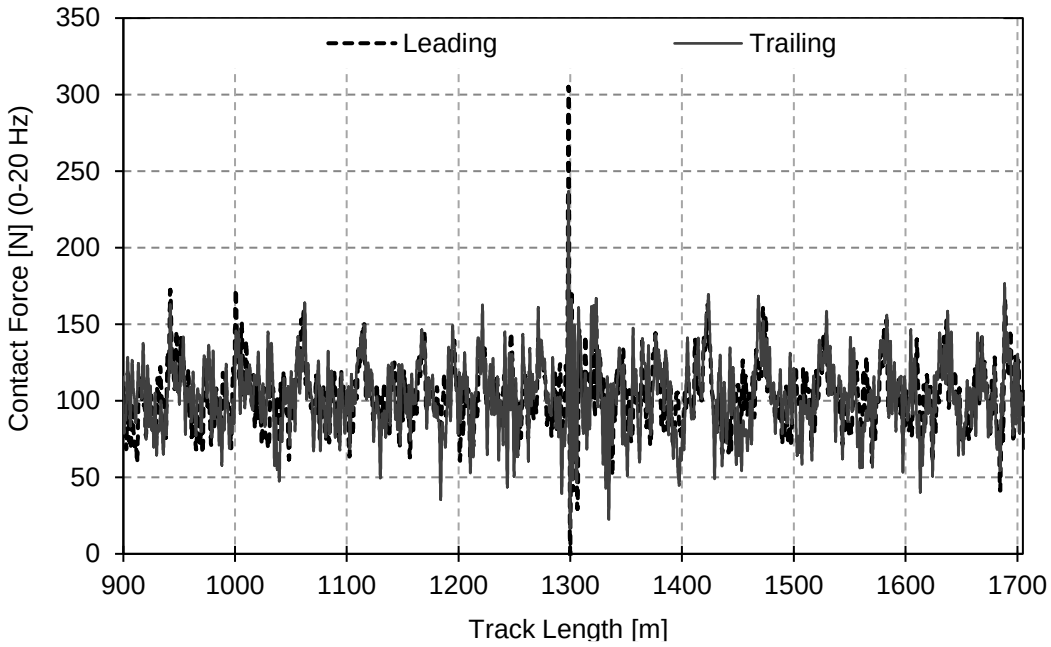

Figure 4.19: Contact forces results for LP10_Pant1_S100_V170

Studying Figure 4.19 the maximum contact force is found to occur in the leading pantograph, instead of the trailing one, and it is located where the two catenary sections overlap. In this figure, the leading pantograph is the one that has the maximum contact force and a contact loss can be observe. These can be located where the two catenary sections overlap. So, the velocity limiting factor is the maximum force that occurs due to the overlap arrangement.

The dynamic analysis results obtained of the interaction of the LP10 catenary and the Pant1 pantograph, considering 2 pantographs, with a separation between them of 200 m, for various speeds are represented in Figure 4.20 and Table 4.9.

Table 4.9: LP10_Pant1_S200 results for multiple pantographs, running at various speeds

Speed [km/h]	Pant	Contact Force [N]								Contact loss			Steady Arm Uplift [m]
		F_{max}	F_{min}	ΔF	F_m	σ	σ/F_m	S_{max}	S_{Min}	$CL_{\#}$	CL_t [s]	$CL_{\%}$ [%]	
120	Leading	250.8	55.8	195.0	96.5	12.3	0.13	133.3	59.7	0	0.0	0.00	0.034
	Trailing	297.6	40.1	257.5	96.5	14.8	0.15	140.9	52.1	0	0.0	0.00	
125	Leading	242.9	56.7	186.2	97.1	13.3	0.14	136.9	57.4	0	0.0	0.00	0.031
	Trailing	227.2	58.4	168.8	97.1	14.3	0.15	139.9	54.4	0	0.0	0.00	
130	Leading	279.5	-2.8	282.3	97.7	16.8	0.17	148.1	47.3	1	0.0	0.02	0.031
	Trailing	214.6	39.8	174.8	97.7	17.5	0.18	150.2	45.3	0	0.0	0.00	
135	Leading	275.0	-0.1	275.1	98.3	18.7	0.19	154.6	42.1	1	0.0	0.00	0.029
	Trailing	232.9	16.7	216.2	98.3	21.0	0.21	161.2	35.4	0	0.0	0.00	
…	…	…	…	…	…	…	…	…	…	…	…	…	…

Speed [km/h]	Pant	Contact Force [N]								Contact loss			Steady Arm Uplift [m]
		F_{max}	F_{min}	ΔF	F_m	σ	σ /F_m	S_{max}	S_{Min}	$CL_{\#}$	CL_t [s]	$CL_{\%}$ [%]	
140	Leading	238.7	52.1	186.6	99.0	17.1	0.17	150.3	47.8	0	0.0	0.00	0.035
	Trailing	293.7	24.9	268.8	99.0	23.5	0.24	169.4	28.7	0	0.0	0.00	
145	Leading	228.1	37.6	190.5	99.7	20.1	0.20	159.9	39.4	0	0.0	0.00	0.047
	Trailing	189.8	29.0	160.8	99.7	24.4	0.24	172.7	26.6	0	0.0	0.00	
150	Leading	228.6	38.9	189.6	100.5	19.6	0.20	159.4	41.6	0	0.0	0.00	0.047
	Trailing	183.9	41.6	142.3	100.4	23.4	0.23	170.7	30.1	0	0.0	0.00	
155	Leading	172.0	56.2	115.8	101.1	19.7	0.20	160.2	41.9	0	0.0	0.00	0.055
	Trailing	282.5	-8.6	291.1	101.0	24.3	0.24	174.0	28.1	1	0.0	0.04	
160	Leading	176.4	58.8	117.6	101.8	18.7	0.18	157.9	45.8	0	0.0	0.00	0.051
	Trailing	279.6	40.2	239.4	101.8	24.2	0.24	174.3	29.3	0	0.0	0.00	
165	Leading	168.8	50.0	118.8	102.5	19.7	0.19	161.5	43.4	0	0.0	0.00	0.062
	Trailing	289.0	-14.0	303.0	102.6	27.1	0.26	183.9	21.3	1	0.0	0.06	
170	Leading	250.6	25.6	225.1	103.2	21.0	0.20	166.3	40.2	0	0.0	0.00	0.064
	Trailing	350.6	-22.9	373.5	103.4	27.3	0.26	185.4	21.5	1	0.0	0.07	
175	Leading	311.9	-5.5	317.4	104.1	22.2	0.21	170.6	37.6	1	0.0	0.04	0.060
	Trailing	340.4	9.8	330.5	104.3	27.3	0.26	186.1	22.4	0	0.0	0.00	
180	Leading	334.4	-19.6	354.0	105.1	24.5	0.23	178.5	31.7	1	0.0	0.07	0.061
	Trailing	260.1	5.1	254.9	105.1	29.1	0.28	192.4	17.7	0	0.0	0.00	

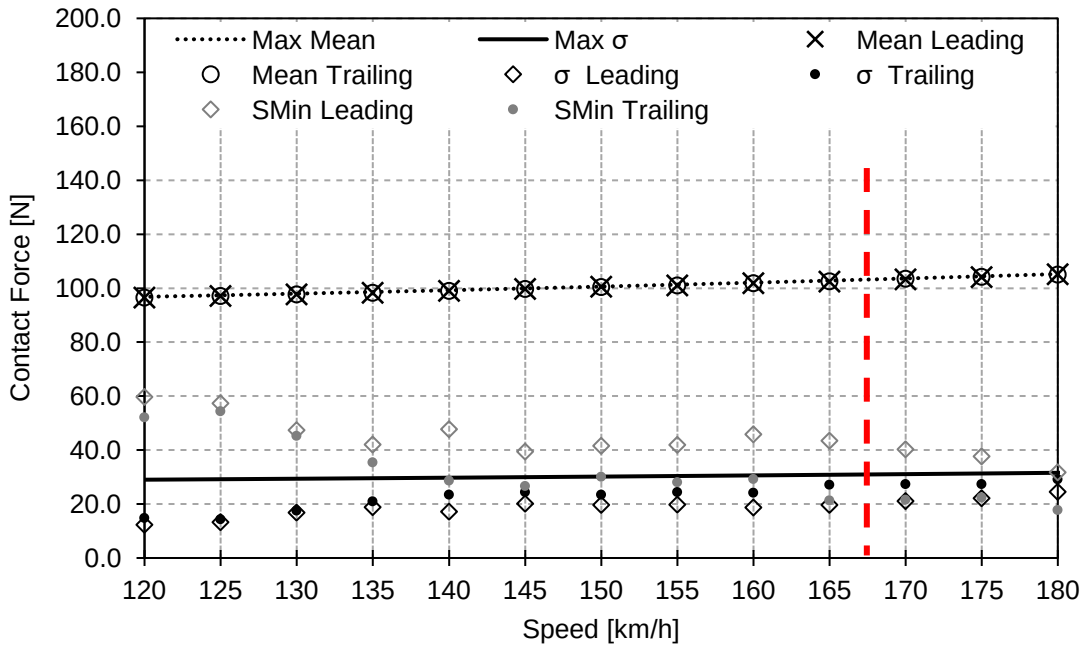

Figure 4.20: LP10_Pant1_S200 results for multiple pantographs, running at various speeds

Studying Figure 4.20 it is observed that the dynamic analysis results obtained are similar to the obtained for LP10_Pant1_S100, since all of the parameters presented in Figure 4.20 and Figure 4.18, are within the validation parameters obtained in Table 4.1. So, to obtain the speed limit for LP10_Pant1_S200 Table 4.9 must be analysed. In this table the maximum force surpasses the 300 N limit, and exists a contact loss inferior to 0,1%, for 170 km/h. The surpassing of the maximum force

threshold occurs in the trailing pantograph, just like it happened for LP10_Pant1_S85. The exploration velocity for the LP10_Pant1_S200 case is 165 km/h and the limiting factor is the maximum force, of the trailing pantograph. Figure 4.21 represents the contact forces along the track for a speed of 170 km/h

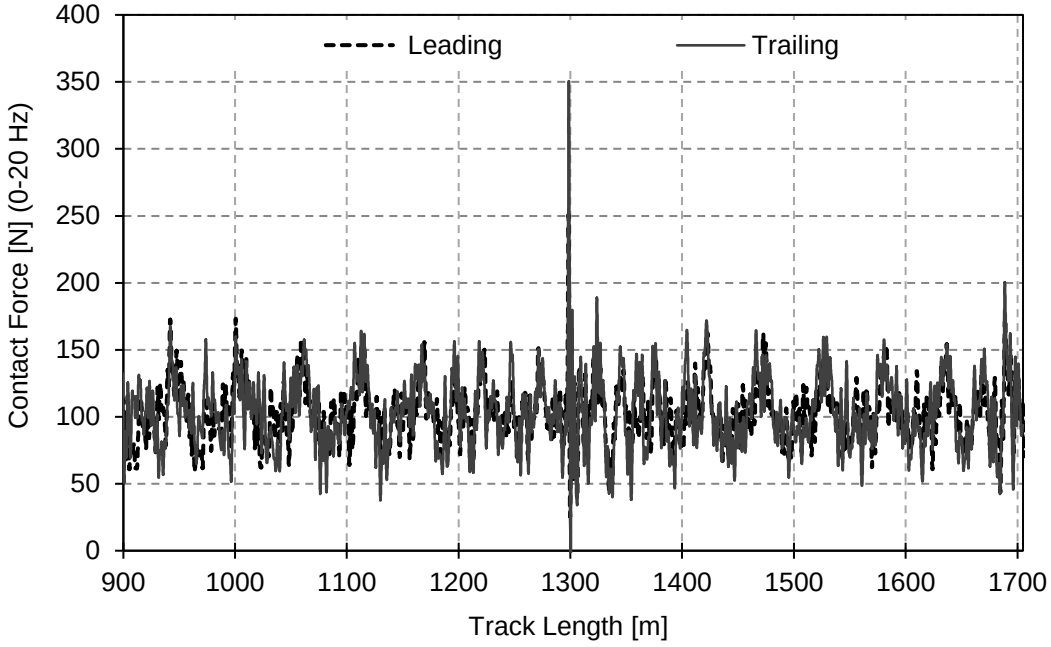

Figure 4.21: Contact forces results for LP10_Pant1_S200_V170

Studying Figure 4.21 the maximum contact force is found to occur in the trailing pantograph, and it is also observed that the trailing pantograph is being affected by the leading pantograph, just like when a separation of 85 m is considered. The maximum force and the contact loss are located where the two catenary sections overlap. So, the velocity limiting factor is the maximum force that occurs due to the overlap arrangement.

In Figure 4.22 represents the maximum steady arm uplift for the LP10_Pant1 pairing, for each velocity and pantograph separation considered. The maximum steady arm uplift occurs for LP10_Pant1_S100 and its value is 0.071 m. In this figure the maximum steady arm uplift occurs for a pantograph separation of 100 m, however the pantograph separation that tends to have a maximum steady arm uplift for each velocity is 35 m.

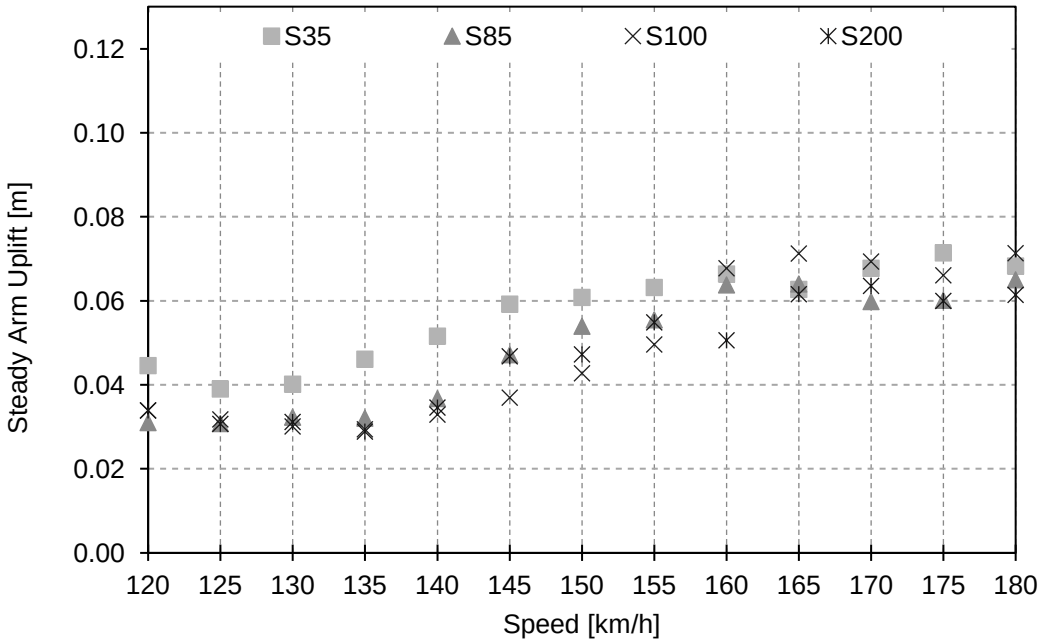

Figure 4.22: LP10_Pant1 steady arm uplift results for multiple pantographs systems, running at various speeds

Considering the cases of LP10_Pant1 operating with multiple pantographs the limit exploration velocity is 160 km/h. Since LP10_Pant1_S35 is the one that has the lowest exploration velocity, so the critical separation is 35 m. Being also possible to conclude that the parameter that restricts this specific catenary pantograph pair to reach higher velocities is the maximum force expressed by the overlapping arrangement.

Comparing the single pantograph operation with multiple pantograph operation the maximum operating velocity lowers from 170 km/h to 160 km/h, while the limiting factor remains the same. The limiting parameter of the LP10_Pant1 pairing is the maximum force for the trailing pantograph that occurs due to the overlap arrangement. Comparing the four pantograph separations, the limiting velocity for LP10_Pant1 occurs for a pantograph separation of 35 m.

When a pantograph is exchanged and assuming that both pantographs have a good representation model and where design to operate at the same speeds, the limit exploration velocity obtained for each case study in the same conditions should be similar. This means that the maximum velocity obtained for the LP10_Pant1 cases should be close to the one obtained from the respective LP10_Pant2 cases.

The dynamic analysis results obtained of the interaction of the LP10 catenary and the Pant2 pantograph, considering 2 pantographs, with a separation between them of 35 m, for various speeds are represented in Figure 4.23 and Table 4.10.

Table 4.10: LP10_Pant2_S35 results for multiple pantographs, running at various speeds

Speed [km/h]	Pant	Contact Force [N]								Contact loss			Steady Arm Uplift [m]
		F_{max}	F_{min}	ΔF	F_m	σ	σ / F_m	S_{max}	S_{Min}	$CL_{\#}$	CL_t [s]	$CL_{\%}$ [%]	
120	Leading	298.1	-8.9	307.0	96.6	19.0	0.20	153.4	39.7	1	0.0	0.05	0.041
	Trailing	251.0	4.8	246.2	96.6	18.5	0.19	152.2	41.0	0	0.0	0.00	
125	Leading	290.2	9.6	280.6	97.0	19.4	0.20	155.2	38.9	0	0.0	0.00	0.039
	Trailing	220.7	19.0	201.8	96.9	19.3	0.20	154.9	39.0	0	0.0	0.00	
130	Leading	293.0	-1.2	294.2	97.6	22.0	0.23	163.5	31.6	1	0.0	0.00	0.046
	Trailing	191.9	23.3	168.5	97.5	18.9	0.19	154.2	40.9	0	0.0	0.00	
135	Leading	295.2	6.4	288.9	98.2	23.4	0.24	168.5	27.9	0	0.0	0.00	0.051
	Trailing	177.4	40.8	136.6	98.1	18.0	0.18	152.0	44.1	0	0.0	0.00	
140	Leading	208.8	31.0	177.9	99.0	23.0	0.23	167.8	30.1	0	0.0	0.00	0.057
	Trailing	215.7	24.2	191.5	99.1	20.9	0.21	161.9	36.3	0	0.0	0.00	
145	Leading	175.6	32.5	143.1	99.2	22.9	0.23	167.9	30.5	0	0.0	0.00	0.057
	Trailing	294.8	20.3	274.5	99.4	24.8	0.25	173.6	25.1	0	0.0	0.00	
150	Leading	256.1	-10.8	266.8	100.3	25.5	0.25	176.7	24.0	1	0.0	0.07	0.058
	Trailing	345.5	22.3	323.2	100.3	28.4	0.28	185.7	15.0	0	0.0	0.00	
155	Leading	227.5	26.7	200.8	100.8	25.4	0.25	177.1	24.5	0	0.0	0.00	0.058
	Trailing	407.0	-22.5	429.5	100.6	33.7	0.34	201.8	-0.6	2	0.0	0.17	
160	Leading	213.4	6.9	206.5	101.9	27.8	0.27	185.2	18.5	0	0.0	0.00	0.062
	Trailing	427.6	-9.7	437.2	101.8	33.0	0.32	200.9	2.7	2	0.0	0.14	
165	Leading	199.3	25.7	173.6	102.7	29.9	0.29	192.4	13.1	0	0.0	0.00	0.059
	Trailing	398.6	2.9	395.6	102.7	36.8	0.36	213.1	-7.7	0	0.0	0.00	
170	Leading	208.3	14.3	194.0	103.1	32.2	0.31	199.7	6.4	0	0.0	0.00	0.069
	Trailing	344.2	-4.7	348.9	103.3	42.3	0.41	230.1	-23.5	1	0.0	0.07	
175	Leading	235.7	4.2	231.6	103.9	33.8	0.33	205.2	2.6	0	0.0	0.00	0.072
	Trailing	302.2	-2.5	304.7	104.0	43.1	0.41	233.4	-25.5	2	0.0	0.16	
180	Leading	323.3	0.6	322.7	105.0	36.5	0.35	214.4	-4.4	0	0.0	0.00	0.071
	Trailing	333.9	1.3	332.6	105.0	42.3	0.40	231.9	-21.9	0	0.0	0.00	

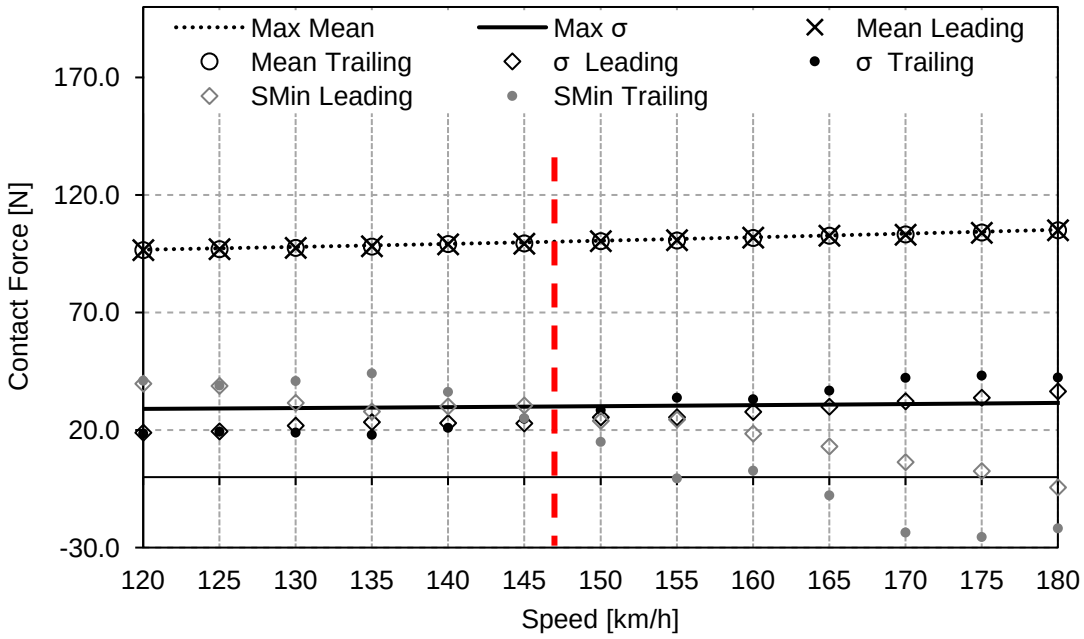

Figure 4.23: LP10_Pant2_S35 results for multiple pantographs, running at various speeds

Looking at Figure 4.23, it is observed that the standard deviation is the only parameter that surpasses its respective limits thresholds and the first velocity where this is observed is 155 km/h for the trailing pantograph. While in Table 4.10 it is found that there is a maximum force exciding the 300 N limit, for 150 km/h. For this velocity there is also a contact loss that is between the limiting parameters. So, the exploration velocity for LP10_Pant2_S35 is 145 km/h and its limiting factor is the maximum contact force on the trailing pantograph. Figure 4.24 represents the contact forces along the track for LP10_Pant2_S35_V150.

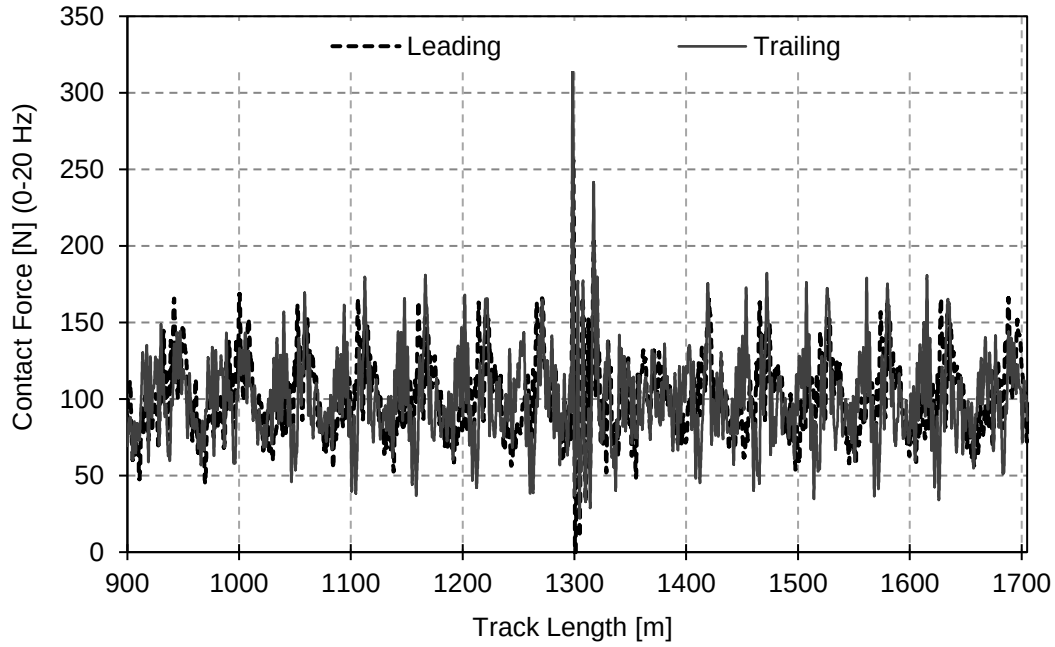

Figure 4.24: Contact forces results for LP10_Pant2_S35_V150

In Figure 4.24 the contact forces along the track are represented for each pantograph, where it is possible to determine that the maximum force occurs near the only contact loss of LP10_Pant2_S35_V150 which is located where the two catenary sections overlap for the trailing pantograph. So, the LP10_Pant2_S35 case is limited by the trailing pantograph due to the overlapping arrangement.

The dynamic analysis results obtained of the interaction of the LP10 catenary and the Pant2 pantograph, considering 2 pantographs, with a separation between them of 85 m, for various speeds are represented in Figure 4.25 and Table 4.11.

Table 4.11: LP10_Pant2_S85 results for multiple pantographs, running at various speeds

Speed [km/h]	Pant	Contact Force [N]								Contact loss			Steady Arm Uplift [m]
		F_{max}	F_{min}	ΔF	F_m	σ	σ / F_m	S_{max}	S_{Min}	$CL_{\#}$	CL_t [s]	$CL_{\%}$ [%]	
120	Leading	276.6	12.8	263.8	96.8	18.5	0.19	152.3	41.2	0	0.0	0.00	0.031
	Trailing	299.0	12.4	286.6	96.7	22.0	0.23	162.8	30.8	0	0.0	0.00	
125	Leading	246.1	39.0	207.1	97.2	18.8	0.19	153.7	40.7	0	0.0	0.00	0.033
	Trailing	299.9	10.5	289.4	97.2	24.0	0.25	169.3	25.0	0	0.0	0.00	
130	Leading	255.6	31.1	224.6	97.7	21.6	0.22	162.5	32.9	0	0.0	0.00	0.037
	Trailing	225.6	25.6	200.0	97.7	26.6	0.27	177.5	17.9	0	0.0	0.00	
135	Leading	214.9	38.2	176.7	98.3	23.2	0.24	167.8	28.8	0	0.0	0.00	0.036
	Trailing	206.9	-0.7	207.6	98.4	33.3	0.34	198.3	-1.5	1	0.0	0.03	
140	Leading	282.4	-7.7	290.1	98.8	26.7	0.27	178.8	18.8	1	0.0	0.07	0.046
	Trailing	232.8	8.4	224.4	99.1	36.9	0.37	209.8	-11.6	0	0.0	0.00	
145	Leading	191.5	37.4	154.1	99.2	25.2	0.25	174.9	23.6	0	0.0	0.00	0.059
	Trailing	213.4	6.1	207.3	99.9	33.3	0.33	199.7	0.0	0	0.0	0.00	
150	Leading	199.3	42.3	157.1	100.0	25.4	0.25	176.1	24.0	0	0.0	0.00	0.062
	Trailing	218.3	19.8	198.5	100.5	30.5	0.30	192.1	8.9	0	0.0	0.00	
155	Leading	195.5	25.9	169.5	100.7	27.0	0.27	181.7	19.6	0	0.0	0.00	0.056
	Trailing	203.9	20.1	183.8	101.2	31.4	0.31	195.5	6.9	0	0.0	0.00	
160	Leading	189.0	29.7	159.2	101.2	28.0	0.28	185.1	17.3	0	0.0	0.00	0.068
	Trailing	206.7	7.6	199.0	102.0	34.6	0.34	205.8	-1.8	0	0.0	0.00	
165	Leading	203.0	19.1	183.9	102.1	29.7	0.29	191.2	13.0	0	0.0	0.00	0.062
	Trailing	394.0	-8.9	402.9	102.6	42.0	0.41	228.5	-23.2	7	0.1	0.69	
170	Leading	208.7	16.2	192.5	103.1	29.7	0.29	192.2	14.1	0	0.0	0.00	0.059
	Trailing	461.2	-12.6	473.9	103.6	49.3	0.48	251.4	-44.3	10	0.1	0.86	
175	Leading	206.3	21.4	184.8	104.2	30.1	0.29	194.4	14.1	0	0.0	0.00	0.062
	Trailing	440.5	-15.2	455.7	104.2	49.2	0.47	251.9	-43.6	6	0.1	0.54	
180	Leading	272.3	-10.1	282.3	105.0	32.5	0.31	202.6	7.5	2	0.0	0.10	0.062
	Trailing	422.4	-10.6	433.1	104.7	51.6	0.49	259.4	-49.9	10	0.2	1.06	

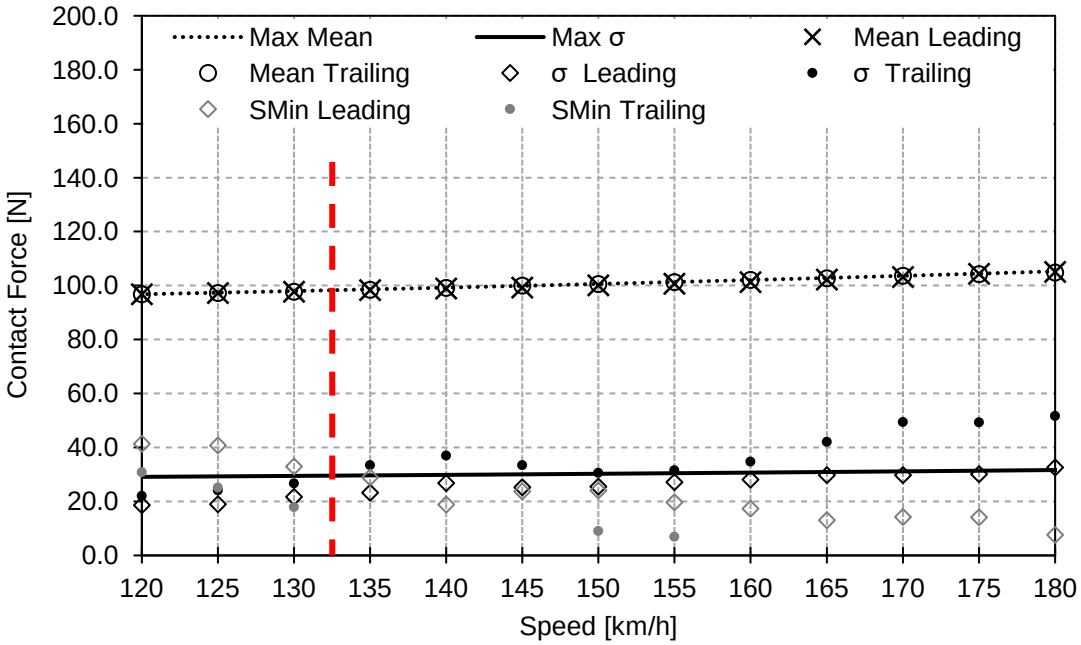

Figure 4.25: LP10_Pant2_S85 results for multiple pantographs, running at various speeds

Figure 4.25 show that for LP10_Pant2_S85 the standard deviation and the minimum statistical of the trailing pantograph surpasses its limit threshold as soon as the pantograph is operating at 135 km/h. In Table 4.11, there is no other dynamic parameter that surpasses their respective thresholds, for lower velocities of operation than 145 km/h, but a contact loss, inferior to 0,1% is observed. The limiting operating velocity is 130 km/h and the limiting factors are the standard deviation and statistical minimum of the trailing pantograph Figure 4.26 represents the contact forces along the track for LP10_Pant2_S85_V130.

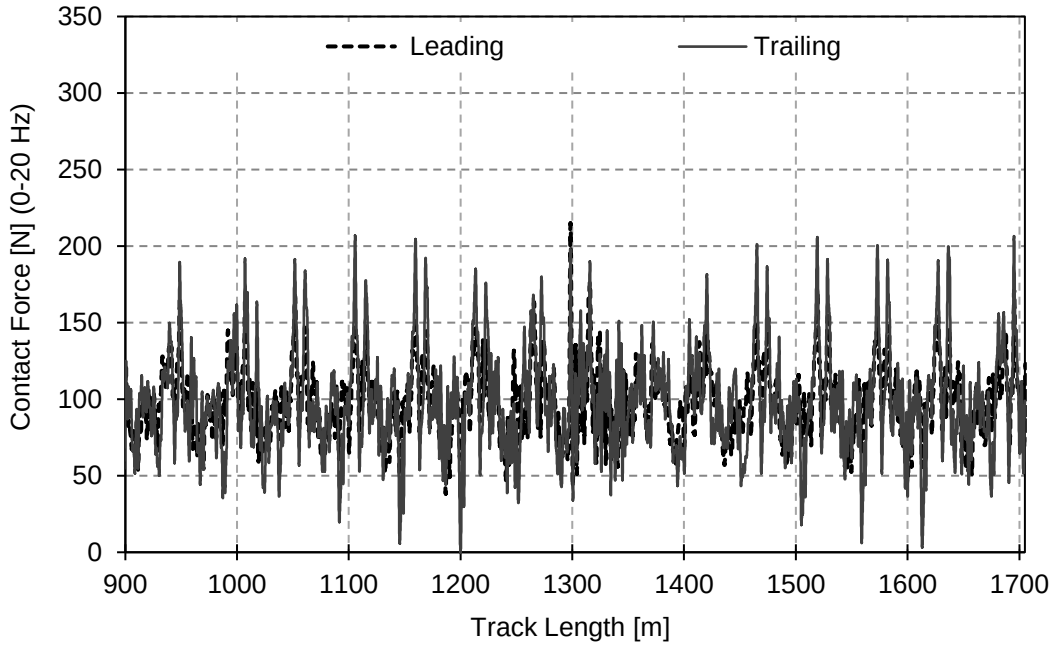

Figure 4.26: Contact forces results for LP10_Pant2_S85_V135

In Figure 4.26 the contact forces along the track are represented for each pantograph, where it is possible to observe that the contact loss occurs in in the steady arm near located at the track length of 1200 m, which is not where the catenary sections overlap. For the LP10_Pant2_S85 operations, the trailing pantograph is affected by the propagation wave creating by the leading pantograph, originating the contact force

The dynamic analysis results obtained of the interaction of the LP10 catenary and the Pant2 pantograph, considering 2 pantographs, with a separation between them of 100 m, for various speeds are represented Figure 4.27and Table 4.12Table 4.10.

Table 4.12: LP10_Pant2_S100 results for multiple pantographs, running at various speeds

Speed [km/h]	Pant	Contact Force [N]								Contact loss			Steady Arm Uplift [m]
		F_{max}	F_{min}	ΔF	F_m	σ	σ / F_m	S_{max}	S_{Min}	$CL_{\#}$	CL_t [s]	$CL_{\%}$ [%]	
120	Leading	280.4	0.2	280.2	96.6	18.6	0.19	152.4	40.9	0	0.0	0.00	0.035
	Trailing	269.4	17.6	251.8	96.8	20.7	0.21	158.9	34.6	0	0.0	0.00	
125	Leading	278.0	1.3	276.7	97.2	20.3	0.21	158.1	36.4	0	0.0	0.00	0.034
	Trailing	215.0	25.9	189.1	97.3	21.2	0.22	160.9	33.8	0	0.0	0.00	
130	Leading	241.6	35.1	206.5	97.7	21.5	0.22	162.1	33.2	0	0.0	0.00	0.032
	Trailing	234.4	24.5	209.9	97.9	23.7	0.24	169.0	26.9	0	0.0	0.00	
135	Leading	233.4	44.3	189.1	98.3	23.5	0.24	168.7	27.8	0	0.0	0.00	0.033
	Trailing	264.2	7.6	256.6	98.4	27.4	0.28	180.6	16.3	0	0.0	0.00	
140	Leading	245.1	40.0	205.2	98.8	25.7	0.26	175.8	21.8	0	0.0	0.00	0.037
	Trailing	274.5	-2.0	276.4	99.0	31.8	0.32	194.4	3.5	1	0.0	0.04	
145	Leading	175.9	50.7	125.2	99.3	24.5	0.25	172.8	25.7	0	0.0	0.00	0.045
	Trailing	336.4	-0.4	336.8	99.6	37.2	0.37	211.3	-12.1	1	0.0	0.00	
150	Leading	176.4	48.4	128.0	100.1	24.8	0.25	174.5	25.6	0	0.0	0.00	0.055
	Trailing	236.8	-4.7	241.5	100.5	38.9	0.39	217.3	-16.4	3	0.0	0.23	
155	Leading	179.9	36.5	143.4	100.7	25.5	0.25	177.1	24.2	0	0.0	0.00	0.064
	Trailing	204.0	-8.8	212.8	101.1	36.1	0.36	209.5	-7.3	2	0.0	0.20	
160	Leading	174.6	21.5	153.2	101.3	25.4	0.25	177.3	25.2	0	0.0	0.00	0.073
	Trailing	184.9	5.0	179.9	102.0	32.1	0.31	198.3	5.7	0	0.0	0.00	
165	Leading	232.1	21.2	210.9	102.2	25.6	0.25	179.0	25.3	0	0.0	0.00	0.070
	Trailing	192.2	19.8	172.4	102.8	28.3	0.28	187.8	18.0	0	0.0	0.00	
170	Leading	402.5	-7.6	410.1	103.0	29.0	0.28	189.9	16.1	1	0.0	0.05	0.070
	Trailing	221.1	16.0	205.1	103.6	31.0	0.30	196.5	10.6	0	0.0	0.00	
175	Leading	411.8	2.2	409.6	103.9	31.1	0.30	197.2	10.6	0	0.0	0.00	0.075
	Trailing	242.4	-23.0	265.4	104.4	35.5	0.34	211.0	-2.2	2	0.0	0.25	
180	Leading	398.6	7.7	391.0	104.8	35.1	0.33	210.1	-0.5	0	0.0	0.0	0.072
	Trailing	242.6	-9.1	251.7	105.2	37.9	0.36	219.0	-8.5	4	0.0	0.3	

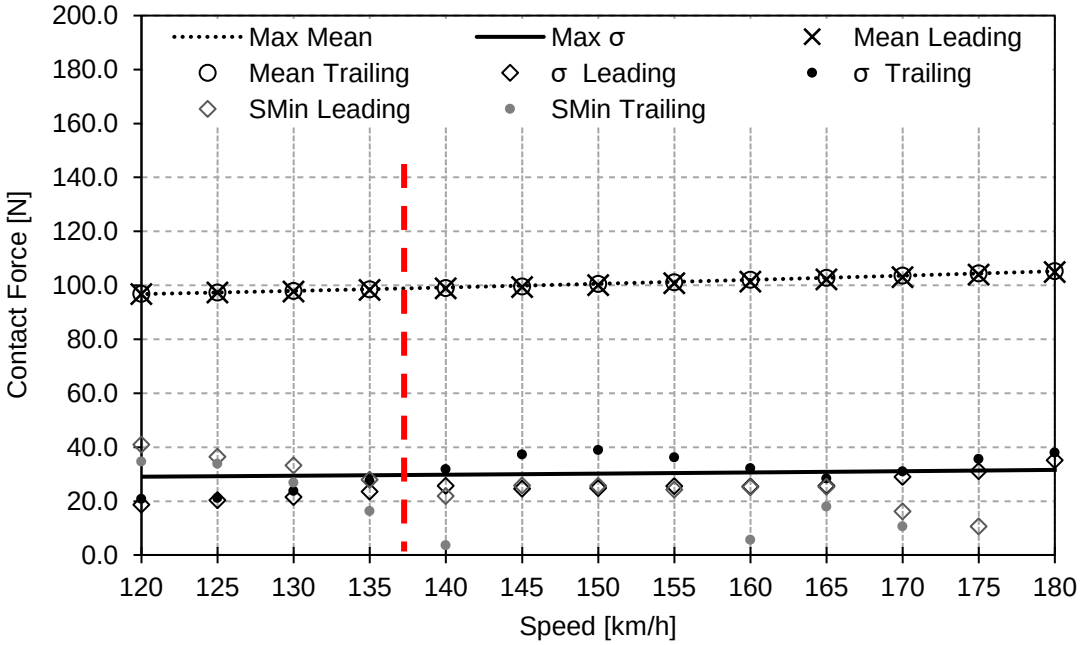

Figure 4.27: LP10_Pant2_S100 results for multiple pantographs, running at various speeds

In Table 4.12 the standard deviation ratio has a value of 0.32, when the velocity considered is 140 km/h, which is above the threshold of 0.3. By observing Figure 4.27 the results obtained from the LP10_Pant2_S100_V165 and LP10_Pant2_S100_V170 simulation stand out, because at these speeds all the parameters represented in the figure respect the threshold limits. However, in this figure the standard deviation for the trailing pantograph is seen to be almost at the limit line, and by looking at Table 4.12 it is observed that the σ/F_m value for the trailing pantograph, for 160 km/h and 175 km/h, is really close to the threshold of 0.3. While the statistical minimum has its first negative value at 145 km/h for the trailing pantograph, and when the speed of 160 km/h is reached returns to be a positive value. Even though these values are almost null, until 175 km/h where the trailing pantograph statistical minimum returns to negative values. This means that, if any system perturbation is found, when the operating velocity is 165 km/h or 170 km/h, their respective trailing standard deviation increases, leading to σ/F_m superior than the threshold of 0.3, while the statistical minimum decreases, possibly to negative values. So, the exploration velocity of LP10_Pant2_S100 is 135 km/h and the limiting factor is the standard deviation of the trailing pantograph. Figure 4.28 represents the contact force for the for LP10_Pant2_S100_V140 operation case.

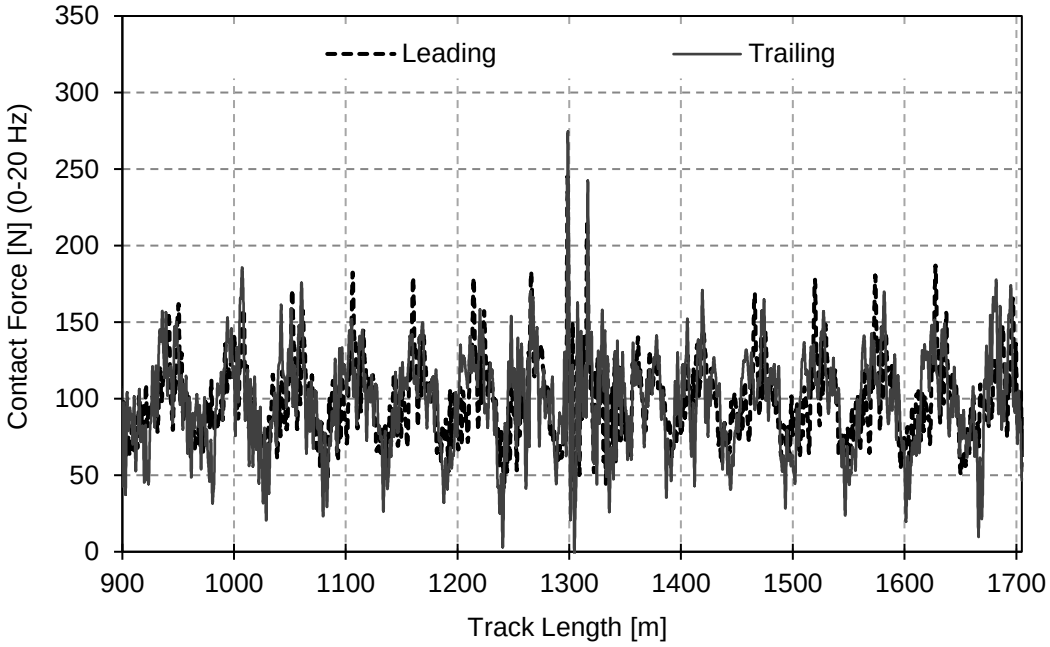

Figure 4.28: Contact forces results for LP10_Pant2_S100_V140

In Figure 4.28 it is observed that the LP10_Pant2_S100_V140 operation has a contact loss located in the catenary section overlap.

The dynamic analysis results obtained of the interaction of the LP10 catenary and the Pant2 pantograph, considering 2 pantographs, with a separation between them of 200 m, for various speeds are represented Figure 4.29and Table 4.13Table 4.10.

Table 4.13: LP10_Pant2_S200 results for multiple pantographs, running at various speeds

Speed [km/h]	Pant	Contact Force [N]								Contact loss			Steady Arm Uplift [m]
		F_{max}	F_{min}	ΔF	F_m	σ	σ/F_m	S_{max}	S_{Min}	$CL_{\#}$	CL_t [s]	$CL_{\%}$ [%]	
120	Leading	187.1	53.7	133.5	96.8	14.6	0.15	140.6	52.9	0.0	0.0	0.0	0.039
	Trailing	209.6	61.0	148.6	96.1	15.5	0.16	142.6	49.6	0.0	0.0	0.0	
125	Leading	248.8	29.3	219.5	97.2	18.9	0.19	154.0	40.5	0	0.0	0.00	0.038
	Trailing	273.0	-0.9	273.9	97.3	22.4	0.23	164.6	30.1	2	0.0	0.00	
130	Leading	291.2	2.4	288.8	97.7	22.8	0.23	166.0	29.3	0	0.0	0.00	0.033
	Trailing	198.9	42.9	156.0	97.9	23.2	0.24	167.5	28.3	0	0.0	0.00	
135	Leading	295.8	-0.7	296.5	98.3	24.6	0.25	172.1	24.5	1	0.0	0.00	0.035
	Trailing	301.9	5.0	296.9	98.3	31.8	0.32	193.8	2.7	0	0.0	0.00	
140	Leading	203.5	26.5	177.0	98.9	24.8	0.25	173.3	24.4	0	0.0	0.00	0.048
	Trailing	356.4	-1.1	357.5	99.1	37.3	0.38	211.0	-12.8	1	0.0	0.03	
145	Leading	190.9	34.6	156.3	99.3	24.9	0.25	174.1	24.6	0	0.0	0.00	0.055
	Trailing	234.3	1.8	232.5	99.6	34.0	0.34	201.6	-2.4	0	0.0	0.00	
150	Leading	178.0	48.8	129.2	100.1	25.4	0.25	176.1	24.0	0	0.0	0.00	0.050
	Trailing	192.3	9.9	182.4	100.4	32.6	0.32	198.1	2.7	0	0.0	0.00	
155	Leading	182.5	31.4	151.1	101.0	26.3	0.26	179.9	22.1	0	0.0	0.00	0.051
	Trailing	298.2	2.0	296.2	101.0	34.3	0.34	203.9	-1.8	0	0.0	0.00	

Speed [km/h]	Pant	Contact Force [N]								Contact loss			Steady Arm Uplift [m]
		F_{max}	F_{min}	ΔF	F_m	σ	σ/F_m	S_{max}	S_{Min}	$CL_{\#}$	CL_t [s]	$CL_{\%}$ [%]	
160	Leading	168.8	53.5	115.2	101.8	20.2	0.20	162.6	41.1	0	0.0	0.00	0.051
	Trailing	344.3	-33.2	377.5	101.8	27.1	0.27	183.2	20.4	1	0.0	0.08	
165	Leading	184.8	12.9	171.9	102.0	27.3	0.27	183.9	20.1	0	0.0	0.00	0.070
	Trailing	282.9	-7.7	290.6	102.7	36.5	0.36	212.2	-6.8	1	0.0	0.07	
170	Leading	306.1	18.3	287.7	102.8	29.0	0.28	189.9	15.7	0	0.0	0.00	0.066
	Trailing	507.8	-30.8	538.6	103.4	39.4	0.38	221.5	-14.7	2	0.1	0.38	
175	Leading	306.2	21.5	284.7	103.9	29.9	0.29	193.7	14.0	0	0.0	0.00	0.066
	Trailing	295.3	-17.7	313.1	104.2	37.1	0.36	215.4	-7.0	3	0.0	0.22	
180	Leading	374.8	-1.5	376.2	105.0	34.0	0.32	207.0	3.0	1	0.0	0.03	0.067
	Trailing	278.0	-8.6	286.6	104.9	40.6	0.39	226.8	-16.9	6	0.1	0.50	

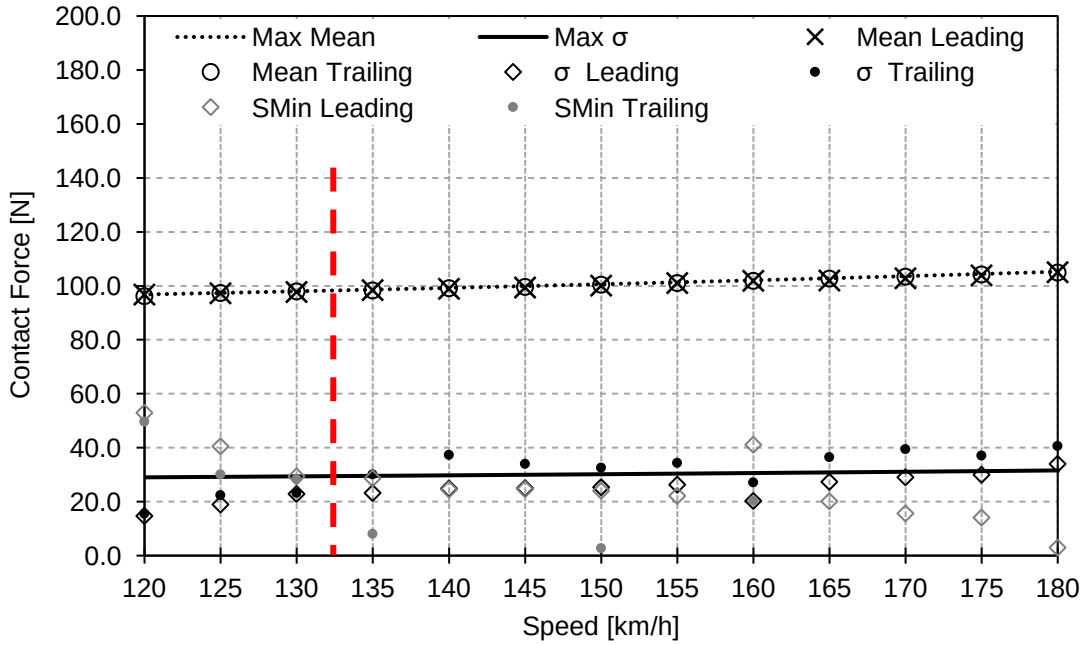

Figure 4.29: LP10_Pant2_S200 results for multiple pantographs, running at various speeds

In Figure 4.29 it is observed that the statistical minimum has negative values for the trailing pantograph for speeds above 135 km/h and that the standard deviation surpasses the maximum standard deviation for 135 km/h. From this image the simulation LP10_Pant2_S200_V160 seems to have all of the parameters within the standard threshold limits. However, Table 4.13 shows that, for this simulation speed, the trailing pantograph has a maximum contact force superior to 300 N. So, the exploration velocity is 130 km/h. Where the limit operating parameter is the standard deviation obtained from the trailing pantograph and its maximum contact force. For this case, the trailing pantograph is affected by the leading pantograph, this can be seen from the higher mean forces and standard deviations observed in the trailing pantograph compared to the leading pantograph. Figure 4.30 represents the contact force for the for LP10_Pant2_S200_V135 operation case.

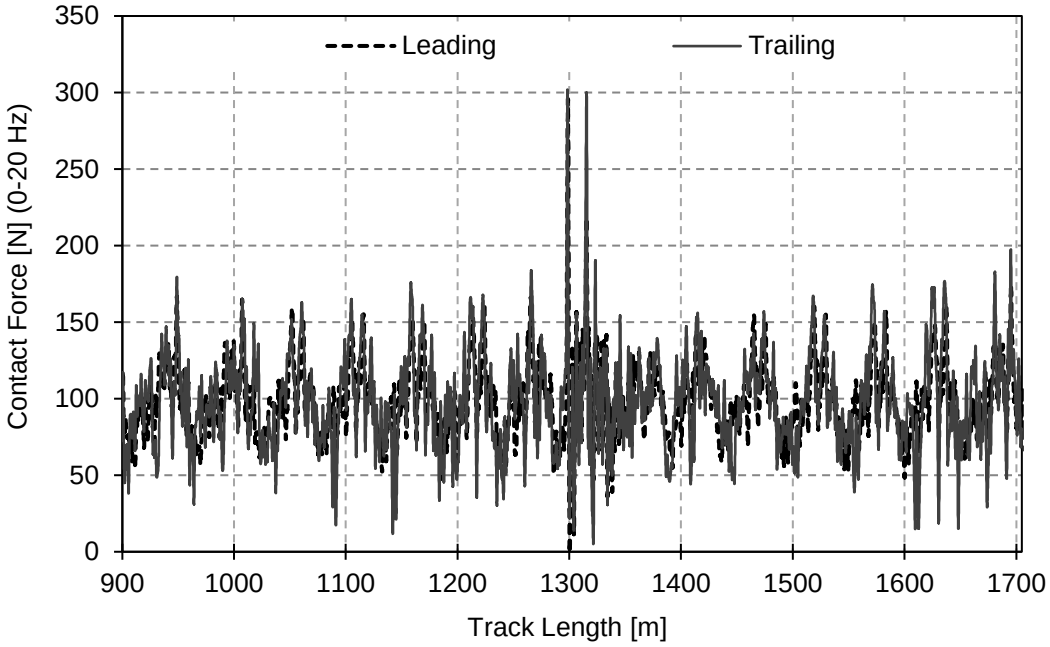

Figure 4.30: Contact forces results for LP10_Pant2_S200_V135

From Figure 4.30 it is possible to determine that the maximum force occurs near the only contact loss of LP10_Pant2_S200_V135 which is located where the two catenary sections overlap for the trailing pantograph. So, the LP10_Pant2_S200 case is limited by the standard deviation and the maximum force of the trailing pantograph. The maximum force occurs due to the overlapping arrangement. Figure 3.1 represents the maximum steady arm uplift for all the pantograph separations considered for the LP10_Pant2 pantograph catenary pairing.

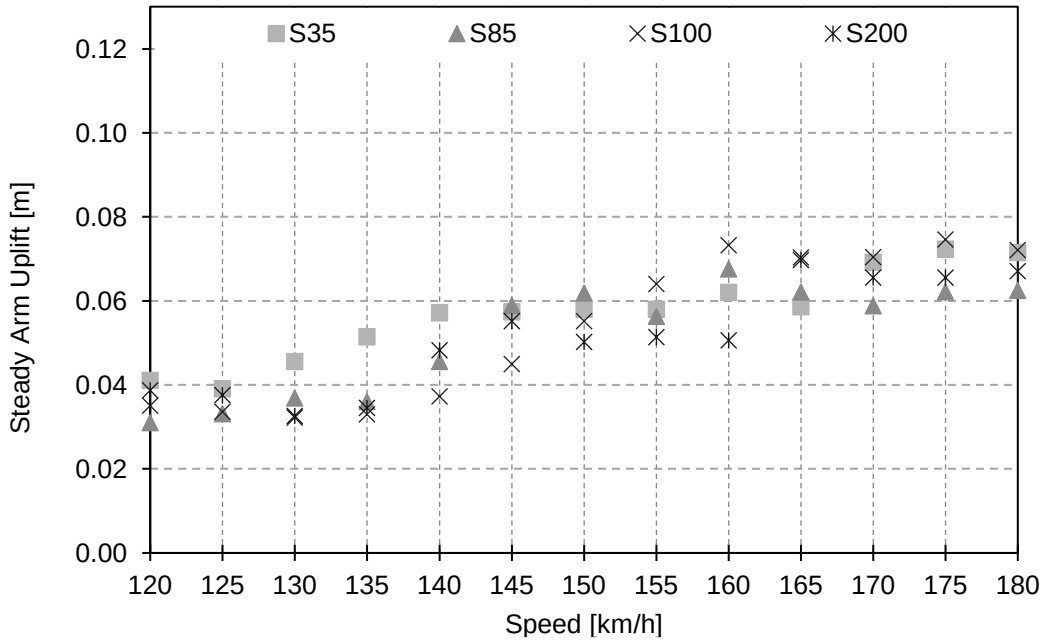

Figure 4.31: LP10_Pant2 steady arm uplift results for multiple pantographs systems, running at various speeds

In Figure 4.31 the maximum steady arm uplift occurs for LP10_Pant2_S100 and its value is 0.075 m. In this figure the maximum steady arm uplift occurs for a pantograph separation of 100 m,

however the pantograph separation that tends to have a maximum steady arm uplift for each velocity is 35 m.

Comparing all the LP10_Pant2 multiple pantographs cases, the maximum exploration velocity is 130 km/h. Even thought, 85 m and 100 m of separation are close to each other, the critical separations are 85 m and 200 m. For this pantograph catenary pair, it is possible to conclude that the parameter that is restricting the use of higher speeds is the trailing pantograph standard deviation.

Comparing the results obtained from LP10_Pant1 and LP10_Pant2 simulations, it is determined that using a Pant1 pantograph the maximum exploration velocity is 35 km/h higher that using a single Pant2 pantograph. It is also observed that the limiting parameters are different. While using multiple Pant1 pantographs the limiting factor is the overlapping model arrangement of the catenary, for the Pant2 pantograph the limiting factor is the standard deviation, that which is a statistical measurement of the evaluated contact force.

4.2.2 LP12 dynamic analysis

The dynamic analysis results obtained of the interaction of the LP12_Pant1 pairing, considering 2 pantographs, with a separation between them of 35 m, for various speeds are represented in Figure 4.32 and Table 4.14.

Table 4.14: LP12_Pant1_S35 results for multiple pantographs, running at various speeds

Speed [km/h]	Pant	Contact Force [N]								Contact loss			Steady Arm Uplift [m]
		F_{max}	F_{min}	ΔF	F_m	σ	σ /F_m	S_{max}	S_{Min}	$CL_{\#}$	CL_t [s]	$CL_{\%}$ [%]	
120	Leading	149.3	62.4	86.9	96.6	11.2	0.12	130.2	63.0	0	0.0	0.00	0.025
	Trailing	146.0	61.5	84.5	96.6	12.5	0.13	134.1	59.0	0	0.0	0.00	
125	Leading	152.0	61.9	90.1	97.2	11.6	0.12	132.1	62.3	0	0.0	0.00	0.025
	Trailing	142.0	54.3	87.7	97.2	10.6	0.11	129.0	65.3	0	0.0	0.00	
130	Leading	151.1	57.2	93.9	97.8	12.1	0.12	134.2	61.4	0	0.0	0.00	0.025
	Trailing	147.0	55.9	91.0	97.8	11.9	0.12	133.5	62.0	0	0.0	0.00	
135	Leading	149.0	52.4	96.6	98.4	12.2	0.12	134.9	61.8	0	0.0	0.00	0.026
	Trailing	143.0	53.9	89.1	98.4	11.2	0.11	131.8	64.9	0	0.0	0.00	
140	Leading	156.5	58.3	98.1	99.1	13.1	0.13	138.3	59.8	0	0.0	0.00	0.024
	Trailing	142.3	55.3	87.0	99.1	11.6	0.12	134.0	64.1	0	0.0	0.00	
145	Leading	155.1	58.0	97.1	99.7	13.9	0.14	141.2	58.1	0	0.0	0.00	0.022
	Trailing	144.3	65.4	78.9	99.6	12.6	0.13	137.5	61.8	0	0.0	0.00	
150	Leading	160.3	47.7	112.6	100.5	15.7	0.16	147.6	53.4	0	0.0	0.00	0.023
	Trailing	170.3	42.2	128.2	100.5	16.4	0.16	149.6	51.4	0	0.0	0.00	
155	Leading	156.7	49.8	106.9	101.1	17.4	0.17	153.3	48.9	0	0.0	0.00	0.026
	Trailing	155.7	50.7	105.1	101.1	17.7	0.18	154.3	47.9	0	0.0	0.00	
160	Leading	167.4	56.2	111.2	102.0	17.8	0.17	155.5	48.5	0	0.0	0.00	0.030
	Trailing	193.4	45.2	148.2	102.0	18.3	0.18	156.9	47.1	0	0.0	0.00	
…	…	…	…	…	…	…	…	…	…	…	…	…	…

Speed [km/h]	Pant	Contact Force [N]								Contact loss			Steady Arm Uplift [m]
		F_{max}	F_{min}	ΔF	F_m	σ	σ /F_m	S_{max}	S_{Min}	$CL_{\#}$	CL_t [s]	$CL_{\%}$ [%]	
165	Leading	161.1	42.5	118.6	102.6	17.4	0.17	154.7	50.4	0	0.0	0.00	0.029
	Trailing	218.3	33.1	185.2	102.6	18.5	0.18	158.0	47.2	0	0.0	0.00	
170	Leading	167.9	46.2	121.7	103.4	17.8	0.17	156.9	49.9	0	0.0	0.00	0.031
	Trailing	204.8	33.5	171.3	103.4	19.3	0.19	161.3	45.5	0	0.0	0.00	
175	Leading	168.7	49.6	119.1	104.3	18.7	0.18	160.4	48.1	0	0.0	0.00	0.033
	Trailing	242.8	9.3	233.5	104.2	21.7	0.21	169.4	38.9	0	0.0	0.00	
180	Leading	270.0	61.5	208.5	105.2	19.4	0.18	163.2	47.1	0	0.0	0.00	0.032
	Trailing	295.9	3.1	292.8	105.1	23.4	0.22	175.4	34.8	0	0.0	0.00	
185	Leading	164.9	56.1	108.8	105.9	19.6	0.19	164.7	47.1	0	0.0	0.00	0.038
	Trailing	253.6	16.7	236.9	105.9	25.0	0.24	180.9	30.9	0	0.0	0.00	
190	Leading	205.3	57.6	147.7	106.8	19.4	0.18	165.1	48.5	0	0.0	0.00	0.040
	Trailing	209.6	18.8	190.9	106.8	27.2	0.25	188.5	25.1	0	0.0	0.00	
195	Leading	171.7	55.8	115.9	107.6	18.9	0.18	164.4	50.8	0	0.0	0.00	0.043
	Trailing	206.5	6.8	199.6	107.7	29.4	0.27	195.9	19.5	0	0.0	0.00	
200	Leading	298.2	58.1	240.1	108.6	19.2	0.18	166.1	51.1	0	0.0	0.00	0.043
	Trailing	261.4	25.4	236.0	108.6	29.5	0.27	197.0	20.2	0	0.0	0.00	
205	Leading	175.6	60.7	114.9	110.6	20.4	0.18	171.7	49.4	0	0.0	0.00	0.046
	Trailing	208.1	9.4	198.7	110.6	29.4	0.27	198.9	22.2	0	0.0	0.00	
210	Leading	176.9	51.5	125.4	112.6	21.4	0.19	176.7	48.5	0	0.0	0.00	0.051
	Trailing	198.1	18.8	179.3	112.6	29.4	0.26	200.6	24.5	0	0.0	0.00	
215	Leading	179.8	46.1	133.8	114.7	23.9	0.21	186.4	43.1	0	0.0	0.00	0.053
	Trailing	205.5	17.8	187.7	114.6	30.5	0.27	206.3	23.0	0	0.0	0.00	
220	Leading	196.3	61.8	134.5	116.8	26.2	0.22	195.4	38.3	0	0.0	0.00	0.054
	Trailing	207.9	11.0	196.8	116.8	30.8	0.26	209.2	24.4	0	0.0	0.00	
225	Leading	194.5	62.9	131.6	118.8	27.7	0.23	201.8	35.7	0	0.0	0.00	0.057
	Trailing	213.3	16.3	197.0	118.7	31.9	0.27	214.6	22.9	0	0.0	0.00	
230	Leading	201.0	51.2	149.8	121.0	28.7	0.24	206.9	35.0	0	0.0	0.00	0.057
	Trailing	242.6	25.5	217.1	120.9	33.6	0.28	221.9	20.0	0	0.0	0.00	
235	Leading	207.9	60.5	147.4	123.1	29.1	0.24	210.3	35.9	0	0.0	0.00	0.054
	Trailing	230.3	12.5	217.8	123.2	35.6	0.29	230.0	16.3	0	0.0	0.00	
240	Leading	225.4	50.5	174.9	125.5	29.2	0.23	213.0	37.9	0	0.0	0.00	0.059
	Trailing	241.1	-11.0	252.2	125.4	38.6	0.31	241.3	9.5	1	0.0	0.12	
245	Leading	246.3	49.5	196.8	127.7	30.1	0.24	218.0	37.4	0	0.0	0.0	0.060
	Trailing	245.2	-9.4	254.6	127.7	40.8	0.32	249.9	5.4	1	0.0	0.1	
250	Leading	501.3	51.5	449.8	130.0	33.3	0.26	230.0	30.0	0	0.0	0.0	0.064
	Trailing	495.4	-19.8	515.2	130.0	45.2	0.35	265.6	-5.6	2	0.0	0.2	
255	Leading	278.1	18.2	259.9	132.9	34.9	0.26	237.6	28.2	0.0	0.0	0.0	0.073
	Trailing	260.0	-20.0	280.0	132.8	45.3	0.34	268.7	-3.1	6.0	0.1	0.7	
260	Leading	337.6	-21.4	359.1	135.3	37.1	0.27	246.5	24.1	1.0	0.0	0.1	0.079
	Trailing	268.9	-2.3	271.2	135.2	44.8	0.33	269.5	0.9	1.0	0.0	0.1	
265	Leading	424.2	-52.2	476.4	137.7	40.3	0.29	258.7	16.6	1.0	0.0	0.2	0.080
	Trailing	327.2	-17.7	344.8	137.6	46.9	0.34	278.4	-3.1	3.0	0.0	0.3	

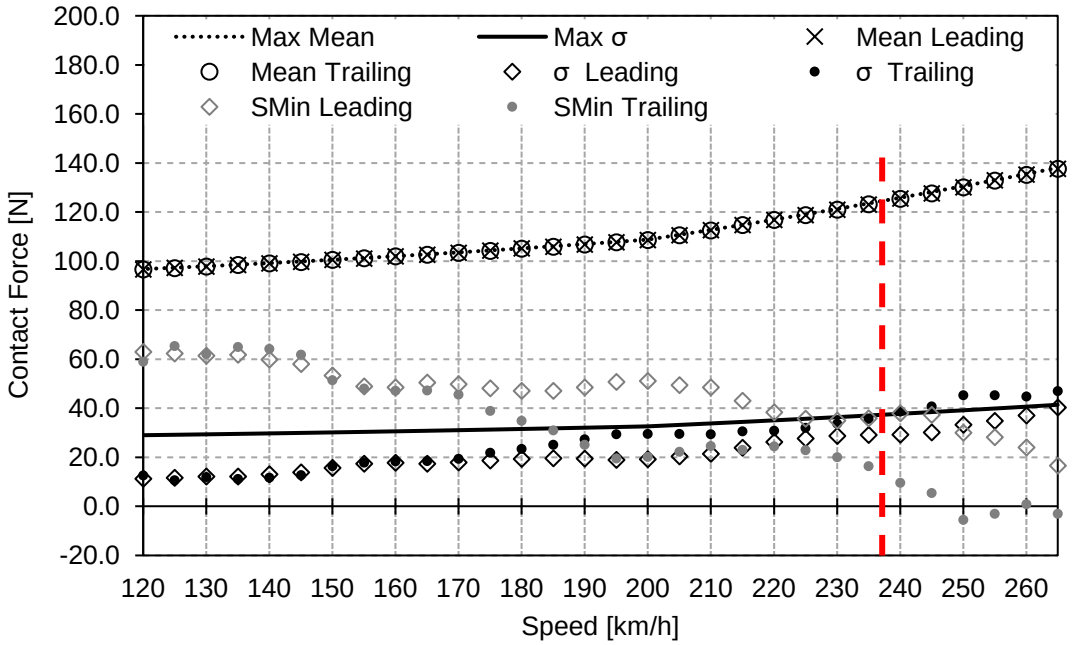

Figure 4.32: LP12_Pant1_S35 results for multiple pantographs, running at various speeds

Looking at Figure 4.32 it is shown that the standard deviation of the trailing pantograph for a travel speed of 240 km/h and higher surpasses the maximum standard deviation line. Table 4.14 shows a contact loss for 240km/h, which also surpasses the limit of 0.1%. So, the limit operation velocity is 235 km/h and the limiting factors for this case scenario are the standard deviation and the loss of contact of the trailing pantograph. Figure 4.33 presents the contact force for LP12_Pant1_S35_V240.

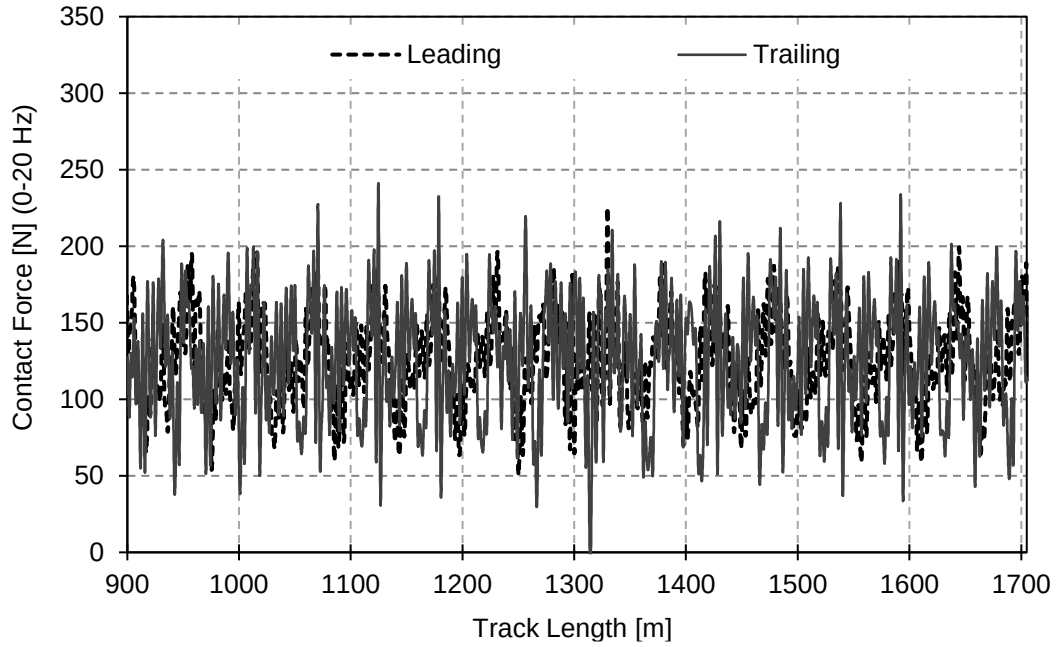

Figure 4.33: Contact forces results for LP12_Pant1_S35_V240

Figure 4.33 shows that the contact loss is located where the two catenary sections overlap, and the trailing pantograph contact force is shown to be affected by the leading pantograph. One of the

limiting factors of this catenary is the contact loss that occurs due to the overlapping arrangement.

The dynamic analysis results obtained of the interaction of the LP12_Pant1 pairing, considering 2 pantographs, with a separation between them of 85 m, for various speeds are represented in Figure 4.34 and Table 4.15.

Table 4.15: LP12_Pant1_S85 results for multiple pantographs, running at various speeds

Speed [km/h]	Pant	Contact Force [N]								Contact loss			Steady Arm Uplift [m]
		F_{max}	F_{min}	ΔF	F_m	σ	σ/F_m	S_{max}	S_{Min}	$CL_{\#}$	CL_t [s]	$CL_{\%}$ [%]	
120	Leading	298.2	65.3	232.9	96.6	10.7	0.11	128.7	64.5	0	0.0	0.00	0.020
	Trailing	259.5	43.9	215.6	96.6	13.0	0.13	135.6	57.7	0	0.0	0.00	
125	Leading	299.5	67.0	232.5	97.2	11.0	0.11	130.2	64.2	0	0.0	0.00	0.019
	Trailing	285.7	61.0	224.7	97.2	12.5	0.13	134.8	59.6	0	0.0	0.00	
130	Leading	149.6	56.5	93.1	97.8	11.0	0.11	130.9	64.7	0	0.0	0.00	0.019
	Trailing	154.9	52.0	102.9	97.8	14.0	0.14	139.7	55.9	0	0.0	0.00	
135	Leading	145.8	57.4	88.3	98.3	10.9	0.11	131.0	65.7	0	0.0	0.00	0.018
	Trailing	175.5	54.7	120.8	98.4	14.3	0.14	141.2	55.6	0	0.0	0.00	
140	Leading	143.1	64.8	78.3	99.0	12.2	0.12	135.8	62.3	0	0.0	0.00	0.017
	Trailing	145.9	52.7	93.1	99.1	16.5	0.17	148.5	49.6	0	0.0	0.00	
145	Leading	149.5	57.5	92.0	99.7	13.4	0.13	139.8	59.5	0	0.0	0.00	0.017
	Trailing	156.6	53.8	102.8	99.6	16.6	0.17	149.5	49.8	0	0.0	0.00	
150	Leading	153.3	44.0	109.3	100.5	16.3	0.16	149.6	51.5	0	0.0	0.00	0.018
	Trailing	168.8	15.8	153.0	100.5	23.0	0.23	169.4	31.6	0	0.0	0.00	
155	Leading	158.2	47.1	111.1	101.1	17.9	0.18	154.7	47.5	0	0.0	0.00	0.020
	Trailing	185.5	28.0	157.4	101.1	26.0	0.26	179.2	22.9	0	0.0	0.00	
160	Leading	194.5	56.9	137.7	101.9	17.2	0.17	153.4	50.3	0	0.0	0.00	0.022
	Trailing	186.9	28.0	158.9	101.9	26.1	0.26	180.1	23.8	0	0.0	0.00	
165	Leading	153.0	56.2	96.8	102.6	16.0	0.16	150.5	54.7	0	0.0	0.00	0.027
	Trailing	168.8	25.0	143.8	102.6	23.9	0.23	174.4	30.8	0	0.0	0.00	
170	Leading	161.8	49.3	112.5	103.4	16.6	0.16	153.2	53.6	0	0.0	0.00	0.029
	Trailing	176.1	26.3	149.8	103.4	24.1	0.23	175.7	31.1	0	0.0	0.00	
175	Leading	165.6	53.6	112.1	104.2	17.1	0.16	155.4	53.0	0	0.0	0.00	0.031
	Trailing	186.1	14.0	172.1	104.2	24.6	0.24	178.0	30.3	0	0.0	0.00	
180	Leading	284.3	61.5	222.8	105.1	17.7	0.17	158.2	52.1	0	0.0	0.00	0.034
	Trailing	298.7	20.4	278.2	105.1	25.4	0.24	181.3	28.9	0	0.0	0.00	
185	Leading	166.2	59.9	106.3	105.9	18.0	0.17	159.8	51.9	0	0.0	0.00	0.033
	Trailing	287.9	25.1	262.8	106.0	24.8	0.23	180.3	31.6	0	0.0	0.00	
190	Leading	164.5	49.5	115.0	106.8	18.0	0.17	160.8	52.7	0	0.0	0.00	0.033
	Trailing	289.8	8.0	281.8	106.9	27.7	0.26	190.1	23.6	0	0.0	0.00	
195	Leading	169.4	54.8	114.6	107.6	17.8	0.17	161.1	54.2	0	0.0	0.00	0.036
	Trailing	270.0	23.4	246.6	107.7	27.9	0.26	191.5	23.8	0	0.0	0.00	
200	Leading	299.0	59.8	239.2	108.6	18.1	0.17	162.9	54.3	0	0.0	0.00	0.040
	Trailing	245.1	20.8	224.3	108.5	26.2	0.24	187.2	29.9	0	0.0	0.00	
205	Leading	181.7	56.2	125.4	110.6	19.0	0.17	167.7	53.5	0	0.0	0.00	0.043
	Trailing	217.4	22.9	194.5	110.5	26.3	0.24	189.4	31.7	0	0.0	0.00	
…	…	…	…	…	…	…	…	…	…	…	…	…	…

Speed [km/h]	Pant	Contact Force [N]								Contact loss			Steady Arm Uplift [m]
		F_{max}	F_{min}	ΔF	F_m	σ	σ/F_m	S_{max}	S_{Min}	$CL_{\#}$	CL_t [s]	$CL_{\%}$ [%]	
210	Leading	167.3	61.2	106.2	112.6	19.6	0.17	171.5	53.7	0	0.0	0.00	0.046
	Trailing	234.5	22.3	212.2	112.6	28.9	0.26	199.2	25.9	0	0.0	0.00	
215	Leading	168.9	52.1	116.8	114.7	21.4	0.19	178.8	50.6	0	0.0	0.00	0.051
	Trailing	286.6	26.4	260.2	114.7	30.2	0.26	205.4	23.9	0	0.0	0.00	
220	Leading	194.3	70.2	124.0	116.8	22.4	0.19	184.1	49.4	0	0.0	0.00	0.050
	Trailing	250.4	16.8	233.6	116.8	30.8	0.26	209.2	24.3	0	0.0	0.00	
225	Leading	184.6	71.2	113.4	118.7	23.3	0.20	188.5	48.9	0	0.0	0.00	0.049
	Trailing	215.6	25.9	189.7	118.7	34.1	0.29	221.0	16.5	0	0.0	0.00	
230	Leading	206.3	64.7	141.5	120.9	25.1	0.21	196.2	45.7	0	0.0	0.00	0.049
	Trailing	225.1	-8.3	233.4	121.0	37.9	0.31	234.8	7.2	3	0.0	0.17	
235	Leading	210.1	65.5	144.6	123.2	25.8	0.21	200.4	45.9	0	0.0	0.00	0.051
	Trailing	220.1	-7.2	227.3	123.2	40.1	0.33	243.4	3.0	4	0.0	0.36	
240	Leading	232.9	62.7	170.2	125.4	26.6	0.21	205.3	45.6	0	0.0	0.00	0.053
	Trailing	224.5	6.9	217.6	125.4	38.6	0.31	241.2	9.7	0	0.0	0.00	
245	Leading	241.3	68.2	173.1	127.6	28.0	0.22	211.5	43.7	0	0.0	0.0	0.057
	Trailing	280.4	14.7	265.7	127.7	43.9	0.34	259.2	-3.9	0	0.0	0.0	
250	Leading	530.3	65.0	465.3	130.1	30.8	0.24	222.6	37.6	0	0.0	0.0	0.060
	Trailing	493.8	2.1	491.7	130.1	48.9	0.38	276.8	-16.6	0	0.0	0.0	
255	Leading	232.4	58.9	173.6	132.9	31.2	0.23	226.4	39.4	0.0	0.0	0.0	0.067
	Trailing	285.0	-4.2	289.2	132.8	49.6	0.37	281.6	-15.9	1.0	0.0	0.1	
260	Leading	296.1	6.4	289.7	135.4	33.3	0.25	235.1	35.6	0.0	0.0	0.0	0.078
	Trailing	289.8	-5.9	295.7	135.3	53.1	0.39	294.5	-23.8	3.0	0.0	0.2	
265	Leading	411.6	-46.2	457.8	137.7	37.2	0.27	249.4	26.0	1.0	0.0	0.2	0.086
	Trailing	334.1	-8.4	342.5	137.8	55.8	0.40	305.1	-29.5	5.0	0.0	0.3	

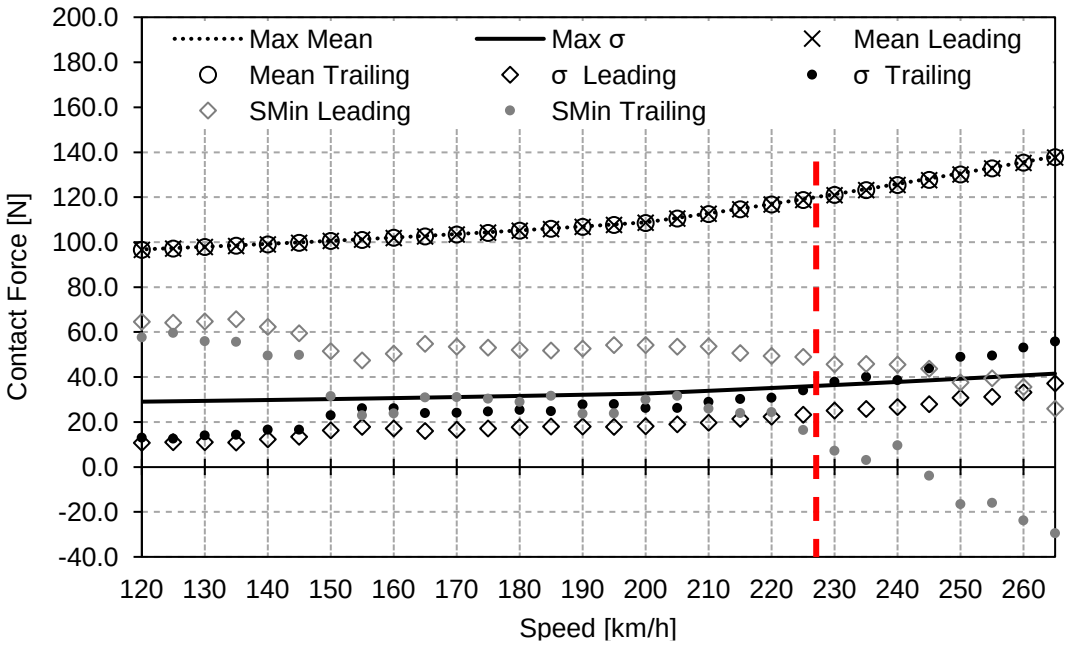

Figure 4.34: LP12_Pant1_S85 results for multiple pantographs, running at various speeds

The dynamic analysis results obtain from the case LP12_Pant1_S85 are similar .to the ones obtained for the case LP12_Pant1_S35 These similarities are that the limit operating parameters are the same and occur for the trailing pantograph. However, the exploration velocity is smaller for a separation of 85 m. In Figure 4.34 the standard deviation surpasses its respective threshold for 230 km/h. For this same speed, Table 4.15 determines that the ratio between the standard deviation and the mean contact force is 0.31, above the threshold of 0.3. This table also shows a contact loss superior that 0.1 % for the trailing pantograph, for 230 km/h. So, the limit operation velocity is 225 km/h and the limiting factors are the contact loss and the standard deviation. Figure 4.35 shows the contact forces along the track of LP12_Pant1_S85_V230.

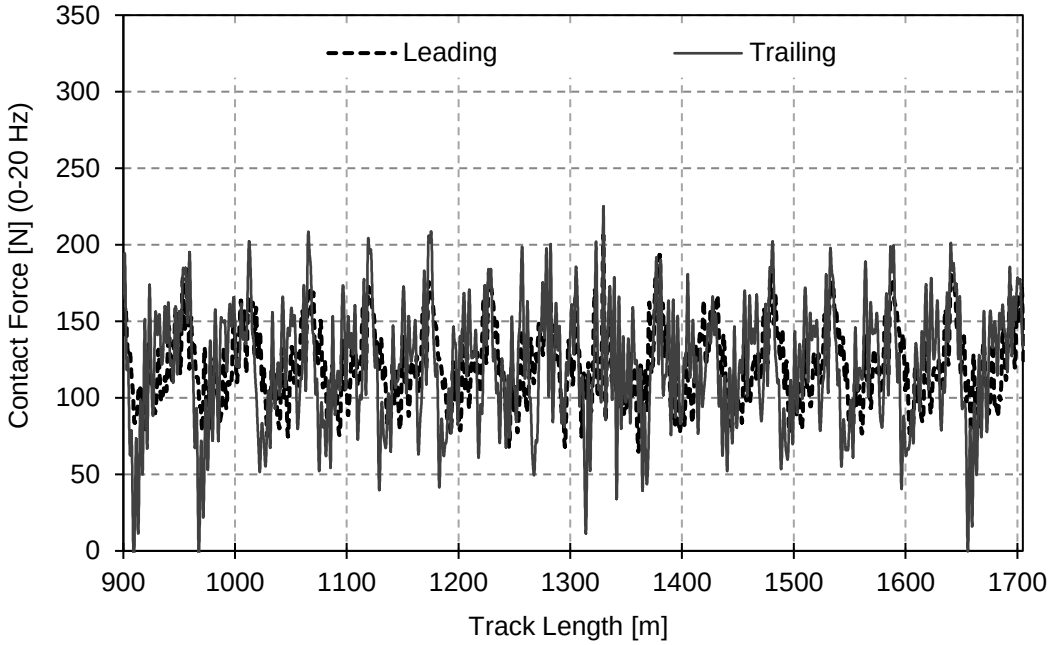

Figure 4.35: Contact forces results for LP12_Pant1_S85_V230

Figure 4.35 shows the contact forces along the track for the LP12_S85_V230 simulation, where the contact losses are shown to occur at steady arms that do not represent the section where the two catenaries overlap. The maximum exploration velocity for this case is 225 km/h and the velocities are the standard deviation and the contact loss.

The dynamic analysis results obtained of the interaction of the LP12_Pant1 pairing, considering 2 pantographs, with a separation between them of 100 m, for various speeds are represented in Figure 4.36 and Table 4.16.

Table 4.16: LP12_Pant1_S100 results for multiple pantographs, running at various speeds

Speed [km/h]	Pant	Contact Force [N]								Contact loss			Steady Arm Uplift [m]
		F_{max}	F_{min}	ΔF	F_m	σ	σ/F_m	S_{max}	S_{Min}	$CL_{\#}$	CL_t [s]	$CL_{\%}$ [%]	
120	Leading	265.5	69.0	196.5	96.6	10.3	0.11	127.6	65.6	0	0.0	0.00	0.018
	Trailing	284.5	57.9	226.6	96.6	11.2	0.12	130.3	62.9	0	0.0	0.00	
…	…	…	…	…	…	…	…	…	…	…	…	…	…

Speed [km/h]	Pant	Contact Force [N]								Contact loss			Steady Arm Uplift [m]
		F_{max}	F_{min}	ΔF	F_m	σ	σ/F_m	S_{max}	S_{Min}	$CL_{\#}$	CL_t [s]	$CL_{\%}$ [%]	
125	Leading	270.6	66.5	204.1	97.2	11.2	0.12	130.8	63.7	0	0.0	0.00	0.018
	Trailing	292.7	53.0	239.7	97.2	12.9	0.13	135.8	58.6	0	0.0	0.00	
130	Leading	147.2	59.2	88.0	97.8	10.9	0.11	130.4	65.1	0	0.0	0.00	0.018
	Trailing	152.1	57.6	94.5	97.8	12.4	0.13	135.1	60.4	0	0.0	0.00	
135	Leading	148.8	63.2	85.6	98.4	10.7	0.11	130.6	66.1	0	0.0	0.00	0.019
	Trailing	181.9	58.7	123.2	98.4	12.2	0.12	135.0	61.8	0	0.0	0.00	
140	Leading	137.1	60.3	76.8	99.1	12.2	0.12	135.6	62.6	0	0.0	0.00	0.018
	Trailing	148.8	60.7	88.1	99.1	13.2	0.13	138.7	59.4	0	0.0	0.00	
145	Leading	150.1	61.3	88.8	99.6	13.2	0.13	139.3	60.0	0	0.0	0.00	0.018
	Trailing	155.1	56.0	99.1	99.7	14.3	0.14	142.7	56.7	0	0.0	0.00	
150	Leading	153.0	47.3	105.6	100.5	16.1	0.16	148.8	52.2	0	0.0	0.00	0.018
	Trailing	191.4	43.4	148.0	100.5	17.3	0.17	152.3	48.7	0	0.0	0.00	
155	Leading	155.6	45.6	110.0	101.1	17.9	0.18	154.8	47.4	0	0.0	0.00	0.019
	Trailing	195.3	23.0	172.3	101.1	22.1	0.22	167.4	34.8	0	0.0	0.00	
160	Leading	189.7	57.8	131.8	102.0	17.3	0.17	153.9	50.1	0	0.0	0.00	0.020
	Trailing	213.5	36.5	177.1	101.9	24.1	0.24	174.3	29.6	0	0.0	0.00	
165	Leading	153.1	55.5	97.6	102.6	16.0	0.16	150.5	54.7	0	0.0	0.00	0.025
	Trailing	193.3	21.1	172.2	102.6	26.8	0.26	182.9	22.3	0	0.0	0.00	
170	Leading	156.6	46.7	109.9	103.5	17.1	0.16	154.7	52.3	0	0.0	0.00	0.028
	Trailing	297.0	14.9	282.2	103.5	30.3	0.29	194.3	12.8	0	0.0	0.00	
175	Leading	193.1	58.3	134.8	104.3	18.0	0.17	158.1	50.4	0	0.0	0.00	0.030
	Trailing	192.8	-3.8	196.6	104.1	31.8	0.31	199.6	8.6	1	0.0	0.14	
180	Leading	297.9	57.0	240.9	105.1	18.5	0.18	160.6	49.6	0	0.0	0.00	0.031
	Trailing	299.8	15.4	284.4	105.1	29.7	0.28	194.1	16.1	0	0.0	0.00	
185	Leading	161.8	54.9	106.8	105.9	18.4	0.17	161.1	50.7	0	0.0	0.00	0.032
	Trailing	210.3	16.5	193.8	105.9	28.6	0.27	191.7	20.1	0	0.0	0.00	
190	Leading	187.6	43.6	144.0	106.8	18.2	0.17	161.3	52.3	0	0.0	0.00	0.038
	Trailing	183.5	9.5	174.0	106.9	28.0	0.26	190.8	23.0	0	0.0	0.00	
195	Leading	193.9	53.3	140.6	107.6	17.4	0.16	159.8	55.4	0	0.0	0.00	0.039
	Trailing	175.0	14.4	160.6	107.7	28.1	0.26	192.1	23.3	0	0.0	0.00	
200	Leading	270.5	54.8	215.7	108.5	17.8	0.16	162.0	55.0	0	0.0	0.00	0.041
	Trailing	266.7	13.8	252.9	108.7	29.9	0.28	198.5	18.9	0	0.0	0.00	
205	Leading	212.4	52.1	160.3	110.6	19.0	0.17	167.5	53.6	0	0.0	0.00	0.041
	Trailing	189.8	3.7	186.1	110.6	31.7	0.29	205.8	15.4	0	0.0	0.00	
210	Leading	180.2	52.8	127.4	112.6	19.6	0.17	171.5	53.7	0	0.0	0.00	0.044
	Trailing	197.0	-6.9	203.8	112.6	33.3	0.30	212.5	12.7	3	0.0	0.27	
215	Leading	177.3	53.4	123.8	114.7	22.1	0.19	181.0	48.4	0	0.0	0.00	0.052
	Trailing	206.2	7.1	199.1	114.6	35.5	0.31	221.2	8.0	0	0.0	0.00	
220	Leading	196.4	58.6	137.9	116.8	24.3	0.21	189.8	43.8	0	0.0	0.00	0.057
	Trailing	223.5	3.4	220.1	116.7	38.6	0.33	232.5	0.9	0	0.0	0.00	
225	Leading	195.3	52.9	142.4	118.8	25.9	0.22	196.3	41.2	0	0.0	0.00	0.067
	Trailing	333.4	-26.5	359.9	118.7	40.4	0.34	239.9	-2.4	2	0.0	0.16	
…	…	…	…	…	…	…	…	…	…	…	…	…	…

Speed [km/h]	Pant	Contact Force [N]								Contact loss			Steady Arm Uplift [m]
		F_{max}	F_{min}	ΔF	F_m	σ	σ/F_m	S_{max}	S_{Min}	$CL_{\#}$	CL_t [s]	$CL_{\%}$ [%]	
230	Leading	206.3	60.0	146.2	121.0	27.4	0.23	203.2	38.7	0	0.0	0.00	0.074
	Trailing	361.9	-15.0	376.9	120.9	41.0	0.34	244.0	-2.2	1	0.0	0.08	
235	Leading	210.8	58.3	152.5	123.1	28.1	0.23	207.4	38.9	0	0.0	0.00	0.076
	Trailing	409.2	-17.2	426.5	123.2	42.2	0.34	249.7	-3.4	1	0.0	0.07	
240	Leading	239.7	57.1	182.6	125.4	28.7	0.23	211.6	39.3	0	0.0	0.00	0.071
	Trailing	420.4	-37.5	457.9	125.5	42.7	0.34	253.5	-2.5	1	0.0	0.11	
245	Leading	244.0	66.2	177.8	127.6	29.3	0.23	215.7	39.6	0	0.0	0.0	0.066
	Trailing	373.1	-38.3	411.5	127.7	42.4	0.33	254.7	0.6	2	0.0	0.2	
250	Leading	530.4	67.2	463.2	130.0	31.9	0.25	225.8	34.3	0	0.0	0.0	0.065
	Trailing	289.4	-15.7	305.0	129.8	41.5	0.32	254.3	5.3	1	0.0	0.1	
255	Leading	251.8	48.5	203.3	132.9	31.9	0.24	228.5	37.2	0.0	0.0	0.0	0.068
	Trailing	368.6	-44.1	412.7	132.7	43.1	0.32	262.1	3.4	2.0	0.0	0.1	
260	Leading	341.7	-11.9	353.6	135.3	33.9	0.25	236.9	33.7	1.0	0.0	0.1	0.073
	Trailing	374.3	-38.0	412.3	135.2	42.0	0.31	261.1	9.3	1.0	0.0	0.1	
265	Leading	439.8	-51.3	491.1	137.7	38.0	0.28	251.8	23.7	1.0	0.0	0.2	0.076
	Trailing	286.8	-15.2	301.9	137.7	42.9	0.31	266.5	8.9	1.0	0.0	0.1	

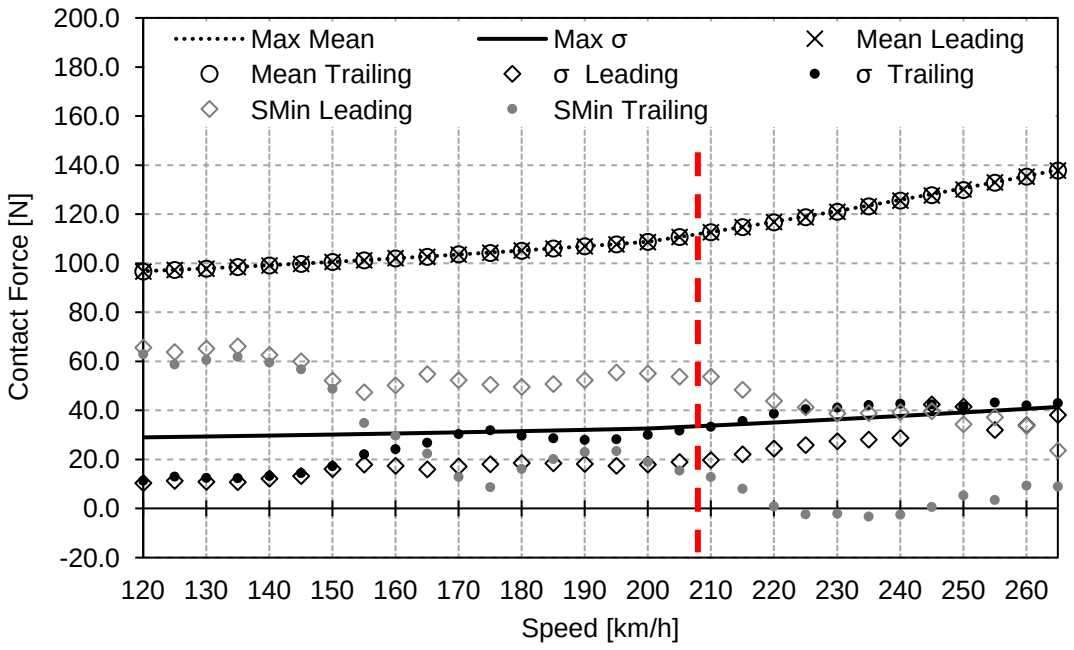

Figure 4.36: LP12_Pant1_S100 results for multiple pantographs, running at various speeds

Looking at Table 4.16, one important note regarding the LP12_Pant1_S100 case is that the dynamic analysis response for a separation operation of 100 m separation, travelling at 175 km/h, it is clearly noticeable that the trailing pantograph presents a contact loss superior to 0.1. It is also observed in Figure 4.36 that the trailing pantograph presents a high standard deviation which, in comparison with the obtained from the surrounding velocities, leads to conclude that the leading pantograph induces a harmonic disturbance in the catenary that resonates with the trailing pantograph. Therefore, the train arrangements with 100 m pantograph spacing should be avoided or the service speed changed to avoid

this harmonic effect. In Figure 4.36 it is seen that the trailing pantograph standard deviation surpasses the limit, again, at 215 km/h. While the statistical minimum has negative values for speeds between 225 and 240 km/h inclusive and suffers a local minimum for 175 km/h, because of the harmonic disturbance. Table 4.16 show that for 210 km/h there is contact losses above the 0.1% for the trailing pantograph. So, the exploration velocity is 205 km/h and the limiting factor is the contact loss that can be seen in Figure 4.37.

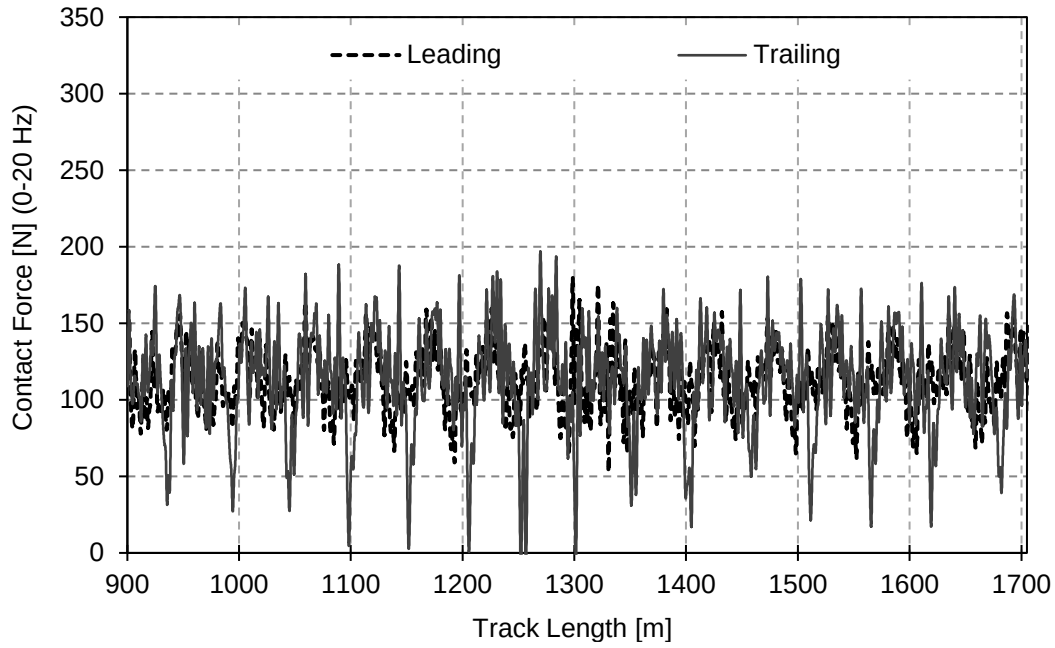

Figure 4.37: Contact forces results for LP12_Pant1_S100_V210

Figure 4.37 shows the contact forces along the track for the LP12_S100_V210 simulation, where the contact losses are shown to occur at steady arms that do not represent the section where the two catenaries overlap.

The dynamic analysis results obtained of the interaction of the LP12_Pant1 pairing, considering 2 pantographs, with a separation between them of 200 m, for various speeds are represented in Figure 4.38 and Table 4.17.

Table 4.17: LP12_Pant1_S200 results for multiple pantographs, running at various speeds

Speed [km/h]	Pant	Contact Force [N]								Contact loss			Steady Arm Uplift [m]
		F_{max}	F_{min}	ΔF	F_m	σ	σ/F_m	S_{max}	S_{Min}	$CL_{\#}$	CL_t [s]	$CL_{\%}$ [%]	
120	Leading	299.1	65.2	233.9	96.6	10.6	0.11	128.6	64.7	0	0.0	0.00	0.020
	Trailing	274.7	63.3	211.4	96.6	12.2	0.13	133.2	60.1	0	0.0	0.00	
125	Leading	299.5	65.9	233.6	97.2	11.0	0.11	130.3	64.2	0	0.0	0.00	0.020
	Trailing	279.9	60.9	219.0	97.2	11.4	0.12	131.3	63.1	0	0.0	0.00	
130	Leading	150.0	57.8	92.3	97.8	10.9	0.11	130.6	65.0	0	0.0	0.00	0.018
	Trailing	226.3	62.7	163.6	97.8	12.3	0.13	134.7	60.9	0	0.0	0.00	
…	…	…	…	…	…	…	…	…	…	…	…	…	…

Speed [km/h]	Pant	Contact Force [N]								Contact loss			Steady Arm Uplift [m]
		F_{max}	F_{min}	ΔF	F_m	σ	σ/F_m	S_{max}	S_{Min}	$CL_{\#}$	CL_t [s]	$CL_{\%}$ [%]	
135	Leading	147.5	59.2	88.3	98.4	10.9	0.11	131.2	65.5	0	0.0	0.00	0.019
	Trailing	151.4	57.8	93.7	98.4	13.1	0.13	137.6	59.1	0	0.0	0.00	
140	Leading	140.7	63.1	77.6	99.1	12.1	0.12	135.3	62.9	0	0.0	0.00	0.017
	Trailing	144.7	57.5	87.2	99.1	13.5	0.14	139.6	58.5	0	0.0	0.00	
145	Leading	148.5	60.4	88.0	99.7	13.0	0.13	138.8	60.5	0	0.0	0.00	0.017
	Trailing	152.3	56.9	95.4	99.7	14.8	0.15	144.0	55.4	0	0.0	0.00	
150	Leading	155.1	46.4	108.8	100.5	16.2	0.16	149.1	51.9	0	0.0	0.00	0.017
	Trailing	182.3	28.1	154.2	100.5	19.5	0.19	159.1	41.9	0	0.0	0.00	
155	Leading	157.3	46.6	110.7	101.1	17.7	0.18	154.2	47.9	0	0.0	0.00	0.019
	Trailing	205.3	31.5	173.7	101.0	23.9	0.24	172.7	29.4	0	0.0	0.00	
160	Leading	201.1	55.3	145.8	101.9	17.2	0.17	153.6	50.3	0	0.0	0.00	0.021
	Trailing	195.6	34.9	160.7	102.0	22.8	0.22	170.4	33.5	0	0.0	0.00	
165	Leading	151.2	54.7	96.5	102.6	15.9	0.15	150.3	55.0	0	0.0	0.00	0.022
	Trailing	174.8	39.6	135.2	102.6	21.0	0.20	165.6	39.6	0	0.0	0.00	
170	Leading	159.0	46.4	112.7	103.5	16.6	0.16	153.4	53.5	0	0.0	0.00	0.034
	Trailing	180.0	20.3	159.7	103.5	21.8	0.21	168.9	38.1	0	0.0	0.00	
175	Leading	177.0	56.2	120.8	104.3	17.2	0.16	155.9	52.7	0	0.0	0.00	0.033
	Trailing	216.8	30.7	186.1	104.2	25.1	0.24	179.5	28.8	0	0.0	0.00	
180	Leading	228.1	59.7	168.5	105.1	17.8	0.17	158.4	51.8	0	0.0	0.00	0.029
	Trailing	297.4	16.0	281.4	105.1	27.3	0.26	187.1	23.1	0	0.0	0.00	
185	Leading	165.2	56.7	108.5	105.9	17.8	0.17	159.3	52.6	0	0.0	0.00	0.032
	Trailing	237.9	15.3	222.6	105.9	26.8	0.25	186.2	25.6	0	0.0	0.00	
190	Leading	160.1	50.6	109.4	106.6	17.6	0.17	159.5	53.7	0	0.0	0.00	0.031
	Trailing	271.8	27.6	244.2	106.8	27.2	0.25	188.3	25.3	0	0.0	0.00	
195	Leading	168.8	53.6	115.2	107.6	17.2	0.16	159.2	56.0	0	0.0	0.00	0.035
	Trailing	221.7	24.2	197.6	107.7	26.0	0.24	185.8	29.7	0	0.0	0.00	
200	Leading	298.0	60.7	237.3	108.6	17.8	0.16	162.1	55.1	0	0.0	0.00	0.036
	Trailing	190.3	16.2	174.2	108.5	26.1	0.24	186.9	30.1	0	0.0	0.00	
205	Leading	195.5	52.7	142.9	110.6	19.0	0.17	167.5	53.6	0	0.0	0.00	0.035
	Trailing	190.5	-1.6	192.1	110.5	27.9	0.25	194.0	26.9	1	0.0	0.00	
210	Leading	170.0	56.6	113.4	112.6	19.7	0.17	171.6	53.6	0	0.0	0.00	0.038
	Trailing	216.0	25.8	190.2	112.6	29.1	0.26	199.9	25.2	0	0.0	0.00	
215	Leading	179.7	54.0	125.8	114.7	22.4	0.20	181.8	47.6	0	0.0	0.00	0.039
	Trailing	202.7	-0.1	202.8	114.6	31.5	0.27	209.0	20.2	1	0.0	0.00	
220	Leading	196.2	62.7	133.6	116.8	24.1	0.21	189.1	44.5	0	0.0	0.00	0.045
	Trailing	219.6	3.2	216.4	116.8	35.3	0.30	222.6	11.0	0	0.0	0.00	
225	Leading	191.6	62.4	129.2	118.7	25.3	0.21	194.7	42.8	0	0.0	0.00	0.058
	Trailing	273.1	14.9	258.2	118.9	39.8	0.33	238.5	-0.6	0	0.0	0.00	
230	Leading	212.5	66.0	146.4	121.0	26.5	0.22	200.3	41.6	0	0.0	0.00	0.065
	Trailing	377.0	-44.5	421.5	121.0	43.5	0.36	251.5	-9.6	1	0.0	0.13	
235	Leading	222.2	62.2	160.0	123.2	26.9	0.22	203.9	42.4	0	0.0	0.00	0.062
	Trailing	255.0	-4.1	259.1	123.0	44.8	0.36	257.5	-11.4	1	0.0	0.08	
…	…	…	…	…	…	…	…	…	…	…	…	…	…

Speed [km/h]	Pant	Contact Force [N]								Contact loss			Steady Arm Uplift [m]
		F_{max}	F_{min}	ΔF	F_m	σ	σ/F_m	S_{max}	S_{Min}	$CL_{\#}$	CL_t [s]	$CL_{\%}$ [%]	
240	Leading	234.1	61.7	172.4	125.5	27.4	0.22	207.7	43.2	0	0.0	0.00	0.072
	Trailing	267.4	-2.8	270.2	125.3	47.3	0.38	267.2	-16.6	2	0.0	0.19	
245	Leading	239.8	63.8	176.0	127.6	28.3	0.22	212.6	42.6	0	0.0	0.0	0.074
	Trailing	239.7	-6.8	246.5	127.5	50.3	0.39	278.4	-23.4	2	0.0	0.2	
250	Leading	535.2	66.7	468.5	130.1	30.8	0.24	222.5	37.7	0	0.0	0.0	0.083
	Trailing	446.7	-8.2	455.0	130.1	54.5	0.42	293.7	-33.5	2	0.1	0.5	
255	Leading	242.9	33.6	209.3	132.9	31.2	0.24	226.6	39.2	0.0	0.0	0.0	0.096
	Trailing	312.6	-6.0	318.5	132.9	56.7	0.43	302.9	-37.2	1.0	0.0	0.2	
260	Leading	279.5	8.3	271.2	135.3	32.9	0.24	233.9	36.7	0.0	0.0	0.0	0.098
	Trailing	303.7	-14.0	317.7	135.3	55.5	0.41	301.9	-31.2	4.0	0.1	0.5	
265	Leading	353.3	-37.5	390.7	137.7	36.0	0.26	245.7	29.7	1.0	0.0	0.1	0.096
	Trailing	288.1	-7.0	295.1	137.7	56.5	0.41	307.3	-31.9	4.0	0.1	0.5	

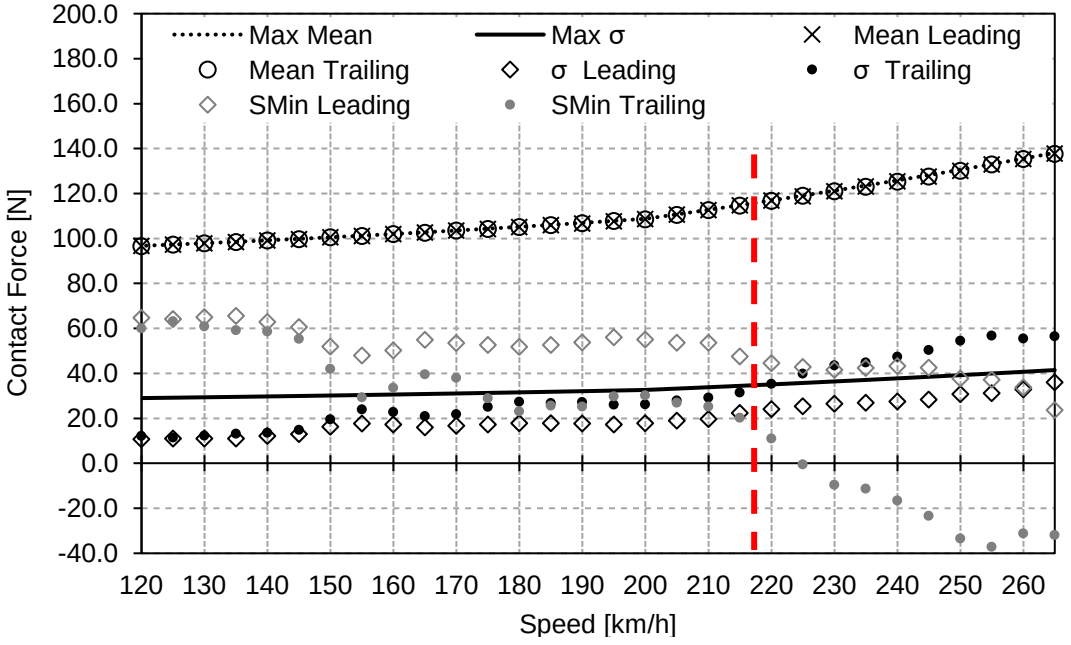

Figure 4.38: LP12_Pant1_S200 results for multiple pantographs, running at various speeds

The last separation considered for the LP12_Pant1 pantograph catenary pair is 200 m. In Figure 4.38 it is observed that the standard deviation of the trailing pantograph for 220 km/h, surpasses its respective threshold. By observing Table 4.17 no other dynamic analysis parameter exceeds their respective threshold. So, the exploration velocity is 215 km/h, where the limiting factor is the standard deviation of the trailing pantograph. Figure 4.39 shows the contact forces along the track of LP12_Pant1_S200_V200 operation.

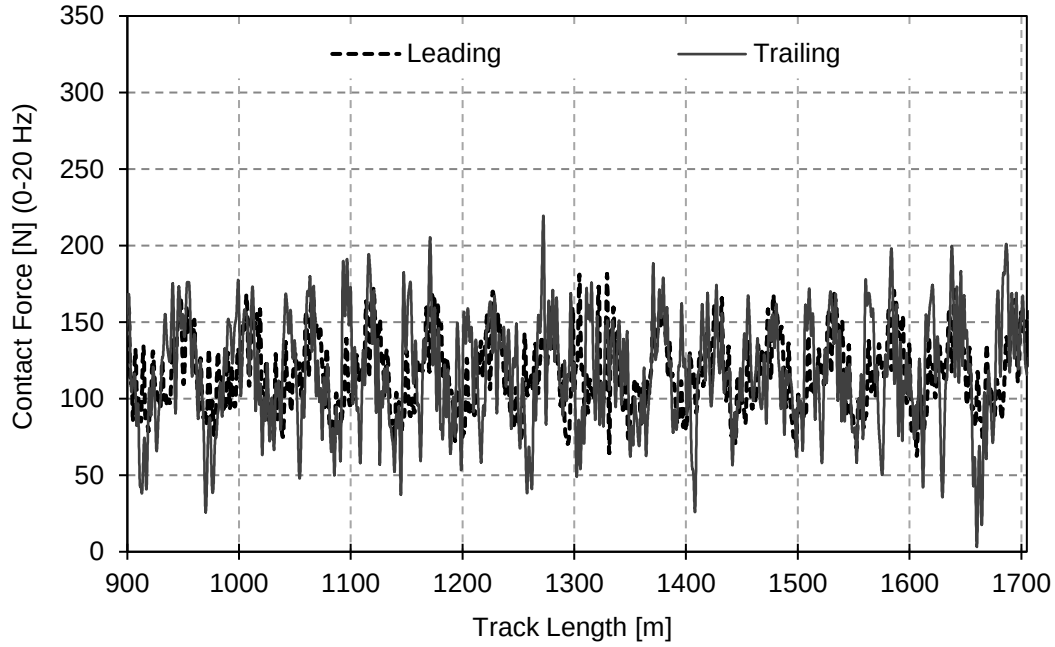

Figure 4.39: Contact forces results for LP12_Pant1_S200_V220

In Figure 4.39 the contact loss that occurs for LP12_Pant1_S200_V220 operation is located near the end of the zone of interest considered. This means that the limiting of the operation velocity has nothing to do with the overlapping arrangement. This figure also permits to conclude that the trailing pantograph is affected by the leading pantograph propagation wave.

Figure 4.40 represents the maximum steady arm uplift for all the pantograph separations considered for the LP12_Pant1 pantograph catenary pairing.

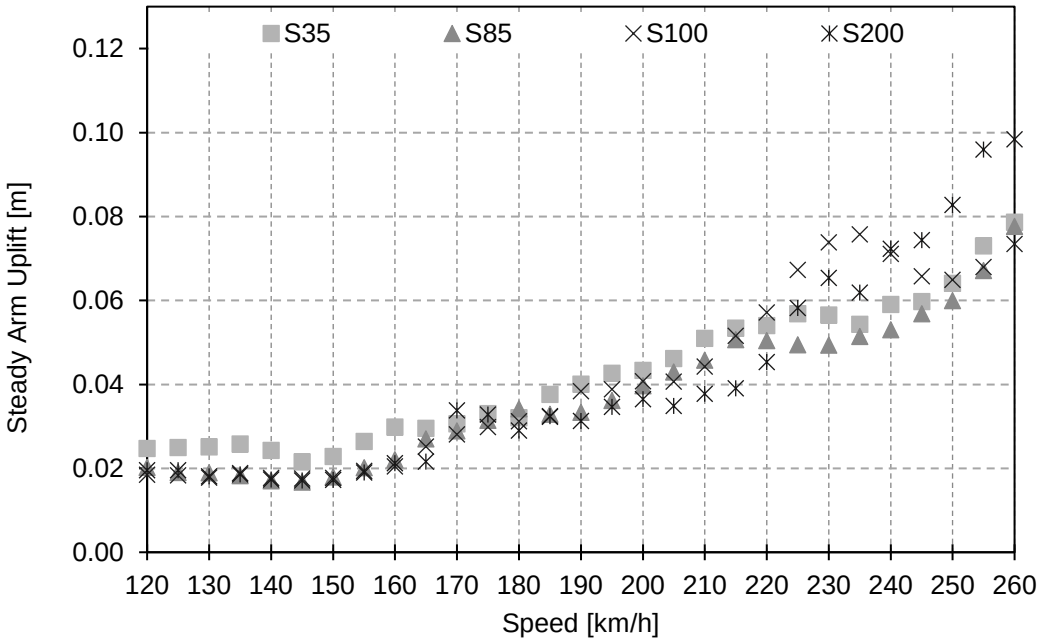

Figure 4.40: LP12_Pant1 steady arm uplift results for multiple pantographs systems, running at various speeds

In Figure 4.40 the maximum steady arm uplift is seen to occur for LP12_Pant1_S200_V260 with 0.098. In this figure, the maximum steady arm uplift can be observed to increase with the velocity considered, where its maximum is shown to occur for a pantograph separation of 200 m. Even though, the separation that tends to have a bigger maximum steady arm uplift is 35 m.

When comparing all the LP12_Pant1 multiple pantographs cases, the maximum exploration velocity is 205 km/h. The critical separation is 100 m for this pantograph catenary pair, and it is possible to conclude that the factor that is restricting the use of higher speeds is the loss of contact forces for the trailing pantograph. So, the maximum exploration velocity for a multiple pantograph scenario for LP12_Pant1 is 45 km/h lower than obtained from the single operating pantograph simulations.

When a pantograph is exchanged and assuming that both pantographs have a good representation model, and where design to operate at the same conditions. The speed limit obtained for each case study in the same conditions should be similar. This means that the maximum speed obtained for the LP12_Pant1 simulations should be similar to the one obtained from the LP12_Pant2 simulations.

The dynamic analysis results obtained of the interaction of the LP12_Pant2 pairing, considering 2 pantographs, with a separation between them of 35 m, for various speeds are represented in Figure 4.41 and Table 4.18.

Table 4.18: LP12_Pant2_S35 results for multiple pantographs, running at various speeds

Speed [km/h]	Pant	Contact Force [N]								Contact loss			Steady Arm Uplift [m]
		F_{max}	F_{min}	ΔF	F_m	σ	σ / F_m	S_{max}	S_{Min}	$CL_{\#}$	CL_t [s]	$CL_{\%}$ [%]	
120	Leading	154.6	41.2	113.5	96.6	13.1	0.14	135.9	57.2	0	0.0	0.0	0.024
	Trailing	152.2	13.7	138.5	96.4	12.3	0.13	133.3	59.5	0	0.0	0.0	
125	Leading	182.9	32.8	150.1	97.3	13.8	0.14	138.6	56.0	0	0.0	0.0	0.025
	Trailing	166.5	30.8	135.7	97.1	12.2	0.13	133.9	60.4	0	0.0	0.0	
130	Leading	172.3	35.7	136.6	97.8	14.6	0.15	141.6	54.1	0	0.0	0.0	0.025
	Trailing	167.5	43.2	124.3	97.7	13.0	0.13	136.9	58.6	0	0.0	0.0	
135	Leading	153.2	31.7	121.6	98.4	15.4	0.16	144.5	52.3	0	0.0	0.0	0.024
	Trailing	154.5	44.6	109.9	98.4	13.2	0.13	137.9	59.0	0	0.0	0.0	
140	Leading	164.3	47.0	117.3	99.0	16.3	0.17	148.0	50.0	0	0.0	0.0	0.022
	Trailing	152.9	39.0	113.9	98.9	14.2	0.14	141.5	56.3	0	0.0	0.0	
145	Leading	165.2	39.5	125.7	99.8	17.6	0.18	152.5	47.1	0	0.0	0.0	0.023
	Trailing	152.6	48.1	104.5	99.8	15.1	0.15	145.0	54.6	0	0.0	0.0	
150	Leading	186.3	24.6	161.6	100.2	19.3	0.19	158.3	42.2	0	0.0	0.0	0.025
	Trailing	192.8	40.1	152.7	100.4	18.7	0.19	156.6	44.3	0	0.0	0.0	
155	Leading	176.3	32.8	143.5	100.9	20.9	0.21	163.5	38.3	0	0.0	0.0	0.028
	Trailing	171.7	37.2	134.5	101.2	20.1	0.20	161.6	40.8	0	0.0	0.0	
160	Leading	169.8	40.0	129.7	101.6	20.8	0.20	164.0	39.1	0	0.0	0.0	0.030
	Trailing	175.3	11.8	163.5	102.0	20.9	0.20	164.6	39.4	0	0.0	0.0	
…	…	…	…	…	…	…	…	…	…	…	…	…	…

Speed [km/h]	Pant	Contact Force [N]								Contact loss			Steady Arm Uplift [m]
		F_{max}	F_{min}	ΔF	F_m	σ	σ / F_m	S_{max}	S_{Min}	$CL_{\#}$	CL_t [s]	$CL_{\%}$ [%]	
165	Leading	163.2	39.4	123.8	102.5	20.9	0.20	165.1	39.9	0	0.0	0.0	0.029
	Trailing	232.7	5.8	226.9	102.6	22.3	0.22	169.4	35.9	0	0.0	0.0	
170	Leading	169.7	39.0	130.6	103.4	21.8	0.21	168.6	38.1	0	0.0	0.0	0.030
	Trailing	211.9	-7.6	219.6	103.5	22.8	0.22	171.8	35.2	1	0.0	0.1	
175	Leading	176.7	40.8	135.9	104.3	23.0	0.22	173.3	35.2	0	0.0	0.0	0.033
	Trailing	250.1	16.1	234.0	104.3	24.8	0.24	178.6	29.9	0	0.0	0.0	
180	Leading	176.7	47.9	128.8	105.1	23.9	0.23	176.9	33.3	0	0.0	0.0	0.033
	Trailing	297.4	26.9	270.5	105.0	26.9	0.26	185.8	24.3	0	0.0	0.0	
185	Leading	171.8	51.5	120.3	106.0	24.4	0.23	179.3	32.7	0	0.0	0.0	0.035
	Trailing	222.7	19.4	203.3	105.8	28.5	0.27	191.4	20.2	0	0.0	0.0	
190	Leading	172.0	52.8	119.2	106.9	24.1	0.23	179.2	34.6	0	0.0	0.0	0.040
	Trailing	222.3	5.3	217.0	106.7	31.2	0.29	200.3	13.2	0	0.0	0.0	
195	Leading	183.3	47.8	135.5	107.6	24.0	0.22	179.7	35.5	0	0.0	0.0	0.043
	Trailing	216.4	1.4	215.0	107.7	31.6	0.29	202.5	12.9	0	0.0	0.0	
200	Leading	197.6	49.2	148.4	108.6	24.0	0.22	180.5	36.7	0	0.0	0.0	0.043
	Trailing	218.7	-3.9	222.6	108.5	32.1	0.30	204.7	12.3	1	0.0	0.1	
205	Leading	196.2	47.0	149.2	110.6	25.0	0.23	185.5	35.7	0	0.0	0.0	0.046
	Trailing	217.4	8.2	209.2	110.5	33.0	0.30	209.5	11.6	0	0.0	0.0	
210	Leading	188.2	57.0	131.2	112.5	26.4	0.24	191.9	33.2	0	0.0	0.0	0.047
	Trailing	204.7	5.2	199.5	112.7	33.5	0.30	213.1	12.3	0	0.0	0.0	
215	Leading	193.7	59.7	134.0	114.3	28.7	0.25	200.3	28.3	0	0.0	0.0	0.050
	Trailing	231.1	6.4	224.7	114.7	33.0	0.29	213.6	15.9	0	0.0	0.0	
220	Leading	201.6	49.9	151.7	116.5	30.3	0.26	207.3	25.7	0	0.0	0.0	0.051
	Trailing	238.0	5.5	232.5	116.9	32.0	0.27	213.0	20.8	0	0.0	0.0	
225	Leading	204.6	50.8	153.9	118.4	32.7	0.28	216.7	20.2	0	0.0	0.0	0.055
	Trailing	212.6	3.1	209.5	118.9	32.6	0.27	216.6	21.1	0	0.0	0.0	
230	Leading	233.0	28.2	204.8	120.2	35.2	0.29	225.9	14.5	0	0.0	0.0	0.056
	Trailing	215.8	-4.5	220.3	120.8	36.1	0.30	229.0	12.6	1	0.0	0.1	
235	Leading	243.4	39.6	203.8	122.4	37.3	0.30	234.3	10.5	0	0.0	0.0	0.056
	Trailing	243.4	7.9	235.5	122.8	40.5	0.33	244.4	1.2	0	0.0	0.0	
240	Leading	262.9	30.5	232.4	124.9	39.8	0.32	244.4	5.4	0	0.0	0.0	0.058
	Trailing	482.4	-39.9	522.2	125.2	47.3	0.38	267.1	-16.7	4	0.1	0.6	
245	Leading	282.1	25.1	257.1	124.4	40.5	0.33	245.9	2.9	0	0.0	0.0	0.066
	Trailing	558.1	-24.6	582.6	126.5	53.2	0.42	286.0	-33.0	6	0.1	0.8	
250	Leading	376.1	-18.9	395.0	129.5	58.0	0.45	303.5	-44.4	5	0.0	0.4	0.080
	Trailing	547.6	-66.3	613.9	127.7	65.5	0.51	324.1	-68.7	13	0.2	1.9	
255	Leading	583.6	-40.1	623.8	131.6	81.2	0.62	375.1	-111.9	18	0.3	2.5	0.110
	Trailing	647.8	-56.0	703.8	132.8	82.3	0.62	379.8	-114.2	24	0.4	3.7	
260	Leading	440.4	-23.4	463.8	132.2	75.7	0.57	359.3	-95.0	9	0.1	1.0	0.100
	Trailing	603.0	-65.2	668.2	132.2	107.7	0.81	455.2	-190.8	53	0.9	8.2	
265	Leading	750.3	-67.6	817.9	135.2	104.0	0.77	447.3	-176.9	43	0.7	6.6	0.127
	Trailing	684.7	-63.0	747.7	137.9	99.0	0.72	434.9	-159.1	34	0.6	5.8	

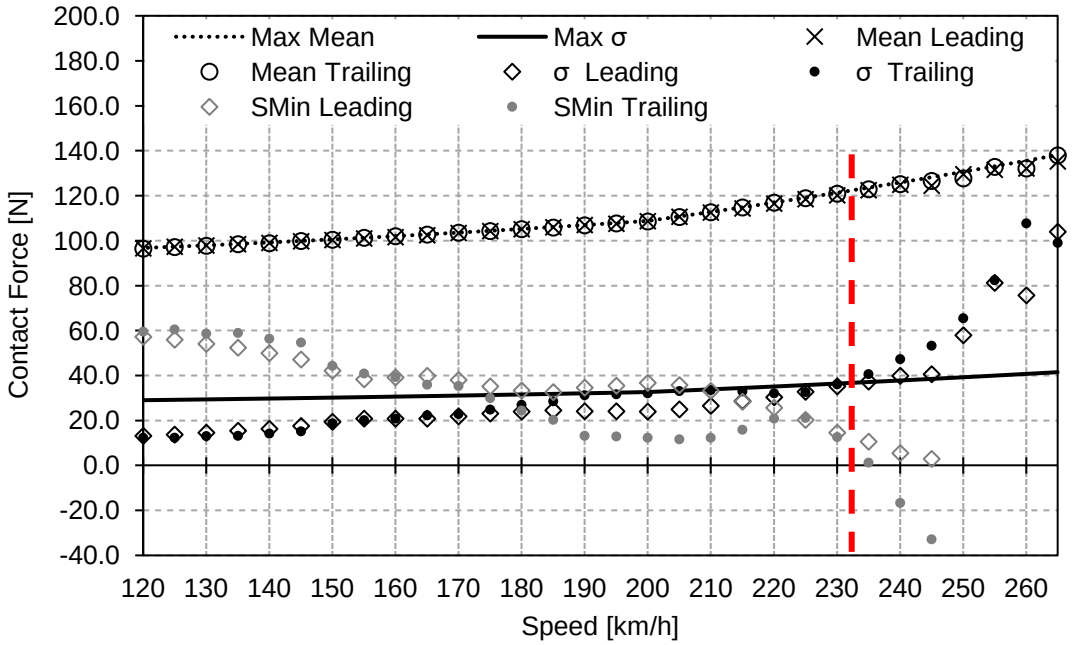

Figure 4.41: LP12_Pant2_S35 results for multiple pantographs, running at various speeds

In Figure 4.41 it is observed that the standard deviation, for 235 km/h exceeds its respective threshold, for both pantographs. While in Table 4.18 it is found that for a lower speed that the 230 km/h previously mention, and there are some cases of contact losses that do not reach the 0.1% limit. So, the exploration velocity for LP12_Pant2_S35 m is 230 km/h. The limiting factor for the LP12_Pant2_S35 case is the trailing pantograph standard deviation. In Figure 4.42 the contact forces along the track are represented for each pantograph.

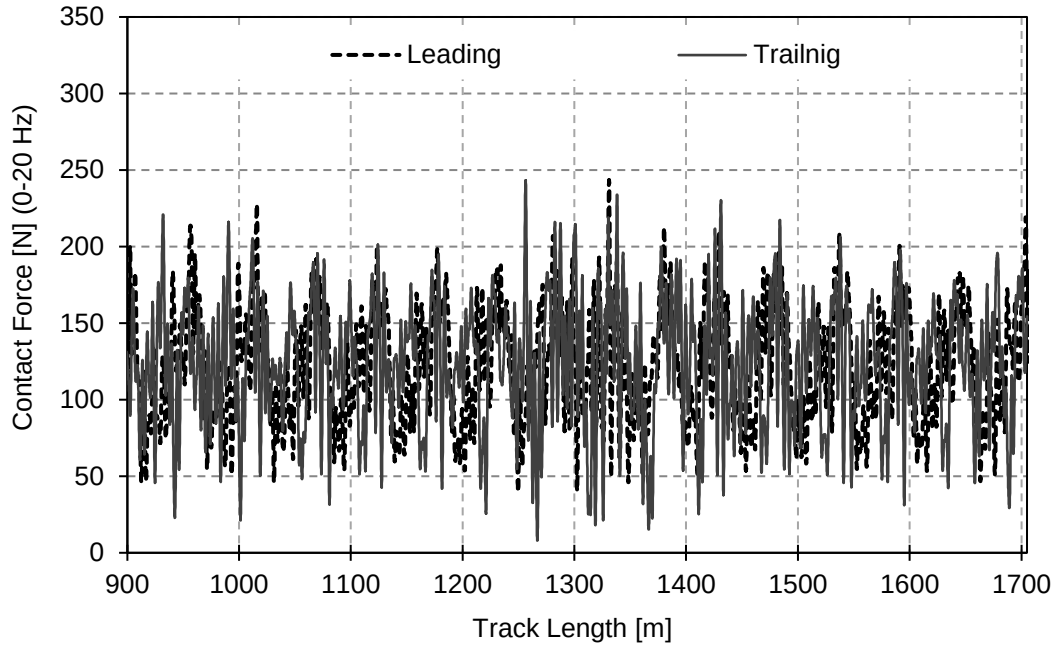

Figure 4.42: Contact forces results for LP12_Pant2_S35_V235

In Figure 4.42 the contact forces along the track, of LP12_Pant2_S35_V235, are represented for each pantograph, where it is possible to determine that the trailing contact force is affected by the leading pantograph. In this figure the overlapping arrangement is shown to have almost no effect on the contact characteristics.

The dynamic analysis results obtained of the interaction of the LP12_Pant2 pairing, considering 2 pantographs, with a separation between them of 85 m, for various speeds are represented in Figure 4.43 and Table 4.19.

Table 4.19: LP12_Pant2_S85 results for multiple pantographs, running at various speeds

Speed [km/h]	Pant	Contact Force [N]								Contact loss			Steady Arm Uplift [m]
		F_{max}	F_{min}	ΔF	F_m	σ	σ / F_m	S_{max}	S_{Min}	$CL_{\#}$	CL_t [s]	$CL_{\%}$ [%]	
120	Leading	160.3	20.4	139.9	96.7	11.7	0.12	131.7	61.7	0	0.0	0.0	0.020
	Trailing	160.6	17.9	142.7	96.7	15.6	0.16	143.6	49.9	0	0.0	0.0	
125	Leading	171.5	45.2	126.3	97.2	12.3	0.13	133.9	60.4	0	0.0	0.0	0.019
	Trailing	175.3	49.1	126.2	97.3	16.2	0.17	145.9	48.7	0	0.0	0.0	
130	Leading	164.9	41.8	123.1	97.7	13.5	0.14	138.3	57.2	0	0.0	0.0	0.019
	Trailing	173.1	25.8	147.3	97.8	19.3	0.20	155.8	39.8	0	0.0	0.0	
135	Leading	159.5	46.6	112.9	98.4	14.3	0.15	141.4	55.4	0	0.0	0.0	0.019
	Trailing	161.5	45.3	116.2	98.5	20.1	0.20	158.9	38.0	0	0.0	0.0	
140	Leading	170.1	51.0	119.1	98.9	15.7	0.16	146.1	51.7	0	0.0	0.0	0.018
	Trailing	163.2	33.9	129.3	99.2	22.2	0.22	165.7	32.6	0	0.0	0.0	
145	Leading	163.8	37.4	126.4	99.6	17.0	0.17	150.6	48.7	0	0.0	0.0	0.020
	Trailing	168.2	37.1	131.1	99.7	22.8	0.23	168.2	31.2	0	0.0	0.0	
150	Leading	175.3	38.9	136.4	100.5	20.5	0.20	162.1	38.8	0	0.0	0.0	0.024
	Trailing	180.3	-2.5	182.8	100.6	31.3	0.31	194.4	6.7	1	0.0	0.1	
155	Leading	171.8	30.2	141.6	100.8	21.4	0.21	165.1	36.6	0	0.0	0.0	0.024
	Trailing	192.2	8.6	183.6	101.2	33.2	0.33	200.8	1.5	0	0.0	0.0	
160	Leading	169.2	42.9	126.3	101.3	20.1	0.20	161.5	41.1	0	0.0	0.0	0.024
	Trailing	201.3	13.8	187.4	102.0	31.4	0.31	196.0	7.9	0	0.0	0.0	
165	Leading	162.0	35.2	126.8	102.2	19.4	0.19	160.5	43.9	0	0.0	0.0	0.028
	Trailing	186.1	6.8	179.2	102.6	29.3	0.29	190.4	14.9	0	0.0	0.0	
170	Leading	163.1	39.8	123.3	103.1	20.4	0.20	164.4	41.8	0	0.0	0.0	0.028
	Trailing	179.7	9.9	169.8	103.5	28.2	0.27	188.2	18.7	0	0.0	0.0	
175	Leading	172.6	41.1	131.5	104.0	20.6	0.20	165.9	42.1	0	0.0	0.0	0.034
	Trailing	196.7	-3.2	199.8	104.2	29.8	0.29	193.6	14.9	1	0.0	0.1	
180	Leading	166.6	52.5	114.1	104.8	21.5	0.21	169.3	40.3	0	0.0	0.0	0.035
	Trailing	179.4	11.8	167.6	105.1	29.8	0.28	194.5	15.7	0	0.0	0.0	
185	Leading	171.8	52.7	119.1	105.8	22.1	0.21	172.2	39.4	0	0.0	0.0	0.034
	Trailing	233.8	1.3	232.5	106.0	30.3	0.29	197.0	15.1	0	0.0	0.0	
190	Leading	172.5	53.0	119.4	106.7	22.4	0.21	173.9	39.5	0	0.0	0.0	0.032
	Trailing	327.6	-11.3	338.9	106.9	33.1	0.31	206.3	7.5	3	0.0	0.2	
195	Leading	185.6	50.8	134.8	107.8	22.6	0.21	175.6	39.9	0	0.0	0.0	0.036
	Trailing	315.9	4.3	311.6	107.8	33.2	0.31	207.4	8.1	0	0.0	0.0	
…	…	…	…	…	…	…	…	…	…	…	…	…	…

Speed [km/h]	Pant	Contact Force [N]								Contact loss			Steady Arm Uplift [m]
		F_{max}	F_{min}	ΔF	F_m	σ	σ / F_m	S_{max}	S_{Min}	$CL_{\#}$	CL_t [s]	$CL_{\%}$ [%]	
200	Leading	200.7	54.1	146.7	108.7	23.2	0.21	178.3	39.1	0	0.0	0.0	0.041
	Trailing	224.2	18.6	205.6	108.5	29.9	0.28	198.1	18.9	0	0.0	0.0	
205	Leading	194.9	47.9	147.1	110.6	24.8	0.22	185.0	36.2	0	0.0	0.0	0.042
	Trailing	234.9	6.6	228.3	110.4	32.2	0.29	207.0	13.8	0	0.0	0.0	
210	Leading	190.9	55.6	135.3	112.8	25.4	0.23	188.9	36.6	0	0.0	0.0	0.045
	Trailing	300.0	2.9	297.1	112.6	38.0	0.34	226.6	-1.3	0	0.0	0.0	
215	Leading	187.5	59.3	128.3	114.7	26.4	0.23	194.0	35.4	0	0.0	0.0	0.051
	Trailing	347.5	-2.5	350.0	114.7	39.3	0.34	232.5	-3.1	1	0.0	0.0	
220	Leading	200.9	51.6	149.2	116.9	27.9	0.24	200.7	33.0	0	0.0	0.0	0.049
	Trailing	244.1	2.3	241.9	116.7	42.2	0.36	243.4	-9.9	0	0.0	0.0	
225	Leading	213.5	47.7	165.8	118.7	30.3	0.26	209.5	27.8	0	0.0	0.0	0.049
	Trailing	269.5	-7.8	277.3	118.5	47.6	0.40	261.4	-24.4	4	0.1	0.6	
230	Leading	218.8	23.0	195.8	110.8	30.2	0.27	201.5	20.2	0	0.0	0.0	0.055
	Trailing	337.2	-1.1	338.3	119.8	53.5	0.45	280.4	-40.8	1	0.0	0.1	
235	Leading	212.9	40.9	172.0	119.4	33.4	0.28	219.6	19.3	0	0.0	0.0	0.065
	Trailing	648.9	-25.5	674.4	120.8	64.5	0.53	314.3	-72.8	8	0.1	0.8	
240	Leading	264.9	45.6	219.2	124.7	37.3	0.30	236.6	12.8	0	0.0	0.0	0.061
	Trailing	411.6	-20.0	431.7	124.8	59.1	0.47	302.2	-52.6	8	0.1	0.8	
245	Leading	282.1	25.1	257.1	124.4	40.5	0.33	245.9	2.9	0	0.0	0.0	0.066
	Trailing	558.1	-24.6	582.6	126.5	53.2	0.42	286.0	-33.0	6	0.1	0.8	
250	Leading	371.7	-9.9	381.6	129.3	57.5	0.45	301.9	-43.3	1	0.0	0.1	0.073
	Trailing	418.6	-45.2	463.8	129.2	75.9	0.59	356.9	-98.5	12	0.2	1.7	
255	Leading	573.9	-65.7	639.6	131.0	91.1	0.69	404.2	-142.1	38	0.5	4.7	0.088
	Trailing	777.7	-71.1	848.8	132.1	112.3	0.85	468.8	-204.7	43	0.9	7.7	
260	Leading	1470.1	-74.3	1544.4	132.4	91.7	0.69	407.3	-142.6	25	0.4	3.4	0.102
	Trailing	654.1	-47.5	701.7	135.2	98.6	0.73	431.1	-160.7	21	0.4	3.5	
265	Leading	674.8	-61.5	736.3	133.1	101.3	0.76	436.9	-170.6	42	0.7	6.4	0.119
	Trailing	651.9	-57.0	709.0	137.2	108.6	0.79	463.0	-188.5	32	0.6	5.4	

Comparing the dynamic analysis results for LP12_Pant2_S85 case with the dynamic analysis results obtained for a separation of 35m it is observed a great difference between the maximum operating velocity found. In Figure 4.43 the standard deviation surpasses the validating standard deviation for 150 km/h, then returns to be within the standard limits between 165 km/h and 180 km/h, to again surpass the standard deviation threshold at 190 km/h and 195 km/h and finally it is within the limits until 210 km/h. While the statistical minimum is negative for the trailing pantograph running at 210 km/h or higher speeds In Figure 4.43 the trailing pantograph standard deviation is shown to be close to the threshold for 165 km/h to 185 km/h and 200 km/h to 205 km/h. So lit is essential to look at Table 4.19, where it is found that the values of the standard deviation for the trailing pantograph are so close to the limit that any perturbation in the system puts them above respective thresholds. This leads to the exploration velocity of 145 km/h, where the limiting factors for the LP12_Pant2_S85 case is the standard deviation on the trailing pantograph. Figure 4.44 shows the contact force of each pantograph along the track.

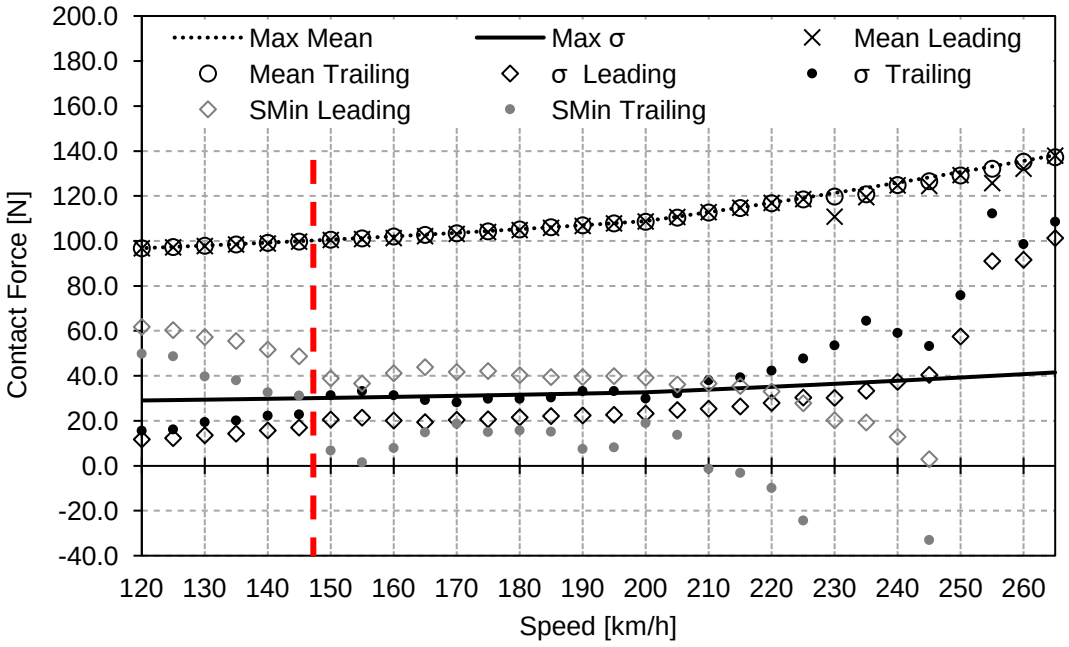

Figure 4.43: LP12_Pant2_S85 results for multiple pantographs, running at various speeds

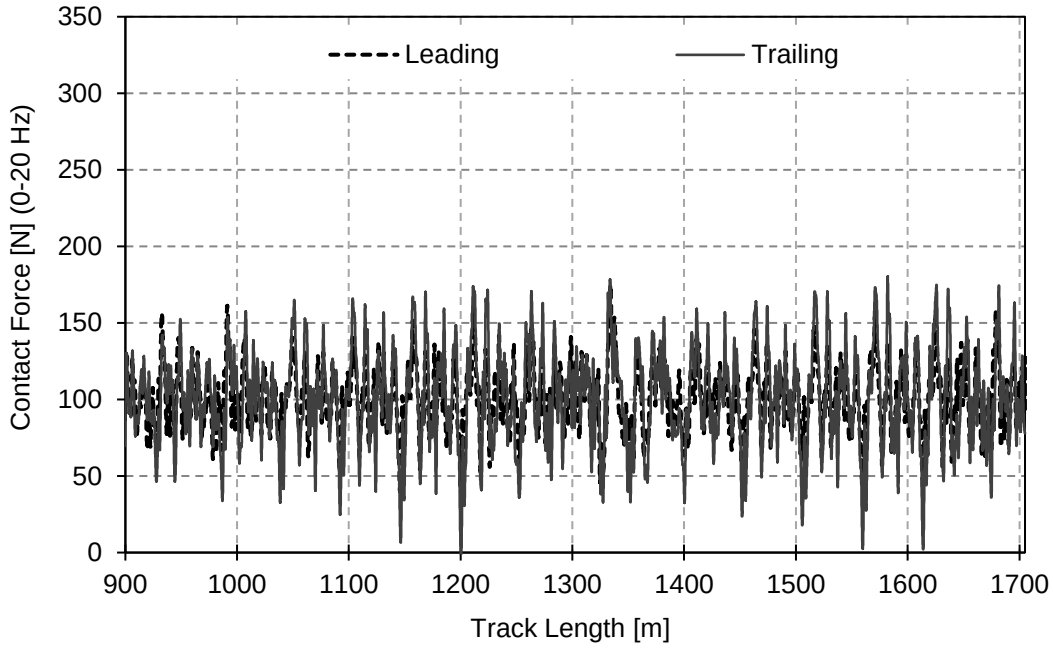

Figure 4.44: Contact forces results for LP12_Pant2_S85_V150

Figure 4.44 shows the contact force of each pantograph along the track, where the trailing pantograph is visibly affected by the leading pantograph. In this figure the contact losses do not occur when the two catenary sections overlap, so the overlapping arrangement has little effect in the limiting of the velocity.

The dynamic analysis results obtained of the interaction of the LP12_Pant2 pairing, considering 2 pantographs, with a separation between them of 100 m, for various speeds are represented in Figure 4.45 and Table 4.20.

Table 4.20: LP12_Pant2_S100 results for multiple pantographs, running at various speeds

Speed [km/h]	Pant	Contact Force [N]								Contact loss			Steady Arm Uplift [m]
		F_{max}	F_{min}	ΔF	F_m	σ	σ/F_m	S_{max}	S_{Min}	$CL_{\#}$	CL_t [s]	$CL_{\%}$ [%]	
120	Leading	156.6	27.1	129.5	96.7	11.6	0.12	131.6	61.9	0	0.0	0.0	0.018
	Trailing	154.4	-1.1	155.4	96.7	12.4	0.13	133.8	59.6	1	0.0	0.0	
125	Leading	179.3	45.0	134.3	97.2	12.6	0.13	135.0	59.3	0	0.0	0.0	0.018
	Trailing	176.1	34.1	142.0	97.2	13.6	0.14	138.1	56.3	0	0.0	0.0	
130	Leading	162.9	47.0	115.9	97.7	13.4	0.14	138.0	57.5	0	0.0	0.0	0.019
	Trailing	162.8	44.9	117.8	97.5	15.1	0.15	142.7	52.4	0	0.0	0.0	
135	Leading	157.9	51.6	106.3	98.4	14.0	0.14	140.4	56.4	0	0.0	0.0	0.020
	Trailing	149.6	38.5	111.1	98.3	16.1	0.16	146.6	50.1	0	0.0	0.0	
140	Leading	165.8	52.9	112.9	99.1	15.7	0.16	146.3	52.0	0	0.0	0.0	0.017
	Trailing	161.6	40.3	121.3	99.1	16.9	0.17	149.9	48.3	0	0.0	0.0	
145	Leading	163.3	46.4	116.9	99.6	16.8	0.17	150.0	49.3	0	0.0	0.0	0.020
	Trailing	185.7	45.1	140.6	99.7	18.5	0.19	155.1	44.3	0	0.0	0.0	
150	Leading	184.3	28.8	155.4	100.5	19.8	0.20	159.8	41.2	0	0.0	0.0	0.020
	Trailing	188.1	33.6	154.5	100.5	21.9	0.22	166.1	34.9	0	0.0	0.0	
155	Leading	165.9	45.3	120.6	101.2	21.1	0.21	164.6	37.7	0	0.0	0.0	0.020
	Trailing	205.7	15.9	189.8	101.0	29.8	0.29	190.3	11.7	0	0.0	0.0	
160	Leading	164.7	52.2	112.5	101.8	20.4	0.20	163.1	40.6	0	0.0	0.0	0.025
	Trailing	234.1	19.3	214.7	101.7	30.6	0.30	193.4	10.0	0	0.0	0.0	
165	Leading	162.3	44.4	117.9	102.4	19.6	0.19	161.3	43.6	0	0.0	0.0	0.029
	Trailing	236.2	0.9	235.3	102.6	34.9	0.34	207.4	-2.2	0	0.0	0.0	
170	Leading	163.6	50.6	113.1	103.5	20.8	0.20	166.0	41.0	0	0.0	0.0	0.031
	Trailing	220.6	-9.1	229.7	103.6	38.1	0.37	217.8	-10.6	3	0.0	0.2	
175	Leading	177.6	40.3	137.4	104.1	21.7	0.21	169.2	39.0	0	0.0	0.0	0.033
	Trailing	210.4	-3.5	213.9	104.4	38.9	0.37	221.2	-12.4	2	0.0	0.3	
180	Leading	176.6	49.6	127.1	104.8	22.3	0.21	171.6	38.0	0	0.0	0.0	0.035
	Trailing	198.7	6.2	192.5	105.1	36.8	0.35	215.5	-5.3	0	0.0	0.0	
185	Leading	172.0	48.6	123.4	105.6	22.2	0.21	172.2	39.0	0	0.0	0.0	0.033
	Trailing	199.3	0.1	199.2	106.0	35.0	0.33	210.8	1.1	0	0.0	0.0	
190	Leading	176.8	40.6	136.2	106.5	21.7	0.20	171.5	41.5	0	0.0	0.0	0.038
	Trailing	209.2	-10.9	220.1	106.9	36.1	0.34	215.2	-1.4	3	0.0	0.3	
195	Leading	181.4	53.2	128.1	107.5	20.5	0.19	168.9	46.0	0	0.0	0.0	0.041
	Trailing	206.1	-6.1	212.3	107.8	36.4	0.34	217.0	-1.4	4	0.0	0.3	
200	Leading	194.5	40.1	154.4	108.1	21.0	0.19	171.2	45.1	0	0.0	0.0	0.043
	Trailing	204.2	-2.7	206.9	108.7	38.1	0.35	222.9	-5.5	1	0.0	0.1	
205	Leading	180.5	49.4	131.1	110.1	23.7	0.22	181.2	38.9	0	0.0	0.0	0.041
	Trailing	210.1	-11.9	222.0	110.5	40.8	0.37	232.8	-11.8	4	0.1	0.5	
210	Leading	184.1	47.9	136.2	111.9	25.6	0.23	188.8	35.0	0	0.0	0.0	0.049
	Trailing	220.8	-11.4	232.2	112.4	41.8	0.37	238.0	-13.1	5	0.1	0.6	
215	Leading	198.1	49.9	148.2	114.1	28.3	0.25	199.1	29.2	0	0.0	0.0	0.051
	Trailing	228.4	-9.7	238.1	114.7	44.8	0.39	249.0	-19.7	2	0.0	0.2	
…	…	…	…	…	…	…	…	…	…	…	…	…	…

Speed [km/h]	Pant	Contact Force [N]								Contact loss			Steady Arm Uplift [m]
		F_{max}	F_{min}	ΔF	F_m	σ	σ/F_m	S_{max}	S_{Min}	$CL_{\#}$	CL_t [s]	$CL_{\%}$ [%]	
220	Leading	205.3	46.5	158.8	116.4	30.8	0.26	208.6	24.1	0	0.0	0.0	0.058
	Trailing	344.3	-12.6	356.9	116.9	50.8	0.43	269.4	-35.6	5	0.1	0.7	
225	Leading	214.1	31.5	182.6	117.5	34.0	0.29	219.5	15.5	0	0.0	0.0	0.067
	Trailing	465.5	-34.8	500.3	118.2	54.3	0.46	281.1	-44.7	12	0.2	1.5	
230	Leading	226.4	35.6	190.8	118.7	35.8	0.30	226.0	11.4	0	0.0	0.0	0.070
	Trailing	579.4	-35.2	614.6	119.3	51.1	0.43	272.6	-34.1	6	0.1	1.0	
235	Leading	234.1	35.8	198.3	121.8	38.3	0.31	236.7	7.0	0	0.0	0.0	0.075
	Trailing	528.8	-12.8	541.6	122.3	55.4	0.45	288.5	-43.8	6	0.1	0.9	
240	Leading	280.2	35.6	244.7	124.4	39.6	0.32	243.3	5.4	0	0.0	0.0	0.064
	Trailing	676.0	-13.7	689.6	125.6	56.8	0.45	296.1	-44.8	7	0.1	0.8	
245	Leading	322.1	37.7	284.4	127.6	41.3	0.32	251.4	3.7	0	0.0	0.0	0.064
	Trailing	379.6	-9.1	388.8	127.8	48.1	0.38	272.2	-16.6	3	0.0	0.2	
250	Leading	463.9	-30.0	493.9	130.3	59.6	0.46	309.2	-48.6	5	0.1	0.7	0.080
	Trailing	558.6	-55.2	613.8	128.6	60.8	0.47	310.8	-53.7	7	0.1	0.8	
255	Leading	572.8	-64.5	637.3	125.8	79.4	0.63	364.1	-112.6	22	0.4	3.4	0.090
	Trailing	612.6	-57.1	669.7	132.6	83.4	0.63	382.7	-117.6	21	0.4	3.3	
260	Leading	573.5	-53.0	626.6	132.2	75.6	0.57	359.1	-94.7	11	0.1	1.2	0.097
	Trailing	711.0	-66.5	777.5	134.2	96.9	0.72	425.0	-156.6	27	0.6	5.4	
265	Leading	552.0	-45.2	597.2	138.0	79.9	0.58	377.8	-101.9	13	0.2	2.1	0.095
	Trailing	703.2	-63.0	766.2	133.8	98.5	0.74	429.2	-161.6	31	0.5	4.5	

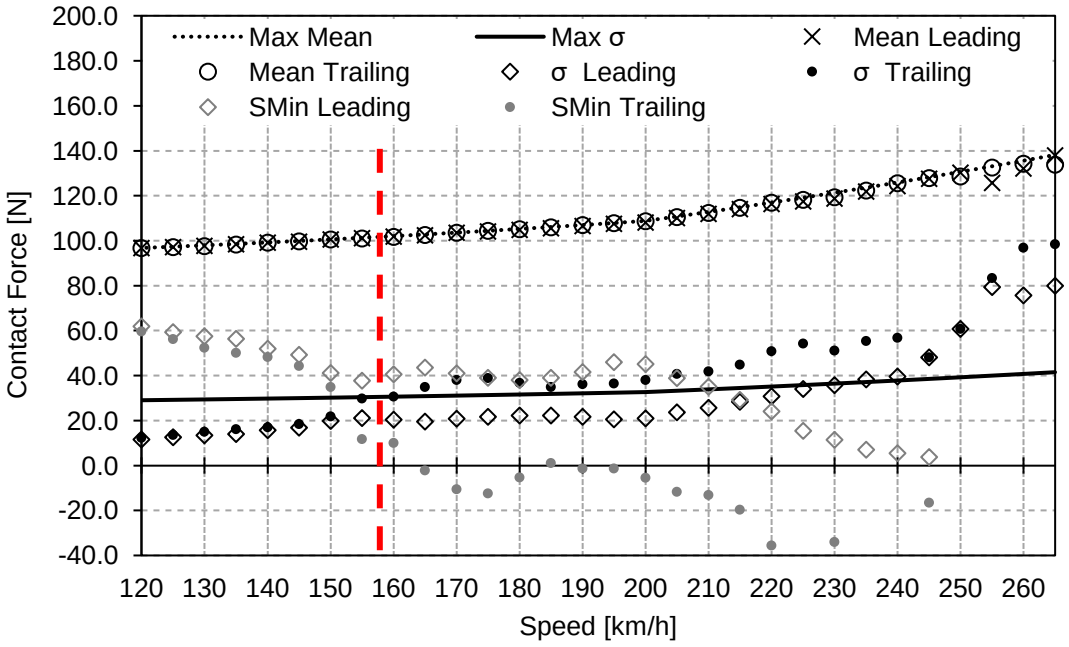

Figure 4.45: LP12_Pant2_S100 results for multiple pantographs, running at various speeds

Figure 4.45 shows that the statistical minimum of the trailing pantograph has negative values for velocities equal or above 165 km/h. In this figure the standard deviation of the trailing pantograph surpasses their respective threshold for 165 km/h. However, form Table 4.20 it is observed that the

trailing pantograph has the standard deviation mean contact force ratio superior to 0.3 for 160 km/h, since this parameter is in grey. This is possible because the line for the maximum standard deviation is obtained calculating the maximum standard deviation, with the maximum mean contact force, while the ratio that validates the velocity is calculated with the mean contact force of each pantograph obtained from the dynamic analysis simulation, which is less than the maximum mean contact force. So, the exploration velocity is 155 km/h, where the limiting factor is the standard deviation of the trailing pantograph. Figure 4.46 shows the contact force for each pantograph for LP12_Pant2_S100_V160.

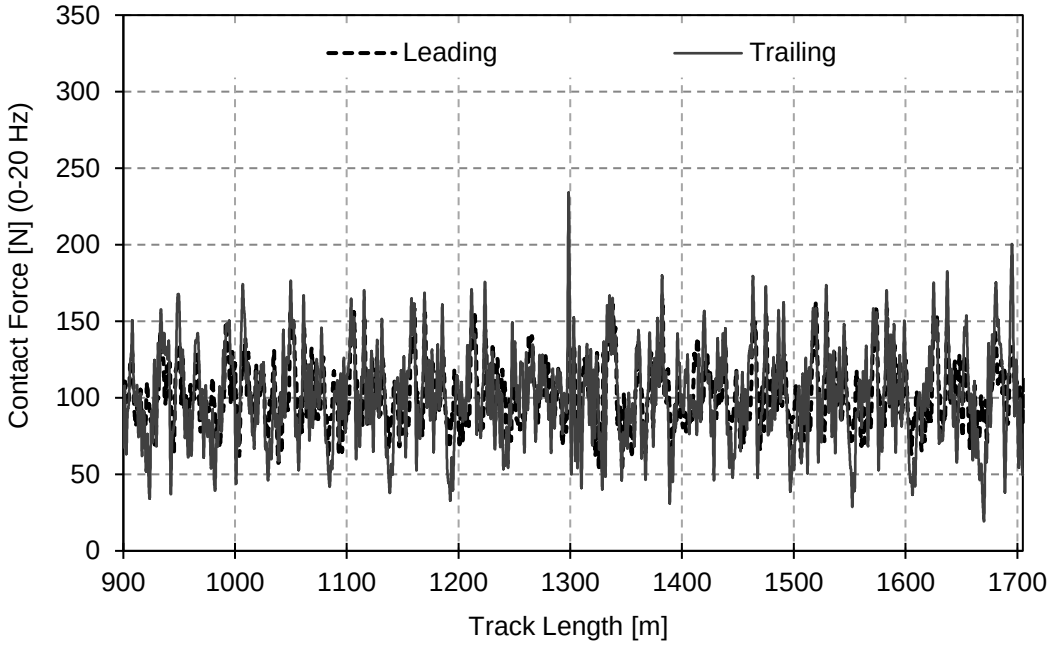

Figure 4.46: Contact forces results for LP12_Pant2_S100_V160

Figure 4.46 shows the contact force for each pantograph, along the track for LP12_Pant2_S100_V160, where the trailing pantograph is shown to be affected by the leading pantograph and the maximum force is shown to be located at the catenary overlap.

Table 4.21: LP12_Pant2_S200 results for multiple pantographs, running at various speeds

Speed [km/h]	Pant	Contact Force [N]								Contact loss			Steady Arm Uplift [m]
		F_{max}	F_{min}	ΔF	F_m	σ	σ/F_m	S_{max}	S_{Min}	$CL_{\#}$	CL_t [s]	$CL_{\%}$ [%]	
120	Leading	156.6	3.1	153.5	96.6	11.6	0.12	131.5	61.7	0	0.0	0.0	0.018
	Trailing	174.3	6.7	167.5	96.7	14.4	0.15	140.0	53.4	0	0.0	0.0	
125	Leading	173.2	46.9	126.3	97.2	12.4	0.13	134.3	60.1	0	0.0	0.0	0.019
	Trailing	166.1	52.4	113.7	97.3	13.5	0.14	137.9	56.8	0	0.0	0.0	
130	Leading	170.5	45.4	125.1	97.8	13.3	0.14	137.8	57.7	0	0.0	0.0	0.018
	Trailing	165.5	51.0	114.5	97.8	15.1	0.15	143.1	52.5	0	0.0	0.0	
135	Leading	160.3	44.6	115.8	98.4	14.3	0.15	141.3	55.5	0	0.0	0.0	0.020
	Trailing	170.6	42.4	128.1	98.4	17.0	0.17	149.6	47.3	0	0.0	0.0	
…	…	…	…	…	…	…	…	…	…	…	…	…	…

Speed [km/h]	Pant	Contact Force [N]								Contact loss			Steady Arm Uplift [m]
		F_{max}	F_{min}	ΔF	F_m	σ	σ/F_m	S_{max}	S_{Min}	$CL_{\#}$	CL_t [s]	$CL_{\%}$ [%]	
140	Leading	167.2	53.2	114.0	99.1	15.4	0.16	145.5	52.8	0	0.0	0.0	0.018
	Trailing	167.9	40.3	127.6	99.2	17.9	0.18	152.7	45.6	0	0.0	0.0	
145	Leading	161.6	47.7	113.9	99.6	16.6	0.17	149.3	49.9	0	0.0	0.0	0.018
	Trailing	177.4	45.5	131.9	99.7	19.9	0.20	159.4	40.0	0	0.0	0.0	
150	Leading	190.0	24.0	166.1	100.5	19.9	0.20	160.2	40.8	0	0.0	0.0	0.019
	Trailing	193.0	11.7	181.3	100.5	26.0	0.26	178.6	22.4	0	0.0	0.0	
155	Leading	166.1	36.6	129.6	101.2	21.1	0.21	164.5	37.8	0	0.0	0.0	0.022
	Trailing	208.2	6.8	201.4	101.2	31.1	0.31	194.6	7.8	0	0.0	0.0	
160	Leading	169.4	41.4	128.0	101.8	20.3	0.20	162.7	41.0	0	0.0	0.0	0.021
	Trailing	181.0	20.5	160.5	101.9	27.9	0.27	185.5	18.4	0	0.0	0.0	
165	Leading	165.4	37.6	127.8	102.7	19.5	0.19	161.3	44.1	0	0.0	0.0	0.027
	Trailing	178.8	17.5	161.3	102.6	25.6	0.25	179.4	25.8	0	0.0	0.0	
170	Leading	161.9	44.2	117.6	103.5	20.5	0.20	165.0	42.0	0	0.0	0.0	0.036
	Trailing	205.1	3.0	202.1	103.5	27.7	0.27	186.6	20.4	0	0.0	0.0	
175	Leading	164.4	45.6	118.8	104.2	20.7	0.20	166.2	42.2	0	0.0	0.0	0.031
	Trailing	202.3	13.7	188.6	104.2	31.4	0.30	198.3	10.1	0	0.0	0.0	
180	Leading	169.1	55.9	113.1	105.0	21.4	0.20	169.1	40.9	0	0.0	0.0	0.032
	Trailing	219.6	5.3	214.3	105.2	34.0	0.32	207.2	3.2	0	0.0	0.0	
185	Leading	171.9	52.6	119.4	105.9	21.5	0.20	170.3	41.5	0	0.0	0.0	0.031
	Trailing	283.9	4.9	279.0	106.1	32.2	0.30	202.8	9.4	0	0.0	0.0	
190	Leading	165.5	46.2	119.3	106.4	21.1	0.20	169.7	43.0	0	0.0	0.0	0.032
	Trailing	249.0	9.6	239.4	106.9	32.1	0.30	203.3	10.6	0	0.0	0.0	
195	Leading	187.9	50.1	137.8	107.6	20.9	0.19	170.3	44.8	0	0.0	0.0	0.038
	Trailing	223.0	13.5	209.4	107.8	31.6	0.29	202.6	12.9	0	0.0	0.0	
200	Leading	202.8	40.3	162.4	108.6	22.0	0.20	174.6	42.6	0	0.0	0.0	0.043
	Trailing	247.0	11.8	235.2	108.7	32.8	0.30	207.2	10.2	0	0.0	0.0	
205	Leading	184.8	46.7	138.1	110.6	24.4	0.22	183.8	37.4	0	0.0	0.0	0.038
	Trailing	214.0	20.9	193.2	110.5	36.3	0.33	219.5	1.4	0	0.0	0.0	
210	Leading	187.9	45.1	142.8	112.5	26.0	0.23	190.5	34.4	0	0.0	0.0	0.045
	Trailing	233.1	10.5	222.6	112.6	38.4	0.34	227.8	-2.6	0	0.0	0.0	
215	Leading	201.9	51.1	150.9	114.6	28.9	0.25	201.3	27.9	0	0.0	0.0	0.043
	Trailing	275.1	-5.2	280.2	114.7	42.4	0.37	241.8	-12.4	3	0.0	0.2	
220	Leading	207.5	40.9	166.6	116.4	31.5	0.27	210.9	21.8	0	0.0	0.0	0.049
	Trailing	286.2	-11.3	297.5	116.9	48.7	0.42	262.9	-29.1	5	0.1	0.5	
225	Leading	211.9	48.7	163.1	118.0	33.7	0.29	219.0	17.0	0	0.0	0.0	0.059
	Trailing	630.6	-28.0	658.6	118.4	62.9	0.53	307.3	-70.4	12	0.2	1.6	
230	Leading	237.2	34.0	203.2	120.8	36.2	0.30	229.4	12.1	0	0.0	0.0	0.068
	Trailing	366.8	-9.9	376.7	120.7	58.3	0.48	295.6	-54.1	6	0.1	0.8	
235	Leading	261.1	34.0	227.1	123.3	37.5	0.30	235.7	10.8	0	0.0	0.0	0.069
	Trailing	354.5	-15.8	370.3	123.1	63.2	0.51	312.8	-66.5	13	0.2	1.7	
240	Leading	287.0	42.9	244.1	125.8	38.6	0.31	241.6	10.0	0	0.0	0.0	0.073
	Trailing	326.0	-10.9	336.9	125.6	65.0	0.52	320.7	-69.5	10	0.2	1.4	
…	…	…	…	…	…	…	…	…	…	…	…	…	…

Speed [km/h]	Pant	Contact Force [N]								Contact loss			Steady Arm Uplift [m]
		F_{max}	F_{min}	ΔF	F_m	σ	σ/F_m	S_{max}	S_{Min}	$CL_{\#}$	CL_t [s]	$CL_{\%}$ [%]	
245	Leading	278.9	33.6	245.3	124.9	38.4	0.31	240.2	9.7	0	0.0	0.0	0.079
	Trailing	401.8	-16.6	418.4	127.3	74.5	0.59	350.9	-96.2	13	0.2	1.6	
250	Leading	482.6	22.3	460.3	130.3	50.7	0.39	282.3	-21.7	0	0.0	0.0	0.099
	Trailing	467.5	-28.8	496.3	127.4	81.7	0.64	372.5	-117.7	22	0.4	3.1	
255	Leading	436.9	-64.3	501.2	127.0	68.3	0.54	332.0	-78.1	13	0.2	1.5	0.100
	Trailing	568.5	-51.2	619.7	132.3	97.8	0.74	425.8	-161.1	25	0.4	3.8	
260	Leading	706.5	-67.5	774.0	129.6	93.3	0.72	409.5	-150.3	34	0.5	4.6	0.127
	Trailing	841.7	-79.9	921.5	132.1	99.6	0.75	430.9	-166.8	28	0.5	4.3	
265	Leading	567.5	-70.3	637.8	136.3	90.0	0.66	406.5	-133.8	25	0.5	4.5	0.106
	Trailing	640.9	-54.9	695.8	138.0	104.4	0.76	451.2	-175.2	24	0.5	4.3	

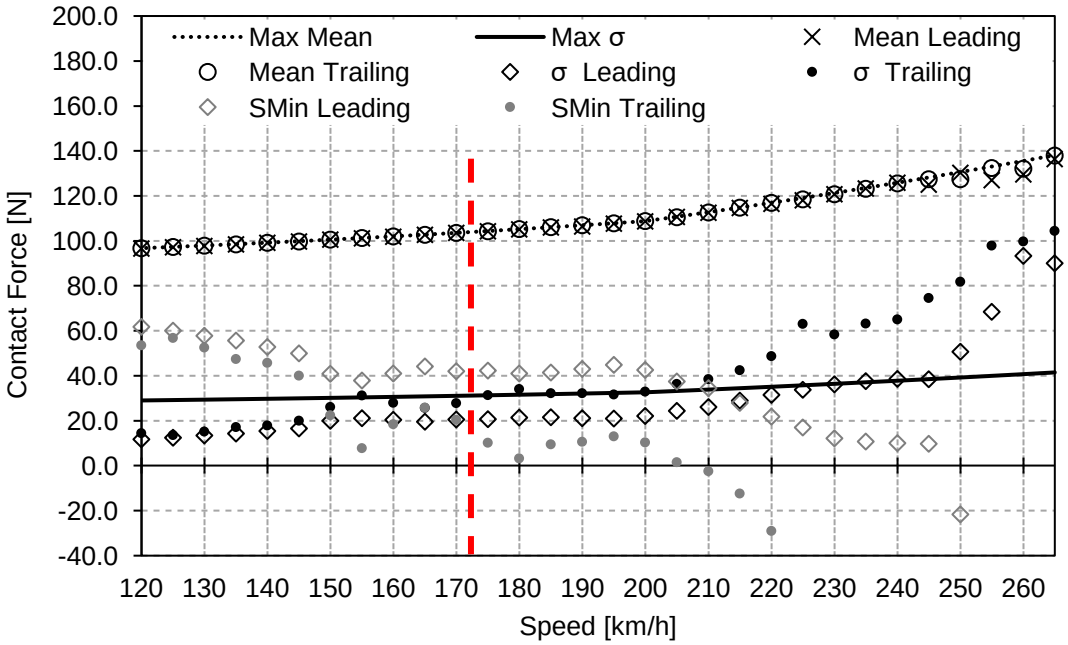

Figure 4.47: LP12_Pant2_S200 results for multiple pantographs, running at various speeds

For the LP12_Pant2_S200 case, Figure 4.47 shows that the statistical minimum of the trailing pantograph has negative values for velocities equal or above 210 km/h. In this figure the standard deviation of the trailing pantograph also surpasses maximum standard deviation line, for 175 km/h. This standard deviation continues to stay above the limit higher velocities. Table 3.1 shows that outside of the contact parameters represented in Figure 4.47, the maximum force is only superior to 350 N, as well as, the contact loss above 0.1% for 215 km/h and above. Since for the adjacent velocities of 155 km/h the standard deviation is within their respective threshold, these dynamic analysis results represent a harmonic effect felt by the trailing pantograph, and the exploration velocity is 170 km/h, where the limiting factor for this case is the standard deviation of the trailing pantograph.

One important note regarding the LP12_Pant2_S200 case, is that travelling at 155 km/h is clearly noticeable that the trailing pantograph presents a high standard deviation which, in comparison with the other separations and a minimum localized minimum for the statistical minimum is observed,

this leads to conclude that the leading pantograph induces a harmonic disturbance in the catenary that resonates with the trailing pantograph. Therefore, the train arrangements with 200 m pantograph spacing should be avoided or the speed of 155 km/h changed as soon as it is reached to avoid this harmonic effect. Another important note regarding the LP12_Pant2_S200 case is that at 195 km/h all of the validating parameters are within the limits. However, the trailing standard deviation is so close to the limit that any small perturbation in the system leads to a trailing standard deviation higher than the limit. Figure 4.48 represents the contact forces for LP12_Pant2_S200_V170.

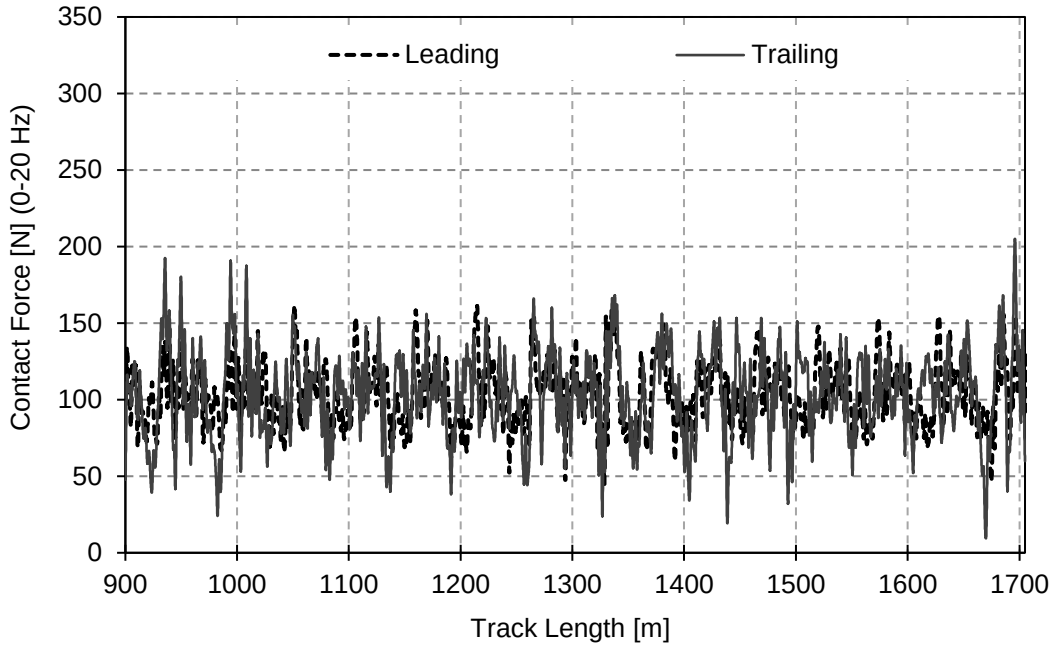

Figure 4.48: Contact forces results for LP12_Pant2_S200_V170

Figure 4.48 represents the contact forces for LP12_Pant2_S200_V170 simulation, where the trailing pantograph is visibly affected by the leading pantograph, in this figure the overlapping arrangement is shown to have similar results to the rest of the zone of interest, so this geometry singularity has no effect in the limiting of higher velocities.

Figure 4.49 represents the maximum steady arm uplift for all the pantograph separations considered for the LP12_Pant2 pantograph catenary pairing. The maximum steady arm uplift is seen to occur for the pair LP12_Pant2 occurs for 35 m and 200 m with 0.127 m of uplift, however this steady arm uplift occurs for speeds at least 40 km/h above the maximum speed of each pantograph separation. When only the exploration velocity are considered the maximum steady arm uplift is 0.056m for the simulation LP12_Pant2_S35_V230, the exploration velocity for a pantograph separation of 35 m is 50 km/h higher than the second higher exploration velocity for multiple pantographs operation In this figure, the maximum steady arm can be observed to increase at a steady pace, until it reaches 200 km/h and the maximum steady arm uplift increases at a much faster pace.

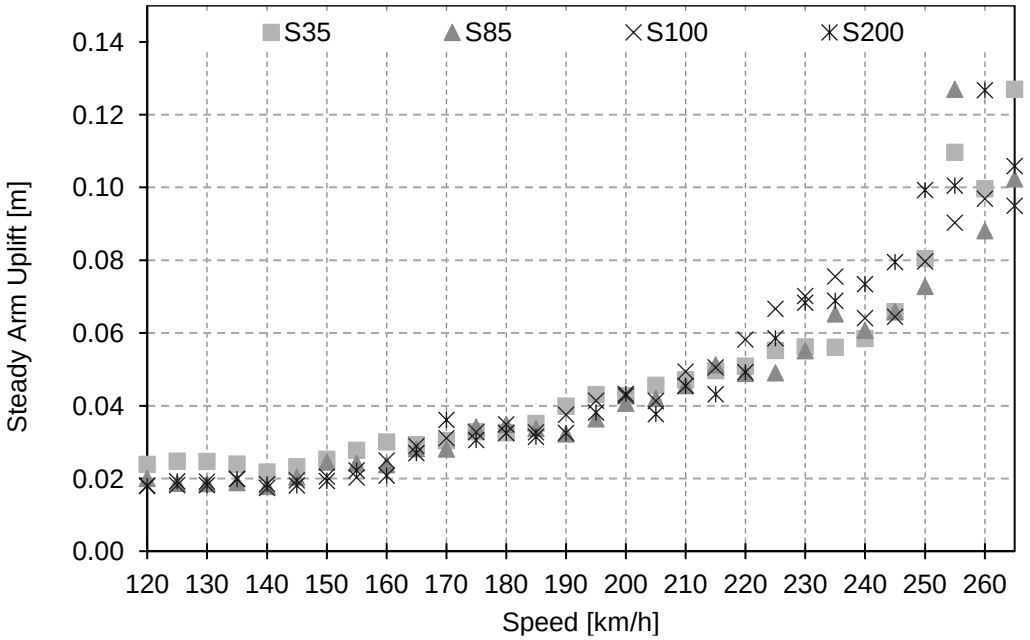

Figure 4.49: LP12_Pant2 steady arm uplift results for multiple pantographs systems, running at various speeds

When comparing all the LP12_Pant2 multiple pantographs cases, the maximum exploration velocity is 145 km/h. Even thought, 85 m and 100 m of separation are close to each other, the critical separation is 85 m. Operating the LP12 catenary with the Pant2 pantograph, with multiple pantographs lowers the exploration velocity by 85 km/h. This difference is significantly high, compared with the difference of 45 km/h for when the Pant1 pantograph is considered. So, when possible, the Pant1 pantograph should be used instead of the Pant2.

4.3 Results Discussion

When the LP10 catenary is paired with the Pant1 pantograph the exploration velocity is found to be 170 km/h for a single pantograph train operation, which is 88 km/h lower than the maximum operating velocity, when the pantograph catenary is not considered, of 258 km/h. This happens because of the effect of the overlapping arrangement since this is the limiting factor of the LP10_Pant1_S0 simulation. When the train operates with multiple pantographs, for the separations observed above, the difference between the exploration velocity is minimal. This is 5 km/h for all separations, except when the separation is 35m, where the exploration velocity is 160 km/h. So, the critical separation between pantographs is 35 m. When a train needs to operate with multiple pantographs their separation should be different from 35 m, and any other separation tested for this pantograph-catenary pair should be chosen instead.

Looking at the LP10 catenary is paired with the Pant2 pantograph the exploration velocity is found to be 165 km/h for a single pantograph train operation, this is a little bit lower than when using the Pant1 pantograph and it is close to 93 km/h lower than the maximum operating velocity. This pantograph catenary case also has the same limiting factor of the maximum force, due to the overlapping arrangement. For the LP10_Pant2 case, when the train operates with multiple pantographs, for the separations observed above, the maximum difference is of 35 km/h, with the exploration velocity of 130 km/h for 85m and 200 m of pantograph separation. For this pantograph the separation of the

pantographs should be 35 m, where the velocity of exploration is 145 km/h, if this separation is not possible to obtain it should be 100 m, that leads to a velocity of exploration of 135km/h. Only for a last case scenario should the separation be 85 m or 200 m.

In order to obtain better results for the LP10 catenary the overlapping arrangement should be redesigned until the limiting factor stops being the maximum force that occurs in this location.

When the LP12 catenary is paired with the Pant1 pantograph the exploration velocity is found to be 260 km/h for a single pantograph train operation. Considering that the maximum operating velocity, when the pantograph catenary is not considered, of 283 km/h, this catenary loses almost 23 km/h. This happens because of the force singularity existing due to the overlapping arrangement. This singularity includes not only a contact force above the 350 N limit, but also a contact loss above the 0.1%, for 265 km/h. When the train operates with multiple pantographs, for the pantograph separations already mentioned, this velocity difference is close to .78 km/h, since the exploration velocity is 205 km/h for a pantograph separation of 100m. For this pantograph catenary pair, the limiting factor is the trailing pantograph standard deviation. The pantograph separation that should be chosen for this operation is 35 m, or, as a second option, 85 m followed by a pantograph separation of 200 m. Only in last case scenario should the train operate at 100 m, and if this pantograph separation is used it should not operate at velocities near 175 km/h, because of the harmonic disturbances.

When the LP12 catenary is paired with the Pant2 pantograph, the exploration velocity is found to be 230 km/h for a single pantograph train operation, this velocity is lower than the one obtained using the Pant1 pantograph and it is close to 53 km/h less than the maximum operation velocity. This pantograph catenary case also has the same limiting factor, as when the Pant1 pantograph is considered, the limiting factor being the standard deviation. For the LP12_Pant2 case, when the train operates with multiple pantographs, with the pantograph separations already mentioned, the maximum difference between the operating and exploration velocity is of 138 km/h, when the exploration velocity is 145km/h, where the critical pantograph separation is 85 m. For this pantograph the separation of the pantographs should be 35 m, if this separation is not possible to obtain it should be 200 m, keeping in mind that for this separation the train velocity should never stay at 155 km/h, it can pass this velocity, but it cannot maintain it because of the harmonic disturbances. If these separations are not possible the pantograph separations should be 100 m and for the last option 85 m. The limiting factor for most of these separations is the standard deviation of the trailing pantograph. This means that the limiting factor for the LP12_Pant2 case is the pantograph used, since it is known that this catenary paired with a different pantograph has a better contact force interaction

With this the Pant2 pantograph should not be used when the alternative of using the Pant1 pantograph is available. If one of these catenaries has to use the Pant2 pantograph, it should be the LP10 catenary, since it is the less affected by this pantograph.

5 Conclusion and future work

5.1 Conclusions

In this work, two catenary models were developed, with three sections each, for a straight railway line. The pantograph-catenary interaction of contact is studied for simulations considering velocities from 120km/h until the exploration velocity with a single pantograph allowed by the norms is reached. The velocity increments between simulations is 5 km/h. The separation of 5 km/h from one simulation to another is capable to pick contact singularities that would not be noticed if the simulations used a much larger increment. Two different types of pantographs, representing the range of pantographs that equip common railway vehicles, are used in the simulations.

This work focusses on the interaction pantograph-catenary. Where it is visible that the LP12 catenary has a higher exploration velocity than LP10, when the same pantograph and pantograph separation is considered. As seen when comparing the simulations with the higher exploration velocity and lower exploration velocity with its equivalent simulation for the other catenary. The case with higher exploration velocity is the LP12_Pant1_S0 that can reach 260 km/h, without surpassing any parameters threshold. While this equivalent case simulation for the LP10 catenary, designated by LP12_Pant1_S0, has a exploration velocity of 170 km/h. If the minimum exploration velocity is considered this occurs for LP10_Pant2_S85 that can reach 130 km/h, and its equivalent for the other catenary is LP12_Pant2_S85 has an exploration velocity of 145 km/h. This leads to the confirmation that the LP12 catenary was designed to operate at higher velocities than LP10, when subjected to the same conditions.

Comparing the pantographs used, the Pant1 pantograph has an advantage, since the exploring velocities for the cases where the Pant1 pantograph is operated are always higher than their equivalent cases considering the Pant2 pantograph. Besides this, the contact quality difference when using the Pant1 or the Pant2 pantograph is intensifies with the velocity. As seen when comparing the difference of velocities between LP10_Pant1_S0 to LP10_Pant2_S0 and LP12_Pant1_S0 to LP12_Pant2_S0. When the LP10 catenary is considered the difference of velocities between the cases is 5 km/h, however when the catenary is exchanged to one with higher exploration velocities LP12 the difference in velocities observed by the exchange of pantographs is 30 km/h. So the use of the Pant2 pantograph should not be used if operating the railway vehicle the Pant1 pantograph is an option. The Pant2 pantograph model has an unusual topology and nonlinearities. When this pantograph is modelled, the dynamic analysis results can differ due to the assumptions made, just like the initial height of the top masses.

Comparing the different pantograph configurations, it is possible to conclude that the best configuration is when only one pantograph is in operation, where the exploring velocities are 260 km/h for LP12_Pant1, 230 km/h for LP12_Pant2, 170 km/h for LP10_Pant1 and 165 km/h for LP10_Pant2. When operations with multiple pantographs are considered the best overall pantograph separation is of 35 m, where the exploration velocities are 235 km/h for LP12_Pant1, 230 km/h for LP12_Pant2, 160 km/h for LP10_Pant1 and 145 km/h for LP10_Pant2. However, for LP10_Pant1 the pantograph separation of 35 m is the one that leads to the slowest exploration velocities, the other separations considered in this work have the same exploration velocity of 165 km/h for this pantograph-catenary

pair. The separation where the lowest exploration velocity for the pantograph-catenary interaction is obtained differs according to the operating pair considered. For LP12_Pant1 it is a separation of 100 m where the exploration velocity is 205 km/h, however if only the pantograph is changed to the Pant2 this separation is 85 m and the exploring velocity is 145 km/h. Considering the LP10 catenary the separation is 35 m for the operation with Pant1 pantograph and 85 m and 200 m for operations with Pant2 pantograph, where the exploration velocity is 130 km/h. So, if only one pantograph separation can be used the chosen is of 35 m, because is the one that has better contact interaction for most of the pantograph-catenary pairs and when this is false the exploration velocity lowers by only 5 km/h.

The limit of the track exploration velocity is the minimum of the exploration velocities obtained. So when no pantograph or pantograph separation is defined the exploration velocity of LP10 is 130 km/h and of LP12 is 145km/h.

5.2 Future work

The limiting factor of the railway operations with the LP10_Pant1 pair is always an effect of the overlap of the two catenaries sections. So, in an attempt obtain a better contact quality with this pantograph-catenary pair, and consequentially increase the exploration velocity, the overlapping can be redesigned. This overlapping redesign would focus on the study of different catenary heights on this zone.

The track exploration velocity considering the different pantographs is visibly different. This can occur, because the Pant2 pantograph is designed to operate at lower velocities than the Pant1. However, the differences in exploration velocities obtained from this work are too high. This can occur if the pantograph does not have a good model representation or if the pantograph was not designed to operate at these velocities. However, most of the pantograph data is not commonly available. If the pantograph owner were able to provide the amplitude and frequency responses obtained from the test rig experimentation, the Pant2 pantograph lump-mass model can be verified.

This study only considers straight railway lines. However, all railway tracks have changes in their geometry, just like curves or contact wire gradients and geometric defects. When this track singularities are considered the exploration velocity can decrease. If a railway operator is capable to provide this geometry singularities, the dynamic analysis results can better represent the reality and new exploration velocities can be found for these catenaries.

6 References

[1] Collina A, Bruni S. Numerical Simulation of Pantograph-Overhead Equipment Interaction. Vehicle System Dynamics [Internet]. 2002;38:261–291. Available from: http://www.tandfonline.com/doi/abs/10.1076/vesd.38.4.261.8286.

[2] Shing AWC, Wong PPL. Wear of pantograph collector strips. Journal of Rail and Mass Transit [Internet]. 2008;222:169–176. Available from: http://journals.sagepub.com/doi/10.1243/09544097JRRT156.

[3] Bucca G, Collina A. A Procedure for the Wear Prediction of Collector Strip and Contact Wire in Pantograph-Catenary System. Wear. 2009;266:46–59.

[4] Mentel JP. Technical developments in superstructure. Communication at Highspeed 2008: 6th World Congress on High Speed Rail. Amsterdam, Netherlands; 2008.

[5] Harada S, Shimizu M, Ikeda K, et al. Development of Simple Catenary Equipment Using PHC Contact Wire for Sinkansen. QR of RTRI. 2008;49:96–102.

[6] California High Speed Train Project. OCS Requirements. Sacramento, California; 2010.

[7] Poetsch G, Evans J, Maisinger R, et al. Pantograph/Catenary Interaction and Control. Vehicle System Dynamics. 1997;28:159–195.

[8] Oura Y, Mochinaga Y, Nagasawa H. Railway Electric Power Feeding Systems. Japan Railway & Transport Review. 1998;16:48–58.

[9] Ambrósio J, Pombo J, Pereira M, et al. A computational procedure for the dynamic analysis of the catenary-pantograph interaction in high-speed trains. Journal of Theoretical and Applied Mechanics. 2012;50.

[10] Ambrósio J, Pombo J, Antunes P, et al. PantoCat statement of method. Vehicle System Dynamics. 2015;53:314–328.

[11] Bruni S, Bucca G, Collina A, et al. Numerical and Hardware-In-the-Loop Tools for the Design of Very High Speed Pantograph-Catenary Systems. Journal of Computational and Nonlinear Dynamics [Internet]. 2012;7:41013. Available from: http://computationalnonlinear.asmedigitalcollection.asme.org/article.aspx?articleid=1475931.

[12] Ambrósio J, Pombo J, Pereira M, et al. Optimization of high-speed railway pantographs for improving pantograph-catenary contact. Theoretical and Applied Mechanics Letters. 2013;3.

[13] Gregori S, Tur M, Nadal E, et al. An approach to geometric optimisation of railway catenaries. Vehicle System Dynamics [Internet]. 2017;3114:1–25. Available from: https://www.tandfonline.com/doi/full/10.1080/00423114.2017.1407434.

[14] Antunes P, Ambrósio J, Pombo J, et al. Dynamic Analysis of the Pantograph-Catenary Interaction on Overlap Sections for High-Speed Railway Operations. Proceedings of the Second International Conference on Railway Technology: Research, Development and Maintenance [Internet]. Stirlingshire, UK: Civil-Comp Press; 2014. Available from: http://www.ctresources.info/ccp/paper.html?id=7792.

[15] Harèll P, Drugge L, Reijm M. Study of Critical Sections in Catenary Systems During Multiple Pantograph Operation. Proceedings of the Institution of Mechanical Engineers, Part F: Journal of Rail and Rapid Transit [Internet]. 2005;219:203–211. Available from: http://pif.sagepub.com/lookup/doi/10.1243/095440905X8934.

[16] Mei G, Zhang W, Zhao H, et al. A hybrid method to simulate the interaction of pantograph and catenary on overlap span. Vehicle System Dynamics. 2006;44:571–580.

[17] Nåvik P, Rønnquist A, Stichel S. Identification of system damping in railway catenary wire systems from full-scale measurements. Engineering Structures. 2016;113:71–78.

[18] Bucca G, Carnevale M, Collina A, et al. Adoption of different pantographs preloads to improve multiple collection and speed up existing lines. Vehicle System Dynamics. 2012;50:403–418.

[19] Liu Z, Jönsson PA, Stichel S, et al. Implications of the operation of multiple pantographs on the soft catenary systems in Sweden. Proceedings of the Institution of Mechanical Engineers, Part F: Journal of Rail and Rapid Transit. 2016;230:971–983.

[20] Pombo J, Antunes P. A Comparative Study Between Two Pantographs In Multiple Pantograph High-Speed Operations. Internatinal Journal of Railway Technology. 2013;2:83–108.

[21] Pombo J, Ambrósio J. Influence of the Track Irregularities on the Railway Vehicle Dynamics. Proceedings of the 4th Asian Conference on Multibody Dynamics (ACMD 2008). Jeju Island, Korea; 2008.

[22] Carnicero A, Jimenez-Octavio JR, Sanchez-Rebollo C, et al. Influence of Track Irregularities in the Catenary-Pantograph Dynamic Interaction. Journal of Computational and Nonlinear Dynamics [Internet]. 2012;7:41015. Available from: http://computationalnonlinear.asmedigitalcollection.asme.org/article.aspx?articleid=1475933.

[23] Van OV, Massat JP, Laurent C, et al. Introduction of variability into pantograph-catenary dynamic simulations. Vehicle System Dynamics [Internet]. 2014;52:1254–1269. Available from: https://doi.org/10.1080/00423114.2014.922199.

[24] J. Pombo, J. Ambrósio, M. Pereira, et al. Influence of the Aerodynamic Forces on the Pantograph-Catenary System for High Speed Trains. Vehicle System Dynamics. 2009;47 (11), 1327–1347.

[25] Bruni S, Ambrosio J, Carnicero A, et al. The results of the pantograph-catenary interaction benchmark. Vehicle System Dynamics [Internet]. 2015;53:412–435. Available from: http://dx.doi.org/10.1080/00423114.2014.953183.

[26] Facchinetti A, Bruni S. Special issue on the pantograph–catenary interaction benchmark. Vehicle System Dynamics [Internet]. 2015;53:303–304. Available from: http://www.tandfonline.com/doi/full/10.1080/00423114.2015.1017308.

[27] EN 50367:2020 Railway applications - Current collection systems -Technical criteria for the interaction between pantograph and overhead line. CENELEC; 2020.

[28] Antunes P, Ambrósio J, Pombo J. Catenary finite element model initialization using optimization. Civil-Comp Proceedings. 2016;110.

[29] Kiessling F, Puschmann R, Schmieder A, et al. Contact Lines for Electric Railways. Berlin, Germany: Siemens AG; 2002.

[30] EN 50119:2020 Railway applications - Fixed installations - Electric traction overhead contact lines. CENLEC; 2020.

[31] Bathe K-J. Finite element procedures. Englewood Cliffs, N.J.: Prentice Hall; 1996.

[32] Przemieniecki JS. Theory of Matrix Structural Analysis. New York: McGraw-Hill; 1968.

[33] Newmark N. A Method of Computation for Structural Dynamics. ASCE Journal of the Engineering Mechanics Division. 1959;85:67–94.

[34] Vyasarayani CP, Uchida T, Carvalho A, et al. Parameter identification in dynamic systems using the homotopy optimization approach. Multibody System Dynamics. 2011;26:411–424.

[35] Antunes P. Co-Simulation Methods for Multidisciplinary Problems in Railway Dynamics. 2018;

[36] Ambrósio J, Pombo J, Pereira M, et al. Recent Developments in Pantograph-Catenary Interaction Modelling and Analysis. International Journal of Railway Technology [Internet]. 2012;1:249–278. Available from: http://www.ctresources.info/ijrt/paper.html?id=12.